

## **General Disclaimer**

### **One or more of the Following Statements may affect this Document**

- This document has been reproduced from the best copy furnished by the organizational source. It is being released in the interest of making available as much information as possible.
- This document may contain data, which exceeds the sheet parameters. It was furnished in this condition by the organizational source and is the best copy available.
- This document may contain tone-on-tone or color graphs, charts and/or pictures, which have been reproduced in black and white.
- This document is paginated as submitted by the original source.
- Portions of this document are not fully legible due to the historical nature of some of the material. However, it is the best reproduction available from the original submission.

# NUMERICAL MODELING OF TWO-DIMENSIONAL CONFINED FLOWS

by

**Mahesh S. Greywall**

**August 1979**



**PREPARED FOR NASA LEWIS RESEARCH CENTER**

**UNDER**

**NASA GRANT NSG-3186**



**Department of Mechanical Engineering  
Wichita State University  
Wichita, Kansas 67208**

ME-MG79-1

NUMERICAL MODELING OF  
TWO-DIMENSIONAL CONFINED FLOWS

by

Mahesh S. Greywall  
Department of Mechanical Engineering  
Wichita State University  
Wichita, KS 67208

August, 1979

Prepared for NASA Lewis Research Center under NASA Grant NSG-3186

## ABSTRACT

A new approach to numerically model two-dimensional confined flows is presented. The flow in the duct is partitioned into finite streams. The difference equations are then obtained by applying conservation principles directly to the individual streams. Also presented is a listing of a computer code based on this approach in FORTRAN IV language. The code computes two-dimensional compressible turbulent flows in ducts when the duct area along the flow is specified and the pressure gradient is unknown.

## TABLE OF CONTENTS

	page
ABSTRACT. . . . .	i
1. INTRODUCTION. . . . .	1
2. STREAMWISE COMPUTATION OF DUCT FLOWS. . . . .	4
3. PROGRAM LISTING . . . . .	10
3.1 Introduction . . . . .	10
3.2 Main Program and Common Subroutines. . . . .	12
3.3 Four Subroutines for Circular Ducts. . . . .	32
3.4 Sample Computations--Pipe Flow . . . . .	37
3.5 Four Subroutines for Rectangular Ducts . . . . .	44
3.6 Sample Computations--Rectangular Diffuser Flow . . . . .	50
REFERENCES. . . . .	56
APPENDIX A -- Pressure Drop Forecasting and Pressure Iteration. . . .	57
APPENDIX B -- Streamwise Computation of Duct Flows--Original Paper. .	

## 1. INTRODUCTION

Two-dimensional effects, such as the growth of momentum and thermal boundary layers, in flows through nozzles, channels, and diffusers have been traditionally studied by separating the flow into a core and a boundary layer.<sup>1</sup> The core flow is then calculated by one-dimensional potential flow equations and the boundary layer by momentum integral approach. Some flows cannot be accurately calculated with this approach. For example, in flows with large differences between the core and the wall temperatures substantial heat flow in or out of the core weakens the assumption of a radially uniform core. Again in calculating performance of diffusers with high inlet blockage factor, as in MHD diffusers, the flow cannot be meaningfully separated into a core and a boundary layer.

Recently many approaches, based on finite difference methods, have been developed to calculate confined flows without the separation into core and boundary layer. These approaches can be broadly divided into two classes. In one class the finite difference equations are obtained by differencing the flow differential equations either in their primitive form or in some transformed form. In the other class the finite difference equations are obtained directly from the conservation principles. Examples of these two classes, along with their interrelationship, are given in Fig. 1.

This report deals with the approach of Ref. 7--shown bordered by heavy line in Fig. 1. The original paper describing this approach is

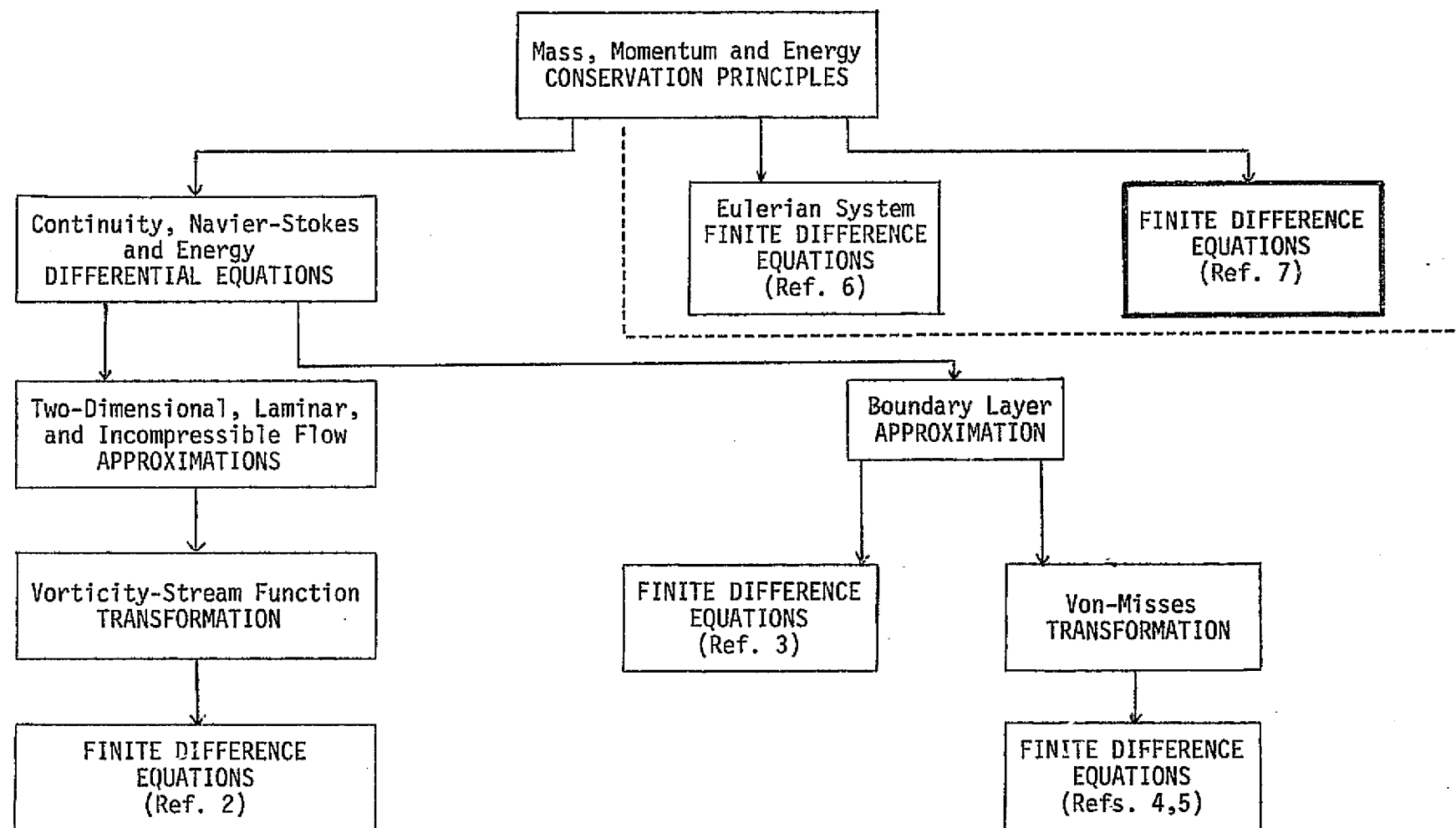


Figure 1

included in Appendix B. In section 2 of this report are given the underlying ideas of this approach, summary of the difference equations and a discussion of the solution technique. Based on this approach a computer code, called NEMCO (numerical modeling of confined flows), has been developed. This code computes basically two-dimensional mass, momentum, and energy transfer. Thus it can handle flow which is either strictly two-dimensional--flow through nozzles, pipes, conical diffusers, discs, etc.--or is a two-dimensional approximation to the actual flow. An example of the latter is flow through a rectangular channel where the calculations are carried out along one pair of the opposing walls and the presence of the other pair is either completely ignored (case of large aspect ratio) or approximately taken into account by introducing some sort of effective width for the actual width between the ignored walls.

In section 3 is given the program listing of the code NEMCO-U2-79 in FORTRAN IV language. The program listing given was derived, with some FORTRAN language modifications, from the various versions of this code we have used in our computations. To check the code listing included in this report we have run two sets of sample calculations--one for flow through a pipe and another for flow through a rectangular diffuser. The results of the sample calculations are also given in section 3.



## 2. STREAMWISE COMPUTATION OF DUCT FLOWS

In this approach finite difference equations are obtained by first partitioning the flow in the duct into a finite number of streams and then applying conservation principles directly to the individual streams. To partition the flow into streams we draw a series of streamlines  $1, 2, \dots, N$  as shown in Fig. 2. The direction  $x$  is along the flow and  $z$ , measured from the duct wall, normal to it. Duct wall is chosen as streamline 1 and the centerline or the symmetry plane as streamline  $N$ . We define streamline  $j+1/2$  as the streamline in the middle of  $j$  and  $j+1$ . Streamline  $j-1/2$  is defined similarly. We now define the various streams as follows:

Stream 2; flow between the wall and the streamline  $2+1/2$ ,

Stream  $j$  ( $N > j > 2$ ); flow between streamlines  $j-1/2$  and  $j+1/2$ ,

Stream  $N$ ; flow between the streamline  $N-1/2$  and the centerline or the symmetry plane.

Shape of a typical stream depends on the shape of the duct: in rectangular ducts the streams will be plane layers and in circular ducts the streams will be cylindrical shells.

We introduce the following nomenclature:

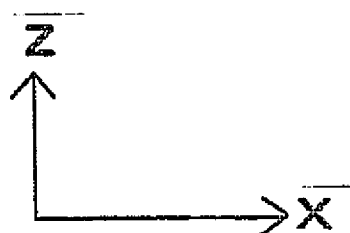
$\psi_j^+$ ; mass flow rate between the streamline  $j$  and  $j+1/2$ .

$\psi_j^-$ ; mass flow rate between the streamline  $j$  and  $j-1/2$ .

$u_j(x)$ ,  $T_j(x)$ ,  $\rho_j(x)$ ,  $h_j(x)$ ,  $C_j(x)$ ; velocity, temperature, density, enthalpy and constant pressure specific heat along the streamline  $j$ .

$z_j(x)$ ; distance of streamline  $j$  from the wall.

$A_j^x$ ; cross-sectional area of stream  $j$ .



FLOW DIRECTION  $\longrightarrow$

DUCT CENTERLINE OR THE SYMMETRY PLANE

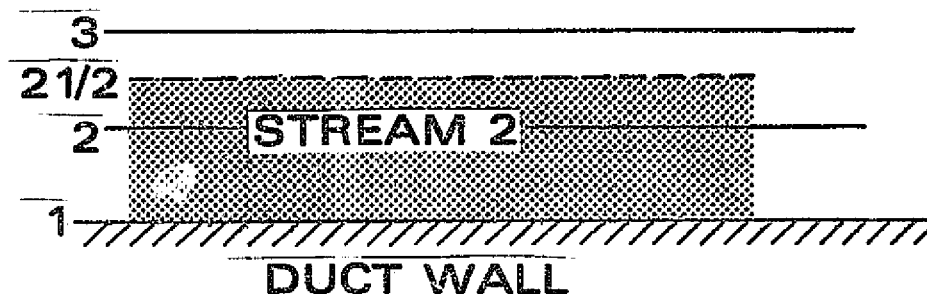
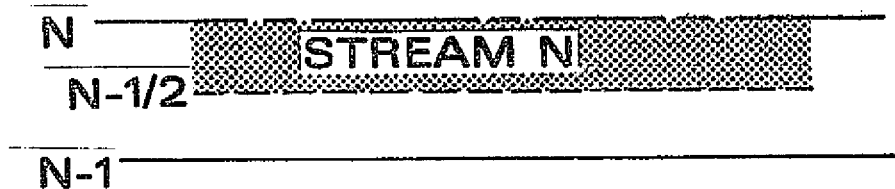


FIG. 2

$A_{j+1/2}^S$ ; interface area between streams  $j$  and  $j+1$ .

$\mu_{j+1/2}(x)$ ,  $k_{j+1/2}(x)$ ; effective viscosity and thermal conductivity (including turbulent contribution) along streamline  $j+1/2$ .

$\Delta p$ ; pressure difference between  $x$  and  $x + \Delta x$ .

$$v_{j+1/2} = \frac{\mu_{j+1/2}}{z_{j+1} - z_j} A_{j+1/2}^S, \quad H_{j+1/2} = \frac{v_{j+1/2}}{Pr_{j+1/2}} \quad \text{where } Pr \text{ is Prandtl's number.}$$

$\alpha, \beta, \delta$ ; correction factors.

Applying conservation principles to individual streams across  $x$  and  $x + \Delta x$  we obtain the following finite difference equations for velocities and enthalpies (see Ref. 7):

#### Stream 2

$$\begin{aligned} & -u_3^+ \left[ -\frac{\psi_2^+}{4} + \frac{1}{2} v_{2+1/2}^+ \right] + u_2^+ \left[ \frac{3}{4} \psi_2^+ + \alpha \psi_2^- + \frac{1}{2} v_{2+1/2}^+ + \frac{1}{2} v_1^+ \right] \\ & = -\Delta p A_2^x + u_3 \left[ \frac{\psi_2^+}{4} + \frac{1}{2} v_{2+1/2} \right] + u_2 \left[ \frac{3}{4} \psi_2^+ + \alpha \psi_2^- - \frac{1}{2} v_{2+1/2} - \frac{1}{2} v_1 \right]. \quad (2-1) \end{aligned}$$

$$\begin{aligned} & -h_3^+ \left( -\frac{\psi_2^+}{4} + \frac{1}{2} H_{2+1/2}^+ \right) + h_2^+ \left( \frac{3}{4} \psi_2^+ + \beta \psi_2^- + \frac{1}{2} H_{2+1/2}^+ + \frac{1}{2} H_1^+ \right) \\ & = h_3 \left( \frac{\psi_2^+}{4} + \frac{1}{2} H_{2+1/2} \right) + h_2 \left( \frac{3}{4} \psi_2^+ + \beta \psi_2^- - \frac{1}{2} H_{2+1/2} - \frac{1}{2} H_1 \right) \\ & + \frac{u_3^+}{2} \left( \frac{\psi_2^+}{4} + \frac{1}{2} v_{2+1/2}^+ \right) - \frac{u_2^+}{2} \left( \frac{3}{4} \psi_2^+ + \delta \psi_2^- + \frac{1}{2} v_{2+1/2}^+ \right) \\ & + \frac{u_3^2}{2} \left( \frac{\psi_2^+}{4} + \frac{1}{2} v_{2+1/2} \right) + \frac{u_2^2}{2} \left( \frac{3}{4} \psi_2^+ + \delta \psi_2^- - \frac{1}{2} v_{2+1/2} \right) + h_w \frac{1}{2} H_1^+ + h_w \frac{1}{2} H_1. \quad (2-2) \end{aligned}$$

In Eq. (2-2)  $h_w$  represents enthalpy evaluated at the wall temperature. This program assumes that the wall temperature is given. When wall heat flux is specified see Ref. 7 for the needed modification.

Streams  $j = 3, 4, \dots, N-1$

$$\begin{aligned}
 & -u_{j+1}^+ \left[ -\frac{\psi_j^+}{4} + \frac{1}{2}v_{j+1/2}^+ \right] + u_j^+ \left[ \frac{3}{4}\psi_j^+ + \frac{3}{4}\psi_j^- + \frac{1}{2}v_{j+1/2}^+ + \frac{1}{2}v_{j-1/2}^+ \right] \\
 & - u_{j-1}^+ \left[ -\frac{\psi_j^-}{4} + \frac{1}{2}v_{j-1/2}^+ \right] \\
 = & -\Delta p A_j^x + u_{j+1} \left[ \frac{\psi_j^+}{4} + \frac{1}{2}v_{j+1/2} \right] + u_j \left[ \frac{3}{4}\psi_j^+ + \frac{3}{4}\psi_j^- - \frac{1}{2}v_{j+1/2} - \frac{1}{2}v_{j-1/2} \right] \\
 & + u_{j-1} \left[ \frac{\psi_j^-}{4} + \frac{1}{2}v_{j-1/2} \right] \cdot
 \end{aligned} \tag{2-3}$$

$$\begin{aligned}
 & -h_{j+1}^+ \left[ -\frac{\psi_j^+}{4} + \frac{1}{2}h_{j+1/2}^+ \right] + h_j^+ \left[ \frac{3}{4}\psi_j^+ + \frac{3}{4}\psi_j^- + \frac{1}{2}h_{j+1/2}^+ + \frac{1}{2}h_{j-1/2}^+ \right] \\
 & - h_{j-1}^+ \left[ -\frac{\psi_j^-}{4} + \frac{1}{2}h_{j-1/2}^+ \right] \\
 = & h_{j+1} \left[ \frac{\psi_j^+}{4} + \frac{1}{2}h_{j+1/2} \right] + h_j \left[ \frac{3}{4}\psi_j^+ + \frac{3}{4}\psi_j^- - \frac{1}{2}h_{j+1/2} - \frac{1}{2}h_{j-1/2} \right] \\
 & + h_{j-1} \left[ \frac{\psi_j^-}{4} + \frac{1}{2}h_{j-1/2} \right] + \frac{u_{j+1}^2}{2} \left[ -\frac{\psi_j^+}{4} + v_{j+1/2}^+ \right] \\
 & - \frac{u_j^2}{2} \left[ \frac{3}{4}\psi_j^+ + \frac{3}{4}\psi_j^- + v_{j+1/2}^+ + v_{j-1/2}^- \right] + \frac{u_{j-1}^2}{2} \left[ -\frac{\psi_j^-}{4} + v_{j-1/2}^+ \right] \\
 & + \frac{u_{j+1}^2}{2} \left[ \frac{\psi_j^+}{4} + v_{j+1/2} \right] + \frac{u_j^2}{2} \left[ \frac{3}{4}\psi_j^+ + \frac{3}{4}\psi_j^- - v_{j+1/2} - v_{j-1/2} \right] \\
 & + \frac{u_{j-1}^2}{2} \left[ \frac{\psi_j^-}{4} + v_{j-1/2} \right] \cdot
 \end{aligned} \tag{2-4}$$

### Stream N

Difference equations for stream N are obtained from Eqs. (2-3) and (2-4) by letting  $j = N$ , and setting

$$\psi_N^+ = V_{N+1/2}^+ = V_{N+1/2} = u_{N+1}^+ = u_{N+1} = 0, \quad \text{and}$$

$$h_{N+1}^+ = h_{N+1} = H_{N+1/2}^+ = H_{N+1/2} = 0$$

In the equations superscripts + indicates the quantities at  $x + \Delta x$ , thus  $u_j$  is the velocity along  $j$  at  $x$  and  $u_j^+$  along  $j$  at  $x + \Delta x$ . In the listing given in section 3 same symbol is used for a given variable, like  $u_j$ , at  $x$  and  $x + \Delta x$ . Program is written such that from the point calculations of new quantities are started there is no further need for old values at  $x$ . Equations (2-1) to (2-4) are supplemented with formulae given in Appendices A and B of Ref. 7. These formulae calculate  $A^X$ ,  $A^S$ ,  $\mu$ , and first at  $x$  calculate  $\psi_j^+$  and  $\psi_j^-$  given  $\rho_j$ ,  $u_j$ , and  $z_j$  and then later at  $x + \Delta x$  calculate  $z_j^+$  from  $\psi_j^+$ ,  $\psi_j^-$ ,  $\rho_j^+$ , and  $u_j^+$ .

The technique to solve these difference equations depends on the specified design variables. The program given in section 3 assumes that the variation of duct area along the flow is specified and the pressure gradient is unknown. For this case the difference equations are solved as follows. Equations (2-1) and (2-3) (and similarly Eqs. (2-2) and (2-4)) are looked at as a system of tri-diagonal linear algebraic equations. This, of course, is true only if  $V_j^+$  and  $\Delta p$  are known. To start with we set  $V_j^+$  equal to  $V_j$  and solve for  $u_j^+$  using standard methods to solve tri-diagonal equations. We then calculate  $V_j^+$  from the new  $u_j^+$  and solve

for  $u_j^+$  again using the new  $V_j^+$ . This iteration process is continued until new  $u_j^+$  differs from the previously calculated  $u_j^+$  by less than some preassigned value. In the early computations  $u_2$ , among all  $u_j$ , was found to change most rapidly from one iteration to another. Thus it has been chosen for all our computations to check for convergence. This iteration loop is called the velocity iteration loop. Solution for  $h_j^+$  is carried on along with the velocity iteration calculating  $H_j^+$  from the latest  $V_j^+$  and using the latest available  $u_j^+$  for kinetic energy terms.

The pressure drop  $\Delta p$  is also not known in advance. We start the calculations with some estimated  $\Delta p$  and carry out the velocity iteration. When the velocity ( $u_2^+$ ) convergence is achieved we check the calculated duct area at  $x + \Delta x$  against the specified duct area. If the difference is larger than some preassigned value we go back, adjust  $\Delta p$ , and start the velocity iteration all over again. Iteration on  $\Delta p$  is called pressure iteration. Note the pressure iteration loop is placed over and above the velocity iteration loop. Initial estimate of  $\Delta p$  at the beginning of a new integration step is obtained by projecting the previous three values using least square method as discussed in Appendix A. Correction to  $\Delta p$  from one pressure iteration to the next is based on the difference between the calculated and the specified duct area.

### 3. PROGRAM LISTING

#### 3.1 Introduction.

The program consists of a MAIN PROGRAM and nine subroutines;

INPUT1	(Provides geometric data for the duct),
START	(Sets up grid normal to the flow and assigns starting velocity, temperature, density and enthalpy profiles),
SIPSIM	(Calculates $\psi_j^+$ and $\psi_j^-$ , the mass flow rates through upper and lower parts of streams),
ZDZ	(Calculates distance of streamlines from the wall),
XSAREA	(Calculates cross-sectional and surface areas of the streams),
VSCSTY	(Calculates laminar and turbulent viscosities),
TDSOLV	(Solves tri-diagonal set of algebraic equations),
THICK	(Calculates various thicknesses associated with the boundary layer),
HPTRHO	(Calculates temperature and density given pressure and enthalpy).

The main program and five of the subroutines are common to all duct shapes.

The four subroutines INPUT1, SIPSIM, ZDZ, and XSAREA depend on the shape of the duct. Subsections 3.2 through 3.6 contain computer listings in

FORTRAN IV as follows:

Subsection 3.2; Main program and subroutines common to all duct shapes,

Subsection 3.3; The four subroutines for circular ducts,

Subsection 3.4; Sample computations--pipe flow,

Subsection 3.5; The four subroutines for rectangular ducts,

### Subsection 3.6; Sample computations--rectangular diffuser flow.

All computer listings are preceded by definitions of the FORTRAN names used in the program.

#### DATA INPUT:

Data input to program is through MAIN program and subroutine INPUT1.

Input statements have been placed at the very beginning of the programs.

Data given through the various programs is as follows:

#### Main Program:

- a) UCNTR, ZBL, TCNTR, TWALL, P, CP, GASK, GASR, PRNDL, DPDX--dynamic and thermodynamic flow data.
- b) XEND--length of the duct.
- c) DPDTL, DXFAC, NJ, MAXIT, NPRNT--pressure gradient convergence tolerance, integration step size, number of grid points normal to the flow, maximum number of iterations allowed, and output frequency.
- d) VZERO, TZERO, EXPV--parameters needed in subroutine VSCSTY to calculate laminar viscosity.
- e) EXPU, EXPH--parameters needed in subroutine START to calculate initial boundary layer profiles.

#### INPUT1 Subroutine:

Duct shape, parameters differ for different duct shapes.

#### PROGRAM OUTPUT

Output of program is of three kinds:

- a) Distribution of velocity, temperature, density, and enthalpy profiles normal to the flow at a given value of x. Frequency of this output is governed by NPRNT.



- b) Distribution of pressure, shear stress, heat transfer to the wall, and various boundary layer parameters along  $x$ . These quantities are calculated at the end of each integration step and stored in vector forms. The results are printed after the calculations reach the end of the duct.
- c) Many subroutines have output statements to print results of intermediate calculations. Frequency of this output is governed through the subscript appended to the subroutine name. This kind of output is used for diagnostic purposes.

### 3.2 Listing main program and common subroutines.

#### MAIN Program:

U(J) = Velocity along streamline J  
 T(J) = Temperature along streamline J  
 H(J) = Enthalpy along streamline J  
 RHO(J) = Density along streamline J  
 USH(J) =  $(1/2)U^2(J)$   
 Z(J) = Distance from the wall of streamline J  
 DZ(J) =  $Z(J+1) - Z(J)$   
 NJ = Number of grid points normal to the flow  
 NJ1 = NJ-1  
 NJ2 = NJ-2  
 NJP = NJ+1  
 NBL = Number of grid points assigned to the boundary layer at the  
       inlet ( $NBL \leq NJ$ )  
 Note: In this program NBL is calculated internally in subroutine START  
 DX = Size of integration step along the flow  
 SIP(J) =  $\psi_j^+/4$   
 SIM(J) =  $\psi_j^-/4$   
 FLORAT = Total mass flow rate through the duct  
 UCNTR = Velocity at the centerline or the symmetry plane  
 TCNTR = Temperature at the centerline or the symmetry plane  
 TWALL = Wall temperature  
 P = Pressure  
 CPINV = Inverse of  $C_p$ , the constant pressure specific heat  
 RINV = Inverse of R, the gas constant  
 GASK = Ratio of the specific heats  
 ZBL = Boundary layer thickness at the inlet  
 AX(J) = Cross-sectional area of stream J  
 AS(J) = Surface area between streams J and J-1  
 ALPHA, BETA, DELTA, GAMMA are the correction factors  $\alpha, \beta, \delta, \gamma$  of Ref. 7.  
 RE = Reynolds number along streamline 2  
 VISC(J) = Viscosity along streamline J - 1/2  
 DEL1 = Displacement thickness of the boundary layer,  $\delta_1$   
 DEL2 = Momentum thickness of the boundary layer,  $\delta_2$   
 HT2 = Shape factor DEL1/DEL2  
 DELO = Boundary layer thickness  
 COMMON/COM8; this common statement contains variable names pertaining to  
 the duct shape. These names are defined later in INPUT1.  
 VF(J), HT(J) defined later by the program listing.  
 UU(J) = Intermediate velocity variable

The tri-diagonal form of the momentum and energy difference equation is

$$-a_j X_{j+1} + b_j X_j - c_j X_{j-1} = d_j ,$$

AA(J),BB(J),CC(J) are used for  $a_j$ ,  $b_j$ , and  $c_j$ , first for momentum and then for energy equation; DD(J) is  $d_j$  for momentum equation and TT(J)  $d_j$  for the energy equation; DU(J) is part of DD(J) and DT(J) part of TT(S).

Note: Subscript I, in what follows, denotes the integration step along x.

EXVEC(I) = Distance along the flow, "x"  
 PVEC(I) = Pressure along x,  
 SHRVEC(I) = Shear stress at wall along x,  
 HTVEC(I) = Heat flux along x,  
 DLOVEC(I) = Boundary layer thickness along x,  
 DL1VEC(I) = Displacement thickness along x,  
 DL2VEC(I) = Momentum thickness along x,  
 SFVEC(I) = Shape factor along x.  
 CP = Constant pressure specific heat  
 GASR = Gas constant, R  
 PRNDL = Prandtl number  
 DPDX = Pressure gradient guess at the entrance

Note: The program requires as input a value of pressure gradient at the duct entrance for its first iteration. We suggest a value calculated approximately for one-dimensional flow.

XEND = Length of the duct  
 DPDTL = Tolerance within which  $dp/dx$  is to be calculated  
 DXFAC = Specifies the size of integration step,  $DX = \text{HEIGHT}/DXFAC$   
 MAXIT = Maximum number of iterations allowed, if this number is exceeded the program will stop and write a message  
 NPRNT = Governs how often along x U(J),T(J), etc., are printed  
 VZERO,TZERO,EXPV: See subroutine VSCSTY  
 EXPU,EXPH; See subroutine START  
 XAMP,DXF,DX; for the first integration step DX is set equal to  $DXF/256$ , where DXF is calculated from  $DXF = \text{HEIGHT}/DXFAC$ . DX is multiplied by XAMP at the end of each integration step when DX reaches DXF XAMP is set equal to 1.

ISTEP = Integration step counter  
 ITRN = Iteration step counter  
 NPI = Counter for NPRNT  
 SNDSPPD = Sound speed at the inlet  
 PTINL = Total pressure at the inlet  
 OLDA = Cross-sectional area of the duct at the previous integration step  
 DPDAMP, ZTLRN, UTLRN; See Appendix A

Symbols appearing in the rest of the MAIN program are either already defined or defined by FORTRAN statements appearing in this part of the program.

### START Subroutine:

This subroutine sets up grid normal to the flow and specifies velocity, temperature, and density profiles at the beginning of the computations. The listing given assumes that the flow at the inlet has a boundary layer of thickness ZBL and that within the boundary layer velocity and enthalpy vary as

$$\frac{U(J)}{UCNTR} = \left( \frac{Z(J)}{ZBL} \right)^{1/EXPU} \quad \text{and}$$

$$\frac{H(J) - HWALL}{HCNTR - HWALL} = \left( \frac{Z(J)}{ZBL} \right)^{1/EXPH}$$

where HWALL and HCNTR refer to enthalpies calculated at wall and center-line temperatures, and EXPU and EXPH are input parameters. Outside the boundary layer H and U are assumed to be uniform.

To set up grid that will compute the flow with maximum possible accuracy is difficult. Algorithm given in this subroutine is guided by the following considerations:

1. Grid points are to have greater density near the wall.  
The grid spacing to increase as Z to the some power, where Z is the distance from wall.
2. Grid point Z(2) (Z(1) is wall) is to be located just outside the laminar sublayer and the transition zone--the formula used to calculate turbulent viscosity for points Z(J),  $J \geq 2$ , is good only for the turbulent region. Also point Z(2) must not be too far away from the wall or we will lose accuracy in calculating flow near the wall.

3. Grid point  $Z(3)$  is to be selected so that  $Z(3)-Z(2)$  is not less than  $Z(2)-Z(1)$ . Otherwise, as noted in Ref. 8, for some flow conditions one may encounter numerical instability.

In the subroutine Reynold's number along  $Z(2)$  is required to be around 1200. Thus  $U(2)$  and  $Z(2)$  are calculated from the two simultaneous equations,

$$\frac{U(2)}{UCNTR} = \left( \frac{Z(2)}{ZBL} \right)^{1.7EXPU} \quad \text{and}$$

$$U(2) Z(2)/VISKIN = 1200$$

where  $VISKIN$  is kinematic viscosity.

Grid location of  $Z(J)$ ,  $J \geq 2$ , are next calculated using a variation of formula given in Ref. 8. We put

$$Z(J) = Z(2) + (HEIGHT - Z(2)) \left( \frac{J}{NJ} \right)^{EXPG}$$

Grid exponent  $EXPG$  is calculated from the requirement

$$Z(3) - Z(2) = Z(2) - Z(1)$$

### VSCSTY Subroutine:

This subroutine calculates viscosity (laminar + turbulent) coefficients along the stream interfaces. Symbol VISC(J) represents the viscosity coefficient along streamline J - 1/2. The laminar contribution to VISC(J) is calculated from the formula

$$\text{VISC}(J) = \frac{1}{2} \left[ \text{VZERO} \left\{ \frac{T(J)}{TZERO} \right\}^{\text{EXPV}} + \text{VZERO} \left\{ \frac{T(J-1)}{TZERO} \right\}^{\text{EXPV}} \right]$$

where VZERO, EXPV, and TZERO are constants and are required input to the subroutine. The turbulent contribution to VISC(J) is calculated from

$$\text{VISC}(J) = \left[ \frac{\text{EL}(J) + \text{EL}(J-1)}{2} \right]^2 \times \left[ \frac{\text{RHO}(J) + \text{RHO}(J-1)}{2} \right] \times \left| \frac{U(J) - U(J-1)}{\text{DZ}(J)} \right|$$

The mixing length, EL, is calculated from the relation for the fully developed turbulent pipe flow [Eq. (20.18), Ref. 1].

$$\text{EL}(J) = \text{ZOUT} \left[ 0.14 - 0.08 \left( \frac{1 - Z(J)}{\text{ZOUT}} \right) - 0.06 \left( \frac{1 - Z(J)}{\text{ZOUT}} \right)^2 \right]$$

The quantity  $1 - Z(J)/\text{ZOUT}$  represents the distance from the centerline normalized by half the channel width.

This subroutine also calculates the correction factors  $\gamma$ ,  $\alpha$ ,  $\delta$ , and  $\beta$ . The formulae used in the subroutine to calculate  $\gamma$ ,  $\alpha$ , and  $\delta$  were obtained by curve fitting the graphs shown in Ref. 7. Factor  $\beta$

was calculated from  $\alpha$  using the relation given in Ref. 8. (This relation is obtained using integrals defining  $\alpha$  and  $\beta$ , and assuming  $\frac{h - h_w}{h - h_0} \sim \frac{u}{u_0}$  ).

The formula to calculate FF from Re was obtained by curve fitting the relation shown in Fig. B-1 of Ref. 7 in the vicinity of  $Re \sim 1000$ .

TDSOLV Subroutine:

This subroutine solves the tri-diagonal set of equations

$$-A_j X_{j-1} + B_j X_j - C_j X_{j+1} = D_j$$

where  $j = 2, 3, \dots, N$ . Method used is the well-known special case of Gauss' reduction formula (see for example Ref. 2). The boundary condition at the wall is already built into the difference equations and appears as

$$C_2 = 0.$$

The boundary condition at the center line used in the present work is that of symmetry and appears as

$$A_N = 0.$$



### THICK Subroutine:

This subroutine calculates boundary layer thickness,  $\delta_0$ , displacement thickness,  $\delta_1$ , momentum thickness,  $\delta_2$ , and shape factor  $H_{12}$ .

Boundary layer thickness is defined as the distance from the wall where the velocity equals 0.995 times center line velocity. The integrals

$$\delta_1 = \int_0^{\infty} \left[ 1 - \frac{\rho u}{\rho_{\infty} u_{\infty}} \right] dz, \quad \text{and}$$

$$\delta_2 = \int_0^{\infty} \frac{\rho u}{\rho_{\infty} u_{\infty}} \left[ 1 - \frac{u}{u_{\infty}} \right] dz$$

were approximated by the sums

$$\delta_1 = \left( 1 - \frac{\gamma \rho_2 u_2}{\rho_{\infty} u_{\infty}} \right) dz_2 + \sum_{j=3}^N \frac{1}{2} \left[ \left( 1 - \frac{\rho_j u_j}{\rho_{\infty} u_{\infty}} \right) + \left( 1 - \frac{\rho_{j-1} u_{j-1}}{\rho_{\infty} u_{\infty}} \right) \right] dz_j$$

and

$$\delta_2 = \left( \frac{\gamma \rho_2 u_2}{\rho_{\infty} u_{\infty}} - \frac{\alpha \gamma \rho_2 u_2^2}{\rho_{\infty} u_{\infty}^2} \right) dz_2 + \sum_{j=3}^N \frac{1}{2} \left[ \frac{\rho_j u_j}{\rho_{\infty} u_{\infty}} \left( 1 - \frac{u_j}{u_{\infty}} \right) + \frac{\rho_{j-1} u_{j-1}}{\rho_{\infty} u_{\infty}} \left( 1 - \frac{u_{j-1}}{u_{\infty}} \right) \right] dz_j$$

HPTRHO Subroutine:

This subroutine calculates temperature and density given pressure and enthalpy. In its present form it uses formulae for perfect gas with constant specific heats.

```

C
C*****NEMCO-U2-79*****
C
COMMON/COM1/U(50),T(50),H(50),RHO(50),USH(50),Z(50),DZ(50)
COMMON/COM2/NJ,NJ1,NJ2,NJP,NBL,DX
COMMON/COM3/SIP(50),SIM(50),FLORAT
COMMON/COM4/UCNTR,TCNTR,TWALL,P,CPINV,RINV,GASK,ZBL
COMMON/COM5/AX(50),AS(50)
COMMON/COM6/ALPHA,BETA,DELTA,GAMMA,RE,VISC(50)
COMMON/COM7/DEL1,DEL2,H12,DELO
COMMON/COM8/HEIGHT,WIDTH,HSLOPE,WSLOPE,AVWIDTH,EFWIDTH,OLDA,ARFAC
COMMON/COM9/VZERO,EXPV,TZERO,EXPU,EXPH
DIMENSION VF(50),HT(50),UU(50)
DIMENSION AA(50),BB(50),CC(50),DD(50),DU(50),DT(50),TT(50)
DIMENSION EXVEC(200),PVEC(200),PRVEC(200),SHRVEC(200),
1HTVEC(200),DLOVEC(200),DL1VEC(200),DL2VEC(200),SFVEC(200)
C
C**DATA INPUT *****
C**DYNAMIC AND THERMODYNAMIC DATA*****
UCNTR=
ZBL=
TCNTR=
TWALL=
P=
CP=
GASK=
GASR=
PRNDL=
DPDX=
C**GEOMETRIC DUCT DATA*****
CALL INPUT1
XEND=
C**CONVERGENCE CRITERIA,GRID SIZE,AND OTHER DATA*****
DPDTL=
DXFAC=
MAXIT=
NJ=
NPRNT=
C**DATA FOR VSCSTY AND START SUBROUTINES*****
VZERO=
TZERO=
EXPV=
EXPU=
EXPH=
C
C**INITIALIZATIONS*****
XAMP=2.0
ISTEP=0
ITRN=0
NPI=NPRNT-1
NJP=NJ+1
NJI=NJ-1
NJ2=NJ-2
SIP(NJ)=0.0

```

```

VF(NJP)=0.
HT(NJP)=0.
U(NJP)=0.
H(NJP)=0.
USH(NJP)=0.
CC(2)=0.
DXF=HEIGHT/DXFAC
DX=DXF/256.
EX=-DX
DP=DPDX*DX
PRLINV=1./PRNDL
CPINV=1./CP
RINV=1./GASR
GASKIN=1./GASK
HWALL=CP*TWALL
SNDSPD=(GASK*GASR*TCNTR)**0.5
PTINL=P*(1.+0.5*(GASK-1.)*(UCNTR/SNDSPD)**2)**(GASK/(GASK-1.))
PINL=P
DPPTI=PTINL-PINL
DP1=0.
DP2=0.
DX1=0.
OLDA=0.0
CALL START
WRITE(6,30)

```

REPRODUCIBILITY OF THE  
ORIGINAL PAGE IS POOR

```

30 FORMAT(1H1, ' VELOCITY U, TEMPERATURE T, DENSITY RHO, AND ENTHALPY H  
1DISTRIBUTIONS AS FUNCTION OF Z.', //)

```

C

C\*\*AXIAL CALCULATIONS\*\*\*\*\*

```

1100 ISTEP=ISTEP+1
EX=EX+DX
CALL VSCSTY(0)
CALL THICK
NPI=NPI+1
EXVEC(ISTEP)=EX
PVEC(ISTEP)=P
PRVEC(ISTEP)=(P-PINL)/DPPTI
SHRVEC(ISTEP)=VISC(2)*U(2)
HTVEC(ISTEP)=VISC(2)*PRLINV*(H(2)-HWALL)
DL0VEC(ISTEP)=DEL0
DL1VEC(ISTEP)=DEL1
DL2VEC(ISTEP)=DEL2
SFVEC(ISTEP)=H12
IF(NPI.LT.NPRNT) GO TO 1200
NPI=0
WRITE(6,46) EX, RE
46 FORMAT('***DIST. ALONG X=', F7.4, '***NEAR WALL RE=', 1P10E11.4)
WRITE(6,40) (Z(J), J=2, NJ)
WRITE(6,41) (U(J), J=2, NJ)
WRITE(6,42) (T(J), J=2, NJ)
WRITE(6,43) (RHO(J), J=2, NJ)
WRITE(6,44) (H(J), J=2, NJ)
40 FORMAT(/, 1X, 'Z', 8X, 1P10E11.4/(10X, 1P10E11.4))
41 FORMAT(/, 1X, 'U', 8X, 1P10E11.4/(10X, 1P10E11.4))

```

```

42 FORMAT(/,1X,'T',8X ,1P10E11.4/(10X,1P10E11.4))
43 FORMAT(/,1X,'RHO',6X ,1P10E11.4/(10X,1P10E11.4))
44 FORMAT(/,1X,'H',8X ,1P10E11.4/(10X,1P10E11.4))
IF (EX.GT.XEND) GO TO 2100

```

C

C\*\* RESETTING DYNAMIC, THERMO, AND GEOM. VARIABLES FOR NEXT ITERATION\*\*\*\*\*

```

1200 ITRN=1
X1=DX1
X2=DX+DX1
SUMX=X1+X2
SUMXX=X1*X1+X2*X2
SUMP=DP+DP1+DP2
SUMXP=X1*DP1+X2*DP
DEN=3.*SUMXX-SUMX*SUMP
DPSLOP=(3.*SUMXP-SUMP*SUMX)/DEN
DPZERO=(SUMP*SUMXX-SUMX*SUMXP)/DEN
DX1=DX
DP2=DP1
DP1=DP
IF (ISTEP.LE.2) GO TO 1205
IF (DX.GE.DXF) XAMP=1.0
DX=DX*XAMP
IF (ISTEP.LT.4) GO TO 1205
DP=DPSLOP*(X2+DX)+DPZERO

```

REPRODUCIBILITY OF THE  
ORIGINAL PAGE IS POOR

```

1205 PSIART=P
DPJAMP=0.5*EXP(-0.115*EX/HEIGHT)
UOLD=U(2)
CALL SIPSIM(0)
CALL XSAREA(0)
ZFAC=FLORAT*U(NJ)/(ULDA-FLORAT*U(NJ)*GASKIN/P)
ADP=ABS(DP1)
ZTLRN=ADP*DPDTL*HEIGHT/ZFAC/ARFAC
UTLRN=ADP*DPDTL*OLDA/FLURAT

```

C

C\*\*\*\*\* EVALUATION OF R.H.S. OF MOM. AND ENERGY EQS. \*\*\*\*\*

```

VF(2)=.5*AS(2)*VISC(2)
HT(2)=VF(2)*PRLINV
DO 1106 J=3,NJ
VF(J)=.5*AS(J)*VISC(J)/DZ(J)
1106 HT(J)=VF(J)*PRLINV
DU(2)=U(3)*(SIP(2)+VF(3))+U(2)*(3.*SIP(2)+ALPHA*SIM(2)-VF(3)-VF(2)
1)
DD(2)=DU(2)-DP*AX(2)
DO 1108 J=3,NJ
UU(J)=U(J+1)*(SIP(J)+VF(J+1))+U(J)*(3.*SIP(J)+3.*SIM(J)-VF(J+1)
1-VF(J))+U(J-1)*(SIM(J)+VF(J))
DD(J)=DU(J)-DP*AX(J)
1108 CONTINUE
DT(2)=H(3)*(SIP(2)+HT(3))+H(2)*(3.*SIP(2)+BETA*SIM(2)-HT(3)-HT(2))
1+USH(3)*(SIP(2)+VF(3))+USH(2)*(3.*SIP(2)+DELTA*SIM(2)-VF(3))+H*WALL
2*HT(2)
DO 1112 J=3,NJ
DT(J)=H(J+1)*(SIP(J)+HT(J+1))+H(J)*(3.*SIP(J)+3.*SIM(J)-HT(J+1)
1-HT(J))+H(J-1)*(SIM(J)+HT(J))+USH(J+1)*(SIP(J)+VF(J+1))+USH(J)*

```

```

      23.*SIP(J)+3.*SIM(J)-VF(J+1)-VF(J)+USH(J-1)*(SIM(J)+VF(J))
1112 CONTINUE
C
C**ITERATIVE CALCULATIONS FOR NEW U , H , Z *****
C**CALCULATIONS OF NEW VELOCITIES*****
      GO TO 95
    90 CONTINUE
      VF(2)=AS(2)*VISC(2)*0.5
      HT(2)=VF(2)*PRLINV
      DO 99 J=3,NJ
        VF(J)=AS(J)*VISC(J)/DZ(J)*0.5
    99 HT(J)=VF(J)*PRLINV
    95 AA(2)=-SIP(2)+VF(3)
      BB(2)=3.*SIP(2)+ALPHA*SIM(2)+VF(3)+VF(2)
      DO 100 J=3,NJ
        AA(J)=-SIP(J)+VF(J+1)
        BB(J)=3.*SIP(J)+3.*SIM(J)+VF(J+1)+VF(J)
        CC(J)=-SIM(J)+VF(J)
    100 CONTINUE
      CALL TDSOLV (AA,BB,CC,DD,UU,0)
      IF (ITRN.GT.1) GO TO 109
      DO 108 J=2,NJ
    108 U(J)=UU(J)
    109 DO 200 J=2,NJ
    200 U(J)=.5*(U(J)+UU(J))
C
C**CALCULATION OF NEW ENTHALPIES*****
      DO 111 J=2,NJ
    111 USH(J)=.5*U(J)*U(J)
      AA(2)=-SIP(2)+HT(3)
      BB(2)=3.*SIP(2)+BETA*SIM(2)+HT(3)+HT(2)
      TT(2)=DT(2)+USH(3)*(-SIP(2)+VF(3))-USH(2)*(3.*SIP(2)+DELTA*SIM(2)
1+VF(3))+HWALL*HT(2)
      DO 115 J=3,NJ
        AA(J)=-SIP(J)+HT(J+1)
        BB(J)=3.*SIP(J)+3.*SIM(J)+HT(J+1)+HT(J)
        CC(J)=-SIM(J)+HT(J)
        TT(J)=DT(J)+USH(J+1)*(-SIP(J)+VF(J+1))-USH(J)*(3.*SIP(J)+3.*SIM(J)
1+VF(J+1)+VF(J))+USH(J-1)*(-SIM(J)+VF(J))
    115 CONTINUE
      CALL TDSOLV(AA,BB,CC,TT,H,0)
C
      P=PSTART+DP
      CALL HPTRHO
      CALL ZDZ
C**CONVERGENCE CHECKS *****
      ZCOR=Z(NJ)-HEIGHT
    80 ITRN=ITRN+1
      UCHEK=ABS(U(2)-UOLD)
      ZCHEK=ABS(ZCOR)
      IF (UCHEK.GT.UTLRN) GO TO 82
      IF (ZCHEK.LT.ZTLRN) GO TO 1100
      IF (ITRN.GT.MAXIT) GO TO 2000
      DPCOR=-ZCOR*ARFAC/Z(NJ)*ZFAC

```

REPRODUCIBILITY OF THE  
ORIGINAL PAGE IS POOR

```
310 DPCOR=DPCOR*DPDAMP
330 DP=DP+DPCOR
    DO 340 J=2,NJ
340 DD(J)=DU(J)-DP*AX(J)
82 CONTINUE
    UOLD=U(2)
    CALL VSCSTY(0)
    GO TO 90
C
2000 WRITE(6,2001)
2001 FORMAT(/,1X,'**VELOCITY-PRESSURE ITERATIONS EXCEEDED THE LIMIT SET
      1 BY MAXIT*****')
2100 WRITE(6,2101)
2101 FORMAT(1H1,9X,'EX',9X,'PRESS',9X,'P-RECV',6X,'WALL SHEAR'
      1,3X,'HEAT FLX',5X,'B-L. THK',5X,'DISP THK',5X,'MOM THK',6X,'SHAPE
      2FAC',/)
      WRITE(6,2105) ( EXVEC(K),PVEC(K),PRVEC(K),SHRVEC(K),
      1HTVEC(K),OLOVEC(K),DL1VEC(K),DL2VEC(K),SFVEC(K), K=1,ISTEP)
2105 FORMAT(1PE16.3,1P8E13.3)
      STOP
      END
```

REPRODUCIBILITY OF THE  
ORIGINAL PAGE IS POOR

5 FORTRAN IV 360N-FO-479 3-8

START

DATE 08/31/79

TIME 15.

```

      SUBROUTINE START
C**SUBROUTINE SETS INITIAL PROFILES AND NORMAL TO THE FLOW GRID*****
      COMMON/COM1/U(50),T(50),H(50),RHO(50),USH(50),Z(50),DZ(50)
      COMMON/COM2/NJ,NJ1,NJ2,NJP,NBL,DX
      COMMON/COM4/UCNTR,TCNTR,TWALL,P,CPINV,RINV,GASK,ZBL
      COMMON/COM8/HEIGHT,WIDTH,HSLOPE,WSLOPE,AVWIDTH,EFWIDTH,OLDA,ARFAC
      COMMON/COM9/VZERO,EXPV,TZERC,EXPU,EXPH
C
      VISKIN=VZERO*(TCNTR/TZERC)**EXPV/(P*RINV/TCNTR)
      FNJ=FLOAT(NJ)
      HCNTR=TCNTR/CPINV
      HWALL=TWALL/CPINV
      DELH=HCNTR-HWALL
      UZZ2=1200.*VISKIN
      U(1)=0.
      Z(1)=0.
      DZ(1)=0.
      H(1)=HWALL
      U(2)=(UCNTR**EXPU*UZZ2/ZBL)**(1./(1.+EXPU))
      Z(2)=UZZ2/U(2)
      DZ(2)=Z(2)-Z(1)
      H(2)=HWALL+DELH*(Z(2)/ZBL)**(1./EXPH)
      EXPG=ALOG(HEIGHT/Z(2)-1.)/ALOG(FNJ/3.)
      DO 20 J=3,NJ
      FJ=FLOAT(J)
      Z(J)=Z(2)+(HEIGHT-Z(2))*(FJ/FNJ)**EXPG
20  DZ(J)=Z(J)-Z(J-1)
      DO 23 J=3,NJ
      U(J)=UCNTR*(Z(J)/ZBL)**(1./EXPU)
      H(J)=HWALL+DELH*(Z(J)/ZBL)**(1./EXPH)
      IF(U(J).GE.UCNTR) GO TO 25
23  CONTINUE
      GO TO 27
25  DO 26 K=J,NJ
      U(K)=UCNTR
26  H(K)=HCNTR
27  CONTINUE
      DZ(NJ+1)=0.
      PRINV=P*RINV
      DO 223 J=2,NJ
      T(J)=H(J)*CPINV
223 RHO(J)=PRINV/T(J)
      T(1)=TWALL
      RHO(1)=P*RINV/T(1)
      DO 31 J=1,NJ
31  USH(J)=U(J)*U(J)*0.5
      RETURN
      END

```



```

      SUBROUTINE VSCSTY(NP)
      COMMON/COM1/U(50),T(50),H(50),RHO(50),USH(50),Z(50),DZ(50)
      COMMON/COM2/NJ,NJ1,NJ2,NJP,NBL,DX
      COMMON/COM6/ALPHA,BETA,DELTA,GAMMA,RE,VISC(50)
      COMMON/COM9/VZERO,EXPV,TZERO,EXPU,EXPH
      DIMENSION EL(50)
      C**MIXING LENGTH, EL, CALCULATIONS*****
      ZOUT=Z(NJ)
      EL(1)=0.
      DO 210 J=2,NJ
      FAC=(1.0-Z(J)/ZOUT)**2
      EL(J)=ZOUT*(0.14-0.08*FAC-0.06*FAC*FAC)
      210 CONTINUE
      C**VISCOSITY (LAMINAR+TURBULENT) CALCULATIONS*****
      VISC(1)=VZERO*(T(1)/TZERO)**EXPV
      VISOLD =VZERO*(T(2)/TZERO)**EXPV
      RE=U(2)*RHO(2)*Z(2)/VISOLD
      DO215 J=3,NJ
      VISNEW =VZERO*(T(J)/TZERO)**EXPV
      VISL=0.5*(VISOLD+VISNEW)
      VISOLD=VISNEW
      ELTS=((EL(J)+EL(J-1))*0.5)**2
      VIST=ELTS*(RHO(J)+RHO(J-1))*0.5
      DUJ=ABS(U(J)-U(J-1))
      VIST=VIST*DUJ/DZ(J)
      VISC(J)=VISL+VIST
      215 CONTINUE
      FF=0.0290106/RE**0.2827065
      VISC(2)=FF*RHO(2)*U(2)
      G=ALOG(RE)
      G2=G*G
      G3=G2*G
      GAMMA=0.6995594-0.1735247*G+0.04343642*G2-0.002524061*G3
      ALPHA=0.8311825-0.2551132*G+0.05791319*G2-0.003226784*G3
      DELTA=0.7987116-0.1194877*G+0.03075327*G2-0.001806241*G3
      BETA=(T(1)+ALPHA*(T(2)-T(1)))/T(2)
      IF (NP.NE.1) GO TO 999
      WRITE (6,102) (EL(J),J=1,NJ)
      WRITE (6,103) (VISC(J),J=1,NJ)
      102 FORMAT(/,' EL ',7X, 10E11.3/(10X,10E11.3))
      103 FORMAT(/,' VISC ',5X, 10E11.3/(10X,10E11.3))
      999 CONTINUE
      RETURN
      END

```

```

      SUBROUTINE TDSOLV(A,B,C,D,X,NP)
      COMMON/COM2/NJ,NJ1,NJ2,NJP,NBL,DX
      DIMENSION A(50),B(50),C(50),D(50),X(50),E(50),F(50)
C   ***** ROUTINE TO SOLVE THE TRIDIAGONAL EQUATIONS *****
      E(2)=A(2)/B(2)
      F(2)=D(2)/B(2)
      DO 500 J=3,NJ1
      DEN=B(J)-C(J)*E(J-1)
      E(J)=A(J)/DEN
500  F(J)=(D(J)+C(J)*F(J-1))/DEN
505  X(NJ1)=(E(NJ1)*D(NJ)+B(NJ)*F(NJ1))/(B(NJ)-E(NJ1)*C(NJ))
      DO 510 I=2,NJ2
      J=NJ-I
510  X(J)=E(J)*X(J+1)+F(J)
      X(NJ)=(D(NJ)+C(NJ)*X(NJ1))/B(NJ)
      IF (NP.NE.1) GO TO 999
      WRITE(6,102) (A(J),J=2,NJ1)
      WRITE(6,103) (B(J),J=2,NJ1)
      WRITE(6,104) (C(J),J=2,NJ1)
      WRITE(6,105) (D(J),J=2,NJ1)
      WRITE(6,106) (E(J),J=2,NJ1)
      WRITE(6,107) (F(J),J=2,NJ1)
102  FORMAT(/,1X,'A',8X ,1P10E11.4/(10X,1P10E11.4))
103  FORMAT(/,1X,'B',8X ,1P10E11.4/(10X,1P10E11.4))
104  FORMAT(/,1X,'C',8X ,1P10E11.4/(10X,1P10E11.4))
105  FORMAT(/,1X,'D',8X ,1P10E11.4/(10X,1P10E11.4))
106  FORMAT(/,1X,'E',8X ,1P10E11.4/(10X,1P10E11.4))
107  FORMAT(/,1X,'F',8X ,1P10E11.4/(10X,1P10E11.4))
999  CONTINUE
      RETURN
      END

```

REPRODUCIBILITY OF THE  
ORIGINAL PAGE IS POOR

```

SUBROUTINE THICK
C*** THIS SUBROUTINE CALCULATES DISP. AND MOM. THICKNESSES *****
COMMON/COM1/U(50),T(50),H(50),RHO(50),USH(50),Z(50),DZ(50)
COMMON/COM2/NJ,NJ1,NJ2,NJP,NBL,DX
COMMON/COM6/ALPHA,BETA,DELTA,GAMMA,RE,VISC(50)
COMMON/COM7/DEL1,DEL2,H12,DELO
COMMON/COM8/HEIGHT,WIDTH,HSLOPE,WSLOPE,AVWIDTH,EFWIDTH,OLDA,ARFAC
DIMENSION RU1(50),RU2(50)
UINV=1./U(NJ)
RUINV=0.5/RHO(NJ)/U(NJ)
DO 20 J=1,NJ
RU1(J)=RHO(J)*U(J)*RUINV
20 RU2(J)=RU1(J)*[1.-U(J)*UINV]
DEL1=(1.-RU1(2)*2.*GAMMA)*DZ(2)
DEL2=RU1(2)*2.*GAMMA*(1.-U(2)*ALPHA*UINV)*DZ(2)
DO 30 J=3,NJ
DEL1=DEL1+(1.-RU1(J)-RU1(J-1))*DZ(J)
30 DEL2=DEL2+(RU2(J)+RU2(J-1))*DZ(J)
H12=DEL1/DEL2
UPBL=0.995*U(NJ)
DO 40 J=2,NJ
IF( U(J).GT.UPBL) GO TO 41
40 CONTINUE
41 DELO=Z(J-1)+DZ(J)*[(UPBL-U(J-1))/(U(J)-U(J-1))]
RETURN
END

```

IS FORTRAN IV 360N-FO-479 3-8

HPTRHO

DATE 08/20/79

TIME 13.

```
SUBROUTINE HPTRHO
COMMON/COM1/U(50),T(50),H(50),RHO(50),USH(50),Z(50),DZ(50)
COMMON/COM2/NJ,NJ1,NJ2,NJP,NBL,DX
COMMON/COM4/UCNTR,TCNTR,TWALL,P,CPINV,RINV,GASK,ZBL
PRINV=P*RINV
DO 223 J=2,NJ
  T(J)=H(J)*CPINV
223 RHO(J)=PRINV/T(J)
RETURN
END
```

### 3.3 Listing of CIRCULAR Geometry Subroutines.

Most of the calculations in these subroutines are carried out in terms of the radial distance  $R(J)$  from the center line. Relations between  $R(J)$  and  $Z(J)$  is given by

$$R(J) = \text{HEIGHT} - Z(J)$$

#### INPUT1 Subroutine:

This subroutine provides data for the duct shape.

HEIGHT = Radius of the duct.  
 HSLOPE = Axial variation of the radius defined as:  
 HEIGHT at  $x + \Delta x$  = HEIGHT at  $x$  + HSLOPE  $\cdot \Delta x$   
 ARFAC = 2. for circular ducts

#### SIPSIM and ZDZ Subroutines:

Given  $U(J)$ ,  $RHO(J)$ , and  $Z(J)$ , subroutine SIPSIM calculates  $SIP(J)$  and  $SIM(J)$ . It is called at the beginning of each integration step. Subroutine ZDZ, called at the end of the integration step, calculates  $Z(J)$  given  $U(J)$ ,  $RHO(J)$ ,  $SIP(J)$ , and  $SIM(J)$ . Fortran statements in these routines are almost direct translations of the formulae given in Appendices A and B of Ref. 7.

#### XSAREA Subroutine:

This subroutine calculates cross-sectional and surface areas of the streams. It also calculates cross-sectional area of the duct called OLDA. This area is used in the pressure iteration formulae.

JS FORTRAN IV 360N-FO-479 3-8

INPUT1

DATE 08/20/79

TIME 13.

```
SUBROUTINE INPUT1
COMMON/COM8/HEIGHT,WIDTH,HSLOPE,WSLOPE,AVWIDH,EFWIDH,OLDA,ARFAC
HEIGHT=
HSLOPE=
ARFAC=2.0
RETURN
END
```

```

SUBROUTINE SIPSIM(NP)
COMMON/COM1/U(50),T(50),H(50),RHO(50),USH(50),Z(50),DZ(50)
COMMON/COM2/NJ,NJ1,NJ2,NJP,NBL,DX
COMMON/COM3/SIP(50),SIM(50),FLORAT
COMMON/COM5/AX(50),AS(50)
COMMON/COM6/ALPHA,BETA,DELTA,GAMMA,RE,VISC(50)
COMMON/COM7/DEL1,DEL2,H12,DELO
COMMON/COM8/HEIGHT,WIDTH,HSLOPE,WSLOPE,AVWIDTH,EFWIDTH,CLDA,ARFAC
DIMENSION R(50),RR(50),RSQ(50),RU(50)
PI=3.141593
PI16TH=PI/16.0
FLORAT=0.0
R(1)=HEIGHT
DO 10 J=2,NJ
RU(J)=RHO(J)*U(J)
R(J)=HEIGHT-Z(J)
RR(J)=R(J)*R(J)
10 RSQ(J)=0.25*(R(J)+R(J-1))**2
C**SI'S, EXCEPT SIM(2), REDUCED BY 4 TO ABSORB 1/4 APPEARING IN SI(J)/4*
DO 30 J=2,NJ1
SIP(J)=PI16TH*(3.*RU(J)+RU(J+1))*(RR(J)-RSQ(J+1))
30 FLORAT=FLORAT+ SIP(J)
SIM(2)=RU(2)*GAMMA*(R(1)+R(2))*PI*(R(1)-R(2))
FLORAT=FLORAT+ SIM(2)*0.25
DO 40 J=3,NJ1
SIM(J)=PI16TH*(3.*RU(J)+RU(J-1))*(RSQ(J)-RR(J))
40 FLORAT=FLORAT+ SIM(J)
SIM(NJ)=PI16TH*(3.*RU(NJ)+RU(NJ1))*RR(NJ1)*0.25
FLORAT=4.0*FLORAT+4.0*SIM(NJ)
IF(NP.NE.1) GO TO 100
WRITE(6,43) ( SIM(J),J=3,NJ)
WRITE(6,44) ( SIP(J),J=2,NJ1)
43 FORMAT(/,' SIM',6X ,10E11.3/(10X,10E11.3))
44 FORMAT(/,' SIP',6X ,10E11.3/(10X,10E11.3))
WRITE(6,53) FLORAT
53 FORMAT (/,10X,'FLOW RATE= ', E11.4)
100 RETURN
END

```

```

SUBROUTINE ZDZ
COMMON/COM1/U(50),T(50),H(50),RHO(50),USH(50),Z(50),DZ(50)
COMMON/COM2/NJ,NJ1,NJ2,NJP,NBL,DX
COMMON/COM3/SIP(50),SIM(50),FLORAT
COMMON/COM6/ALPHA,BETA,DELTA,GAMMA,RE,VISC(50)
COMMON/COM8/HEIGHT,WIDTH,HSLOPE,WSLOPE,AVWIDTH,EFWIDTH,OLDA,ARFAC
DIMENSION R(50),RU(50)
R(NJ)=0.
PI=3.141593
DO 10 J=2,NJ
10 RU(J)=RHO(J)*U(J)
R(NJ1)=(32.*(SIP(NJ1)+SIM(NJ1))/PI/(5.*RU(NJ1)+3.*RU(NJ)))*0.5
DO 20 N=4,NJ
J=NJ+3-N
R(J-1)=(16.*SIP(J-1)/PI/(3.*RU(J-1)+RU(J))+16.*SIM(J)/PI/(3.*RU(J)
1+RU(J-1))+R(J)*R(J))*0.5
20 CONTINUE
R(1)=(SIM(2)/(RU(2)*GAMMA*PI)+R(2)*R(2))*0.5
DO 40 J=2,NJ
Z(J)=R(1)-R(J)
40 DZ(J)=Z(J)-Z(J-1)
RETURN
END

```



```

SUBROUTINE XSAREA(NP)
COMMON/COM1/U(50),T(50),H(50),RHO(50),USH(50),Z(50),DZ(50)
COMMON/COM2/NJ,NJ1,NJ2,NJP,NBL,DX
COMMON/COM5/AX(50),AS(50)
COMMON/COM8/HEIGHT,WIDTH,HSLOPE,WSLOPE,AVWIDTH,CFWIDTH,OLDA,APFAC
DIMENSION R(50),RSQ(50)
PI=3.141593
PIDX=PI*DX
R(1)=HEIGHT
DO 10 J=2,NJ
R(J)=HEIGHT-Z(J)
10 RSQ(J)=0.25*(R(J)+R(J-1))**2
AX(2)=PI* R(2)*(2.*R(1)-R(3)-R(2))
AS(2)=PIDX*R(1)*2.
DO 20 J=3,NJ1
AX(J)=PI*(RSQ(J)-RSQ(J-1))
20 AS(J)=PIDX*(R(J)+R(J-1))
AX(NJ)=PI*RSQ(NJ)
AS(NJ)=PIDX*(R(NJ)+R(NJ1))
OLDA=PI*HEIGHT*HEIGHT
HEIGHT=HEIGHT+HSLOPE*DX
IF(NP.NE.1)GO TO 100
WRITE (6,30) (AX(J),J=2,NJ)
30 FORMAT (/,' AX',7X,10E11.3/(10X,10E11.3))
WRITE(6,40) (AS(J),J=2,NJ)
40 FORMAT(/,' AS',7X,10E11.3/(10X,10E11.3))
100 RETURN
END

```

### 3.4 Sample Computations--Entry Region Pipe Flow

DATA: (SI Units)

MAIN program:

```
C**DYNAMIC AND THERMODYNAMIC DATA*****
      UCNTR=15.0
      ZBL=0.01
      TCNTR=400.0
      TWALL=300.0
      P=70927.5
      CP=1003.5
      GASK=1.4
      GASR=287.0
      PRNDL=0.7
      DPDX=-5000.0
C**GEOMETRIC DUCT DATA*****
      CALL INPUT1
      XEND=10.0
C**CONVERGENCE CRITERIA,GRID SIZE,AND OTHER DATA*****
      DPDTL=0.01
      DXFAC=5.0
      MAXIT=50
      NJ=21
      NPRNT=10
C**DATA FOR VSCSTY AND START SUBROUTINES*****
      VZERO=0.0000386
      TZERO=860.0
      EXPV=.7
      EXPU=7.
      EXPH=7.
C
```

INPUT1 Subroutine:

```
HEIGHT=0.5
HSLOPE=0.0
```

JOB STATISTICS:

Machine: IBM 360/44 with DOS operating system.  
Cards Read: 500  
Core Required: 44K  
Compilation Time: 3.19 mns  
CPU Time: 2.11 mns

\*\*DIST. ALONG X= 0.0 \*\*\*\*NEAR WALL RE=1.2763E 03

Z	3.4106E-03	6.8213E-03	1.0533E-02	1.6020E-02	2.3519E-02	3.3246E-02	4.5403E-02	6.0179E-02	7.7751E-02	9.3291E-02
U	1.2843E 01	1.4202E 01	1.5000E 01	1.5000E 01	1.5000E 01	1.5000E 01	1.5000E 01	1.5000E 01	1.5000E 01	1.5000E 01
T	3.8576E 02	3.9468E 02	4.0000E 02	4.0000E 02	4.0000E 02	4.0000E 02	4.0000E 02	4.0000E 02	4.0000E 02	4.0000E 02
RHO	6.4065E-01	6.2616E-01	6.1784E-01	6.1784E-01	6.1784E-01	6.1784E-01	6.1784E-01	6.1784E-01	6.1784E-01	6.1784E-01
H	3.8711E 05	3.9606E 05	4.0140E 05	4.0140E 05	4.0140E 05	4.0140E 05	4.0140E 05	4.0140E 05	4.0140E 05	4.0140E 05

\*\*DIST. ALONG X= 0.2000\*\*\*\*NEAR WALL RE=1.2875E 03

Z	3.2813E-03	6.5789E-03	1.0195E-02	1.5497E-02	2.2629E-02	3.1838E-02	4.3335E-02	5.7283E-02	7.3833E-02	9.3117E-02
U	1.3183E 01	1.4396E 01	1.5080E 01	1.5582E 01	1.5806E 01	1.5804E 01	1.5804E 01	1.5804E 01	1.5804E 01	1.5804E 01
T	3.8057E 02	3.8851E 02	3.9329E 02	3.9728E 02	3.9986E 02	4.0000E 02	3.9998E 02	3.9998E 02	3.9998E 02	3.9998E 02
RHO	6.4930E-01	6.3604E-01	6.2833E-01	6.2200E-01	6.1799E-01	6.1777E-01	6.1780E-01	6.1779E-01	6.1780E-01	6.1779E-01
H	3.8190E 05	3.8987E 05	3.9467E 05	3.9867E 05	4.0126E 05	4.0140E 05	4.0138E 05	4.0138E 05	4.0138E 05	4.0138E 05

\*\*DIST. ALONG X= 1.2000\*\*\*\*NEAR WALL RE=1.3101E 03

Z	3.5501E-03	7.1089E-03	1.0980E-02	1.6594E-02	2.4024E-02	3.3427E-02	4.4973E-02	5.8850E-02	7.5264E-02	9.4390E-02
U	1.1853E 01	1.3039E 01	1.3783E 01	1.4462E 01	1.5025E 01	1.5464E 01	1.5778E 01	1.5959E 01	1.5991E 01	1.5987E 01
T	3.7063E 02	3.7790E 02	3.8258E 02	3.8700E 02	3.9090E 02	3.9425E 02	3.9704E 02	3.9920E 02	4.0007E 02	3.9996E 02
RHO	6.6670E-01	6.5388E-01	6.4588E-01	6.3849E-01	6.3212E-01	6.2676E-01	6.2235E-01	6.1899E-01	6.1764E-01	6.1781E-01
H	3.7193E 05	3.7922E 05	3.8392E 05	3.8836E 05	3.9227E 05	3.9563E 05	3.9843E 05	4.0059E 05	4.0147E 05	4.0136E 05

\*\*DIST. ALONG X= 2.2000\*\*\*\*NEAR WALL RE=1.3194E 03

Z	3.6739E-03	7.3555E-03	1.1354E-02	1.7139E-02	2.4775E-02	3.4402E-02	4.6162E-02	6.0205E-02	7.6683E-02	9.5764E-02
U	1.1331E 01	1.2481E 01	1.3214E 01	1.3900E 01	1.4495E 01	1.4996E 01	1.5407E 01	1.5727E 01	1.5955E 01	1.6085E 01

REPRODUCIBILITY OF THE  
ORIGINAL PAGE IS POOR

T 3.6676E 02 3.7367E 02 3.7816E 02 3.8245E 02 3.8631E 02 3.8975E 02 3.9277E 02 3.9540E 02 3.9764E 02 3.9941E 02  
4.0005E 02 3.9996E 02 3.9997E 02 3.9997E 02 3.9997E 02 3.9997E 02 3.9996E 02 3.9995E 02 3.9996E 02 3.9999E 02

RHO 6.7373E-01 6.6126E-01 6.5342E-01 6.4609E-01 6.3962E-01 6.3399E-01 6.2911E-01 6.2492E-01 6.2140E-01 6.1866E-01  
6.1766E-01 6.1781E-01 6.1778E-01 6.1779E-01 6.1779E-01 6.1779E-01 6.1779E-01 6.1779E-01 6.1779E-01 6.1776E-01

H 3.6804E 05 3.7498E 05 3.7948E 05 3.8379E 05 3.8767E 05 3.9111E 05 3.9415E 05 3.9679E 05 3.9903E 05 4.0080E 05  
4.0145E 05 4.0136E 05 4.0137E 05 4.0137E 05 4.0137E 05 4.0137E 05 4.0136E 05 4.0135E 05 4.0136E 05 4.0139E 05

\*\*DIST. ALONG X= 3.2000\*\*\*NEAR WALL RE=1.3253E 03

Z 3.7517E-03 7.5114E-03 1.1591E-02 1.7489E-02 2.5263E-02 3.5049E-02 4.6982E-02 6.1193E-02 7.7813E-02 9.6977E-02  
1.1882E-01 1.4349E-01 1.7106E-01 2.0152E-01 2.3468E-01 2.7015E-01 3.0699E-01 3.4392E-01 3.7300E-01 5.0000E-01

U 1.1020E 01 1.2144E 01 1.2866E 01 1.3547E 01 1.4148E 01 1.4669E 01 1.5113E 01 1.5484E 01 1.5783E 01 1.6008E 01  
1.6153E 01 1.6206E 01 1.6201E 01 1.6202E 01 1.6202E 01 1.6202E 01 1.6202E 01 1.6202E 01 1.6201E 01 1.6202E 01

T 3.6431E 02 3.7099E 02 3.7533E 02 3.7951E 02 3.8329E 02 3.8670E 02 3.8975E 02 3.9249E 02 3.9493E 02 3.9706E 02  
3.9879E 02 4.0001E 02 3.9996E 02 3.9996E 02 3.9996E 02 3.9996E 02 3.9996E 02 3.9994E 02 3.9995E 02 3.9999E 02

RHO 6.7824E-01 6.6603E-01 6.5833E-01 6.5108E-01 6.4465E-01 6.3898E-01 6.3397E-01 6.2954E-01 6.2565E-01 6.2230E-01  
6.1960E-01 6.1771E-01 6.1779E-01 6.1778E-01 6.1779E-01 6.1779E-01 6.1780E-01 6.1782E-01 6.1780E-01 6.1775E-01

H 3.6559E 05 3.7229E 05 3.7664E 05 3.8084E 05 3.8463E 05 3.8805E 05 3.9112E 05 3.9387E 05 3.9632E 05 3.9845E 05  
4.0018E 05 4.0141E 05 4.0136E 05 4.0136E 05 4.0136E 05 4.0136E 05 4.0136E 05 4.0134E 05 4.0135E 05 4.0139E 05

\*\*DIST. ALONG X= 4.2000\*\*\*NEAR WALL RE=1.3297E 03

Z 3.8068E-03 7.6219E-03 1.1760E-02 1.7738E-02 2.5614E-02 3.5519E-02 4.7585E-02 6.1935E-02 7.8650E-02 9.7966E-02  
1.1988E-01 1.4453E-01 1.7203E-01 2.0239E-01 2.3546E-01 2.7082E-01 3.0756E-01 3.4347E-01 3.7337E-01 5.0000E-01

U 1.0805E 01 1.1910E 01 1.2622E 01 1.3298E 01 1.3899E 01 1.4427E 01 1.4886E 01 1.5281E 01 1.5615E 01 1.5889E 01  
1.6098E 01 1.6239E 01 1.6301E 01 1.6297E 01 1.6297E 01 1.6297E 01 1.6297E 01 1.6297E 01 1.6297E 01 1.6297E 01

T 3.6250E 02 3.6900E 02 3.7323E 02 3.7731E 02 3.8102E 02 3.8438E 02 3.8742E 02 3.9018E 02 3.9269E 02 3.9495E 02  
3.9696E 02 3.9863E 02 3.9993E 02 3.9996E 02 3.9995E 02 3.9995E 02 3.9995E 02 3.9993E 02 3.9995E 02 3.9998E 02

RHO 6.8161E-01 6.6962E-01 6.6203E-01 6.5487E-01 6.4849E-01 6.4282E-01 6.3778E-01 6.3327E-01 6.2922E-01 6.2561E-01  
6.2245E-01 6.1984E-01 6.1782E-01 6.1777E-01 6.1779E-01 6.1779E-01 6.1780E-01 6.1783E-01 6.1780E-01 6.1774E-01

H 3.6377E 05 3.7029E 05 3.7453E 05 3.7863E 05 3.8235E 05 3.8572E 05 3.8877E 05 3.9154E 05 3.9406E 05 3.9633E 05  
3.9834E 05 4.0003E 05 4.0133E 05 4.0136E 05 4.0135E 05 4.0135E 05 4.0135E 05 4.0135E 05 4.0135E 05 4.0138E 05

\*\*DIST. ALONG X= 5.2000\*\*\*NEAR WALL RE=1.3334E 03

Z 3.8491E-03 7.7072E-03 1.1890E-02 1.7930E-02 2.5884E-02 3.5883E-02 4.8054E-02 6.2519E-02 7.9389E-02 9.8774E-02  
1.2077E-01 1.4547E-01 1.7295E-01 2.0322E-01 2.3619E-01 2.7146E-01 3.0809E-01 3.4391E-01 3.7372E-01 5.0000E-01

U 1.0643E 01 1.1734E 01 1.2437E 01 1.3108E 01 1.3707E 01 1.4238E 01 1.4705E 01 1.5113E 01 1.5468E 01 1.5770E 01  
1.6018E 01 1.6209E 01 1.6337E 01 1.6392E 01 1.6388E 01 1.6389E 01 1.6389E 01 1.6389E 01 1.6388E 01 1.6388E 01

T 3.6105E 02 3.6740E 02 3.7154E 02 3.7553E 02 3.7918E 02 3.8249E 02 3.8550E 02 3.8826E 02 3.9079E 02 3.9311E 02  
3.9523E 02 3.9712E 02 3.9871E 02 3.9995E 02 3.9995E 02 3.9995E 02 3.9994E 02 3.9992E 02 3.9994E 02 3.9998E 02

RHO 6.8435E-01 6.7252E-01 6.6503E-01 6.5795E-01 6.5162E-01 6.4599E-01 6.4094E-01 6.3639E-01 6.3227E-01 6.2853E-01  
6.2516E-01 6.2218E-01 6.1970E-01 6.1779E-01 6.1778E-01 6.1779E-01 6.1780E-01 6.1783E-01 6.1780E-01 6.1773E-01

H 3.6231E 05 3.6868E 05 3.7284E 05 3.7685E 05 3.8051E 05 3.8383E 05 3.8685E 05 3.8961E 05 3.9215E 05 3.9449E 05  
3.9661E 05 3.9851E 05 4.0011E 05 4.0135E 05 4.0135E 05 4.0135E 05 4.0135E 05 4.0134E 05 4.0132E 05 4.0134E 05

\*\*DIST. ALONG X= 6.2000\*\*\*NEAR WALL RE=1.3366E 03

Z	3.8830E-03	7.7748E-03	1.1993E-02	1.8083E-02	2.6099E-02	3.6173E-02	4.8431E-02	6.2989E-02	7.9959E-02	7.9440E-02
	1.2152E-01	1.4629E-01	1.7379E-01	2.0402E-01	2.3690E-01	2.7207E-01	3.0860E-01	3.4433E-01	3.7405E-01	5.0000E-01
U	1.0514E 01	1.1594E 01	1.2291E 01	1.2956E 01	1.3553E 01	1.4084E 01	1.4555E 01	1.4972E 01	1.5340E 01	1.5660E 01
	1.5933E 01	1.6158E 01	1.6329E 01	1.6441E 01	1.6480E 01	1.6476E 01	1.6476E 01	1.6476E 01	1.6476E 01	1.6476E 01
T	3.5982E 02	3.6605E 02	3.7011E 02	3.7403E 02	3.7762E 02	3.8088E 02	3.8386E 02	3.8660E 02	3.8914E 02	3.9148E 02
	3.9366E 02	3.9566E 02	3.9745E 02	3.9895E 02	4.0000E 02	3.9993E 02	3.9793E 02	3.9991E 02	3.9993E 02	3.9998E 02
RHO	6.8667E-01	6.7499E-01	6.6758E-01	6.6058E-01	6.5430E-01	6.4870E-01	6.4366E-01	6.3910E-01	6.3494E-01	6.3113E-01
	6.2765E-01	6.2448E-01	6.2165E-01	6.1932E-01	6.1770E-01	6.1780E-01	6.1780E-01	6.1784E-01	6.1784E-01	6.1772E-01
H	3.6108E 05	3.6733E 05	3.7140E 05	3.7534E 05	3.7894E 05	3.8222E 05	3.8521E 05	3.8796E 05	3.9050E 05	3.9285E 05
	3.9504E 05	3.9704E 05	3.9884E 05	4.0034E 05	4.0140E 05	4.0133E 05	4.0133E 05	4.0131E 05	4.0133E 05	4.0138E 05

\*\*DIST. ALONG X= 7.2000\*\*\*NEAR WALL RE=1.3393E 03

Z	3.9104E-03	7.8297E-03	1.2077E-02	1.8207E-02	2.6275E-02	3.6410E-02	4.8739E-02	6.3377E-02	8.0430E-02	9.9997E-02
	1.2216E-01	1.4699E-01	1.7453E-01	2.0477E-01	2.3758E-01	2.7265E-01	3.0909E-01	3.4472E-01	3.7438E-01	5.0000E-01
U	1.0410E 01	1.1479E 01	1.2170E 01	1.2831E 01	1.3426E 01	1.3956E 01	1.4430E 01	1.4852E 01	1.5228E 01	1.5561E 01
	1.5852E 01	1.6099E 01	1.6301E 01	1.6451E 01	1.6544E 01	1.6564E 01	1.6561E 01	1.6561E 01	1.6561E 01	1.6561E 01
T	3.5876E 02	3.6487E 02	3.6887E 02	3.7273E 02	3.7626E 02	3.7948E 02	3.8242E 02	3.8514E 02	3.8767E 02	3.9003E 02
	3.9223E 02	3.9428E 02	3.9617E 02	3.9787E 02	3.9928E 02	4.0002E 02	3.9991E 02	3.9990E 02	3.9992E 02	3.9998E 02
RHO	6.8869E-01	6.7715E-01	6.6982E-01	6.6208E-01	6.5666E-01	6.5109E-01	6.4607E-01	6.4151E-01	6.3733E-01	6.3348E-01
	6.2992E-01	6.2665E-01	6.2366E-01	6.2099E-01	6.1880E-01	6.1765E-01	6.1782E-01	6.1784E-01	6.1780E-01	6.1771E-01
H	3.6001E 05	3.6615E 05	3.7016E 05	3.7403E 05	3.7757E 05	3.8080E 05	3.8376E 05	3.8649E 05	3.8903E 05	3.9119E 05
	3.9360E 05	3.9566E 05	3.9756E 05	3.9926E 05	4.0068E 05	4.0142E 05	4.0131E 05	4.0130E 05	4.0132E 05	4.0138E 05

\*\*DIST. ALONG X= 8.2000\*\*\*NEAR WALL RE=1.3415E 03

Z	3.9331E-03	7.8755E-03	1.2147E-02	1.8312E-02	2.6423E-02	3.6610E-02	4.8999E-02	6.3704E-02	8.0830E-02	1.0047E-01
	1.2271E-01	1.4760E-01	1.7519E-01	2.0544E-01	2.3823E-01	2.7323E-01	3.0957E-01	3.4511E-01	3.7469E-01	5.0000E-01
U	1.0320E 01	1.1381E 01	1.2067E 01	1.2724E 01	1.3316E 01	1.3847E 01	1.4321E 01	1.4747E 01	1.5129E 01	1.5471E 01
	1.5775E 01	1.6039E 01	1.6263E 01	1.6442E 01	1.6570E 01	1.6640E 01	1.6645E 01	1.6643E 01	1.6643E 01	1.6643E 01
T	3.5781E 02	3.6383E 02	3.6776E 02	3.7156E 02	3.7504E 02	3.7822E 02	3.8113E 02	3.8383E 02	3.8634E 02	3.8870E 02
	3.9091E 02	3.9300E 02	3.9495E 02	3.9674E 02	3.9833E 02	3.9964E 02	3.9997E 02	3.9988E 02	3.9992E 02	3.9998E 02
RHO	6.9051E-01	6.7908E-01	6.7183E-01	6.6495E-01	6.5878E-01	6.5324E-01	6.4825E-01	6.4369E-01	6.3951E-01	6.3563E-01
	6.3203E-01	6.2868E-01	6.2557E-01	6.2275E-01	6.2027E-01	6.1823E-01	6.1772E-01	6.1786E-01	6.1780E-01	6.1770E-01
H	3.5906E 05	3.6510E 05	3.6905E 05	3.7286E 05	3.7635E 05	3.7954E 05	3.8247E 05	3.8517E 05	3.8769E 05	3.9006E 05
	3.9228E 05	3.9437E 05	3.9633E 05	3.9813E 05	3.9972E 05	4.0104E 05	4.0137E 05	4.0128E 05	4.0132E 05	4.0138E 05

\*\*DIST. ALONG X= 9.2000\*\*\*NEAR WALL RE=1.3438E 03

Z	3.9528E-03	7.9147E-03	1.2207E-02	1.8401E-02	2.6548E-02	3.6780E-02	4.9221E-02	6.3994E-02	8.1172E-02	1.0088E-01
	1.2318E-01	1.4813E-01	1.7577E-01	2.0605E-01	2.3884E-01	2.7378E-01	3.1003E-01	3.4549E-01	3.7499E-01	5.0000E-01
U	1.0244E 01	1.1298E 01	1.1979E 01	1.2633E 01	1.3222E 01	1.3751E 01	1.4227E 01	1.4655E 01	1.5042E 01	1.5390E 01
	1.5703E 01	1.5981E 01	1.6221E 01	1.6422E 01	1.6578E 01	1.6683E 01	1.6727E 01	1.6723E 01	1.6723E 01	1.6724E 01
T	3.5695E 02	3.6288E 02	3.6675E 02	3.7050E 02	3.7394E 02	3.7707E 02	3.7996E 02	3.8263E 02	3.8513E 02	3.8747E 02
	3.8969E 02	3.9180E 02	3.9379E 02	3.9565E 02	3.9734E 02	3.9879E 02	3.9989E 02	3.9988E 02	3.9991E 02	3.9998E 02

REPRODUCIBILITY OF THE  
ORIGINAL PAGE IS POOR

RHO 6.9215E-01 6.8084E-01 6.7365E-01 6.6684E-01 6.6071E-01 6.5521E-01 6.5024E-01 6.4570E-01 6.4152E-01 6.3763E-01  
 6.3400E-01 6.3059E-01 6.2741E-01 6.2446E-01 6.2179E-01 6.1954E-01 6.1782E-01 6.1784E-01 6.1781E-01 6.1769E-01  
  
 H 3.5820E 05 3.6415E 05 3.6804E 05 3.7180E 05 3.7525E 05 3.7839E 05 3.8129E 05 3.8397E 05 3.8647E 05 3.8893E 05  
 3.9106E 05 3.9317E 05 3.9516E 05 3.9703E 05 3.9873E 05 4.0019E 05 4.0129E 05 4.0129E 05 4.0131E 05 4.0138E 05  
  
 \*\*DIST. ALONG X=10.1999\*\*\*NEAR WALL RE=1.3458E C3  
  
 Z 3.9696E-03 7.9487E-03 1.2259E-02 1.8478E-02 2.6657E-02 3.6926E-02 4.9411E-02 6.4224E-02 9.1467E-02 1.0123E-01  
 1.2359E-01 1.4859E-01 1.7628E-01 2.0659E-01 2.3939E-01 2.7431E-01 3.1049E-01 3.4585E-01 3.7529E-01 5.0000E-01  
  
 U 1.0178E 01 1.1225E 01 1.1903E 01 1.2553E 01 1.3140E 01 1.3668E 01 1.4143E 01 1.4573E 01 1.4963E 01 1.5317E 01  
 1.5637E 01 1.5925E 01 1.6178E 01 1.6396E 01 1.6575E 01 1.6707E 01 1.6786E 01 1.6806E 01 1.6802E 01 1.6803E 01  
  
 T 3.5616E 02 3.6201E 02 3.6583E 02 3.6953E 02 3.7292E 02 3.7602E 02 3.7887E 02 3.8152E 02 3.8400E 02 3.8634E 02  
 3.8855E 02 3.9067E 02 3.9268E 02 3.9458E 02 3.9635E 02 3.9795E 02 3.9925E 02 3.9995E 02 3.9989E 02 3.9993E 02  
  
 RHO 6.9367E-01 6.8246E-01 6.7534E-01 6.6858E-01 6.6250E-01 6.5704E-01 6.5209E-01 6.4757E-01 6.4339E-01 6.3949E-01  
 6.3584E-01 6.3241E-01 6.2917E-01 6.2614E-01 6.2334E-01 6.2084E-01 6.1882E-01 6.1773E-01 6.1782E-01 6.1768E-01  
  
 H 3.5741E 05 3.6328E 05 3.6711E 05 3.7082E 05 3.7423E 05 3.7734E 05 3.8020E 05 3.8286E 05 3.8534E 05 3.8769E 05  
 3.8991E 05 3.9203E 05 3.9405E 05 3.9596E 05 3.9773E 05 3.9934E 05 4.0064E 05 4.0135E 05 4.0129E 05 4.0138E 05

EX	PRESS	P-RECV	WALL SHEAR (Pa)	HEAT FLX (W/m <sup>2</sup> )	B.L. THK	DISP THK	MQM THK	SHAPE FAC
0.0	7.093E 04	0.0	4.072E-01	3.892E 03	1.018E-02	1.448E-03	1.141E-03	1.269E 00
3.906E-04	7.093E 04	-2.432E-02	4.255E-01	3.978E 03	1.002E-02	1.340E-03	1.100E-03	1.254E 00
7.812E-04	7.092E 04	-4.505E-02	4.407E-01	4.048E 03	9.893E-03	1.331E-03	1.072E-03	1.242E 00
1.562E-03	7.092E 04	-6.126E-02	4.526E-01	4.100E 03	9.819E-03	1.295E-03	1.051E-03	1.232E 00
3.125E-03	7.092E 04	-7.387E-02	4.612E-01	4.136E 03	9.708E-03	1.270E-03	1.039E-03	1.223E 00
6.250E-03	7.092E 04	-8.378E-02	4.668E-01	4.156E 03	9.888E-03	1.255E-03	1.032E-03	1.216E 00
1.250E-02	7.092E 04	-9.189E-02	4.692E-01	4.157E 03	1.132E-02	1.255E-03	1.040E-03	1.208E 00
2.500E-02	7.092E 04	-9.820E-02	4.682E-01	4.138E 03	1.266E-02	1.276E-03	1.069E-03	1.194E 00
5.000E-02	7.092E 04	-1.036E-01	4.628E-01	4.087E 03	1.360E-02	1.333E-03	1.138E-03	1.172E 00
1.000E-01	7.092E 04	-1.081E-01	4.515E-01	3.978E 03	1.493E-02	1.454E-03	1.280E-03	1.135E 00
2.000E-01	7.092E 04	-1.135E-01	4.324E-01	3.788E 03	2.005E-02	1.693E-03	1.563E-03	1.083E 00
3.000E-01	7.092E 04	-1.180E-01	4.183E-01	3.647E 03	2.250E-02	1.919E-03	1.834E-03	1.046E 00
4.000E-01	7.092E 04	-1.216E-01	4.069E-01	3.534E 03	2.789E-02	2.139E-03	2.099E-03	1.019E 00
5.000E-01	7.092E 04	-1.252E-01	3.974E-01	3.441E 03	3.464E-02	2.352E-03	2.355E-03	9.995E-01
6.000E-01	7.092E 04	-1.279E-01	3.894E-01	3.362E 03	3.407E-02	2.560E-03	2.607E-03	9.819E-01
7.000E-01	7.092E 04	-1.306E-01	3.824E-01	3.294E 03	3.866E-02	2.763E-03	2.854E-03	9.681E-01
8.000E-01	7.092E 04	-1.333E-01	3.762E-01	3.234E 03	4.145E-02	2.963E-03	3.098E-03	9.564E-01
9.000E-01	7.092E 04	-1.360E-01	3.707E-01	3.181E 03	4.387E-02	3.159E-03	3.337E-03	9.465E-01
1.000E 00	7.092E 04	-1.387E-01	3.658E-01	3.134E 03	4.854E-02	3.352E-03	3.574E-03	9.379E-01
1.100E 00	7.092E 04	-1.414E-01	3.613E-01	3.090E 03	5.213E-02	3.542E-03	3.808E-03	9.303E-01
1.200E 00	7.092E 04	-1.432E-01	3.572E-01	3.051E 03	5.489E-02	3.730E-03	4.039E-03	9.237E-01
1.300E 00	7.092E 04	-1.450E-01	3.534E-01	3.015E 03	5.735E-02	3.916E-03	4.268E-03	9.177E-01
1.400E 00	7.092E 04	-1.468E-01	3.499E-01	2.981E 03	6.045E-02	4.101E-03	4.494E-03	9.124E-01
1.500E 00	7.092E 04	-1.486E-01	3.467E-01	2.950E 03	6.408E-02	4.283E-03	4.720E-03	9.075E-01
1.600E 00	7.092E 04	-1.505E-01	3.437E-01	2.922E 03	6.808E-02	4.463E-03	4.943E-03	9.030E-01
1.700E 00	7.092E 04	-1.523E-01	3.409E-01	2.894E 03	7.079E-02	4.642E-03	5.164E-03	8.990E-01
1.800E 00	7.092E 04	-1.541E-01	3.383E-01	2.869E 03	7.328E-02	4.820E-03	5.384E-03	8.952E-01
1.900E 00	7.092E 04	-1.559E-01	3.358E-01	2.845E 03	7.557E-02	4.995E-03	5.602E-03	8.917E-01
2.000E 00	7.092E 04	-1.577E-01	3.335E-01	2.822E 03	7.945E-02	5.169E-03	5.818E-03	8.884E-01
2.100E 00	7.092E 04	-1.595E-01	3.313E-01	2.801E 03	8.318E-02	5.342E-03	6.034E-03	8.854E-01
2.200E 00	7.092E 04	-1.613E-01	3.292E-01	2.780E 03	8.623E-02	5.514E-03	6.248E-03	8.825E-01
2.300E 00	7.092E 04	-1.631E-01	3.272E-01	2.761E 03	8.894E-02	5.684E-03	6.461E-03	8.799E-01
2.400E 00	7.092E 04	-1.649E-01	3.253E-01	2.742E 03	9.143E-02	5.854E-03	6.672E-03	8.774E-01
2.500E 00	7.092E 04	-1.667E-01	3.235E-01	2.725E 03	9.376E-02	6.023E-03	6.883E-03	8.750E-01
2.600E 00	7.092E 04	-1.685E-01	3.218E-01	2.708E 03	9.592E-02	6.189E-03	7.092E-03	8.727E-01
2.700E 00	7.092E 04	-1.703E-01	3.202E-01	2.692E 03	9.982E-02	6.356E-03	7.301E-03	8.706E-01
2.800E 00	7.092E 04	-1.721E-01	3.187E-01	2.676E 03	1.033E-01	6.521E-03	7.508E-03	8.685E-01
2.900E 00	7.092E 04	-1.739E-01	3.172E-01	2.661E 03	1.063E-01	6.684E-03	7.714E-03	8.665E-01
3.000E 00	7.092E 04	-1.757E-01	3.157E-01	2.646E 03	1.090E-01	6.848E-03	7.920E-03	8.646E-01
3.100E 00	7.092E 04	-1.775E-01	3.143E-01	2.632E 03	1.116E-01	7.011E-03	8.125E-03	8.629E-01
3.200E 00	7.092E 04	-1.793E-01	3.130E-01	2.619E 03	1.140E-01	7.172E-03	8.329E-03	8.611E-01
3.300E 00	7.091E 04	-1.811E-01	3.118E-01	2.606E 03	1.162E-01	7.334E-03	8.533E-03	8.595E-01
3.400E 00	7.091E 04	-1.829E-01	3.105E-01	2.593E 03	1.183E-01	7.494E-03	8.735E-03	8.579E-01
3.500E 00	7.091E 04	-1.847E-01	3.094E-01	2.581E 03	1.215E-01	7.654E-03	8.937E-03	8.565E-01
3.600E 00	7.091E 04	-1.865E-01	3.082E-01	2.570E 03	1.250E-01	7.813E-03	9.139E-03	8.550E-01
3.700E 00	7.091E 04	-1.883E-01	3.071E-01	2.558E 03	1.281E-01	7.971E-03	9.339E-03	8.535E-01
3.800E 00	7.091E 04	-1.901E-01	3.061E-01	2.547E 03	1.309E-01	8.129E-03	9.539E-03	8.522E-01
3.900E 00	7.091E 04	-1.919E-01	3.050E-01	2.536E 03	1.335E-01	8.287E-03	9.739E-03	8.509E-01
4.000E 00	7.091E 04	-1.937E-01	3.040E-01	2.526E 03	1.360E-01	8.443E-03	9.938E-03	8.496E-01
4.100E 00	7.091E 04	-1.955E-01	3.031E-01	2.516E 03	1.383E-01	8.599E-03	1.014E-02	8.484E-01
4.200E 00	7.091E 04	-1.973E-01	3.021E-01	2.506E 03	1.405E-01	8.755E-03	1.033E-02	8.472E-01
4.300E 00	7.091E 04	-1.991E-01	3.012E-01	2.496E 03	1.425E-01	8.910E-03	1.053E-02	8.460E-01
4.400E 00	7.091E 04	-2.009E-01	3.003E-01	2.486E 03	1.445E-01	9.064E-03	1.073E-02	8.449E-01
4.500E 00	7.091E 04	-2.027E-01	2.995E-01	2.477E 03	1.479E-01	9.218E-03	1.092E-02	8.438E-01
4.600E 00	7.091E 04	-2.045E-01	2.987E-01	2.468E 03	1.512E-01	9.372E-03	1.112E-02	8.428E-01
4.700E 00	7.091E 04	-2.063E-01	2.978E-01	2.459E 03	1.541E-01	9.525E-03	1.132E-02	8.417E-01
4.800E 00	7.091E 04	-2.081E-01	2.971E-01	2.451E 03	1.568E-01	9.677E-03	1.151E-02	8.407E-01
4.900E 00	7.091E 04	-2.099E-01	2.963E-01	2.442E 03	1.594E-01	9.829E-03	1.170E-02	8.397E-01
5.000E 00	7.091E 04	-2.117E-01	2.955E-01	2.434E 03	1.618E-01	9.981E-03	1.190E-02	8.388E-01
5.100E 00	7.091E 04	-2.135E-01	2.948E-01	2.426E 03	1.641E-01	1.013E-02	1.209E-02	8.379E-01

REPRODUCIBILITY OF THE  
ORIGINAL PAGE IS POOR

5.200E 00	7.091E 04	-2.153E-01	2.941E-01	2.418E 03	1.663E-01	1.028E-02	1.229E-02	8.370E-01
5.300E 00	7.091E 04	-2.171E-01	2.934E-01	2.411E 03	1.694E-01	1.044E-02	1.248E-02	8.361E-01
5.400E 00	7.091E 04	-2.189E-01	2.927E-01	2.403E 03	1.704E-01	1.059E-02	1.267E-02	8.353E-01
5.500E 00	7.091E 04	-2.207E-01	2.921E-01	2.396E 03	1.723E-01	1.074E-02	1.297E-02	8.344E-01
5.600E 00	7.091E 04	-2.225E-01	2.914E-01	2.388E 03	1.750E-01	1.089E-02	1.306E-02	8.336E-01
5.700E 00	7.091E 04	-2.243E-01	2.908E-01	2.381E 03	1.782E-01	1.103E-02	1.325E-02	8.328E-01
5.800E 00	7.091E 04	-2.261E-01	2.902E-01	2.374E 03	1.812E-01	1.118E-02	1.344E-02	8.320E-01
5.900E 00	7.091E 04	-2.279E-01	2.896E-01	2.367E 03	1.839E-01	1.133E-02	1.363E-02	8.312E-01
6.000E 00	7.091E 04	-2.297E-01	2.890E-01	2.361E 03	1.865E-01	1.148E-02	1.382E-02	8.305E-01
6.100E 00	7.091E 04	-2.315E-01	2.884E-01	2.354E 03	1.889E-01	1.163E-02	1.402E-02	8.297E-01
6.200E 00	7.091E 04	-2.333E-01	2.878E-01	2.348E 03	1.913E-01	1.178E-02	1.421E-02	8.290E-01
6.300E 00	7.091E 04	-2.351E-01	2.873E-01	2.341E 03	1.935E-01	1.192E-02	1.440E-02	8.283E-01
6.400E 00	7.091E 04	-2.369E-01	2.867E-01	2.335E 03	1.957E-01	1.207E-02	1.459E-02	8.275E-01
6.500E 00	7.091E 04	-2.387E-01	2.862E-01	2.329E 03	1.977E-01	1.222E-02	1.478E-02	8.269E-01
6.600E 00	7.091E 04	-2.405E-01	2.857E-01	2.323E 03	1.997E-01	1.236E-02	1.497E-02	8.262E-01
6.700E 00	7.091E 04	-2.423E-01	2.852E-01	2.317E 03	2.016E-01	1.251E-02	1.515E-02	8.255E-01
6.800E 00	7.091E 04	-2.441E-01	2.847E-01	2.311E 03	2.034E-01	1.266E-02	1.534E-02	8.248E-01
6.900E 00	7.091E 04	-2.459E-01	2.842E-01	2.305E 03	2.058E-01	1.280E-02	1.553E-02	8.242E-01
7.000E 00	7.091E 04	-2.477E-01	2.837E-01	2.299E 03	2.089E-01	1.295E-02	1.572E-02	8.236E-01
7.100E 00	7.091E 04	-2.495E-01	2.833E-01	2.294E 03	2.117E-01	1.309E-02	1.591E-02	8.229E-01
7.200E 00	7.091E 04	-2.514E-01	2.828E-01	2.288E 03	2.144E-01	1.324E-02	1.610E-02	8.223E-01
7.300E 00	7.091E 04	-2.532E-01	2.823E-01	2.283E 03	2.170E-01	1.338E-02	1.629E-02	8.217E-01
7.400E 00	7.091E 04	-2.550E-01	2.819E-01	2.277E 03	2.194E-01	1.353E-02	1.648E-02	8.211E-01
7.500E 00	7.091E 04	-2.568E-01	2.814E-01	2.272E 03	2.217E-01	1.367E-02	1.666E-02	8.205E-01
7.600E 00	7.091E 04	-2.586E-01	2.810E-01	2.267E 03	2.240E-01	1.382E-02	1.685E-02	8.199E-01
7.700E 00	7.091E 04	-2.604E-01	2.806E-01	2.262E 03	2.261E-01	1.396E-02	1.704E-02	8.194E-01
7.800E 00	7.091E 04	-2.622E-01	2.802E-01	2.257E 03	2.282E-01	1.411E-02	1.723E-02	8.188E-01
7.900E 00	7.091E 04	-2.640E-01	2.798E-01	2.252E 03	2.302E-01	1.425E-02	1.742E-02	8.183E-01
8.000E 00	7.091E 04	-2.658E-01	2.793E-01	2.247E 03	2.321E-01	1.440E-02	1.760E-02	8.178E-01
8.100E 00	7.091E 04	-2.676E-01	2.789E-01	2.242E 03	2.339E-01	1.454E-02	1.779E-02	8.172E-01
8.200E 00	7.091E 04	-2.694E-01	2.786E-01	2.237E 03	2.357E-01	1.469E-02	1.798E-02	8.167E-01
8.300E 00	7.091E 04	-2.712E-01	2.782E-01	2.232E 03	2.375E-01	1.483E-02	1.817E-02	8.162E-01
8.400E 00	7.091E 04	-2.730E-01	2.778E-01	2.227E 03	2.399E-01	1.497E-02	1.835E-02	8.157E-01
8.500E 00	7.091E 04	-2.748E-01	2.774E-01	2.223E 03	2.428E-01	1.511E-02	1.854E-02	8.152E-01
8.600E 00	7.091E 04	-2.766E-01	2.771E-01	2.218E 03	2.455E-01	1.526E-02	1.873E-02	8.147E-01
8.700E 00	7.091E 04	-2.784E-01	2.767E-01	2.214E 03	2.481E-01	1.540E-02	1.891E-02	8.142E-01
8.800E 00	7.091E 04	-2.802E-01	2.764E-01	2.209E 03	2.506E-01	1.554E-02	1.910E-02	8.137E-01
8.900E 00	7.091E 04	-2.820E-01	2.760E-01	2.205E 03	2.530E-01	1.568E-02	1.929E-02	8.132E-01
9.000E 00	7.091E 04	-2.838E-01	2.757E-01	2.200E 03	2.553E-01	1.583E-02	1.947E-02	8.127E-01
9.100E 00	7.091E 04	-2.856E-01	2.753E-01	2.196E 03	2.574E-01	1.597E-02	1.966E-02	8.122E-01
9.200E 00	7.091E 04	-2.874E-01	2.750E-01	2.192E 03	2.596E-01	1.611E-02	1.985E-02	8.117E-01
9.300E 00	7.091E 04	-2.892E-01	2.747E-01	2.187E 03	2.616E-01	1.625E-02	2.003E-02	8.112E-01
9.400E 00	7.091E 04	-2.910E-01	2.743E-01	2.183E 03	2.636E-01	1.639E-02	2.022E-02	8.107E-01
9.500E 00	7.091E 04	-2.928E-01	2.740E-01	2.179E 03	2.655E-01	1.653E-02	2.041E-02	8.103E-01
9.600E 00	7.091E 04	-2.946E-01	2.737E-01	2.175E 03	2.673E-01	1.668E-02	2.059E-02	8.098E-01
9.700E 00	7.091E 04	-2.964E-01	2.734E-01	2.171E 03	2.691E-01	1.682E-02	2.078E-02	8.093E-01
9.800E 00	7.091E 04	-2.982E-01	2.731E-01	2.167E 03	2.709E-01	1.696E-02	2.097E-02	8.089E-01
9.900E 00	7.091E 04	-3.000E-01	2.728E-01	2.163E 03	2.726E-01	1.710E-02	2.115E-02	8.084E-01
1.000E 01	7.091E 04	-3.018E-01	2.725E-01	2.159E 03	2.743E-01	1.724E-02	2.134E-02	8.080E-01
1.010E 01	7.091E 04	-3.036E-01	2.722E-01	2.155E 03	2.771E-01	1.738E-02	2.152E-02	8.075E-01
1.020E 01	7.091E 04	-3.054E-01	2.719E-01	2.151E 03	2.798E-01	1.752E-02	2.171E-02	8.071E-01

REPRODUCIBILITY OF THE  
ORIGINAL PAGE IS POOR



### 3.5 Listing of RECTANGULAR Geometry Subroutines.

For rectangular ducts the computations are carried out along one pair of opposing walls. Half the distance between these two walls is called HEIGHT. Half the distance between the other pair of opposing walls is called WIDTH. The effect of the WIDTH walls is taken into account, as in Refs. 5 and 9, by using effective width, EFWIDTH, in calculations involving mass flow rates. Effective width is calculated as,

$$\begin{aligned} \text{EFWIDTH} &= \text{WIDTH} - \delta_1 && \text{for } \delta_0 \leq \text{WIDTH} \\ \text{EFWIDTH} &= \text{WIDTH} \left( 1 - \frac{\delta_1}{\delta_0} \right) && \text{for } \delta_0 > \text{WIDTH} \end{aligned}$$

where  $\delta_0$  and  $\delta_1$  are the boundary layer thickness and the displacement thickness computed along HEIGHT walls.

It is assumed that the flow is symmetric about the midplanes.

The computations are carried out from wall to half the height.

#### INPUT1 Subroutine:

This subroutine provides data for the duct shape.

WIDTH = Half the duct width,  
 HEIGHT = Half the duct height,  
 WSLOPE, HSLOPE = Slope of the duct walls defined as:  
 WIDTH at  $x + \Delta x$  = WIDTH at  $x + \text{WSLOPE} \cdot \Delta x$   
 HEIGHT at  $x + \Delta x$  = HEIGHT at  $x + \text{HSLOPE} \cdot \Delta x$   
 ARFAC = 1 for rectangular ducts

#### SIPSIM and ZDZ Subroutines:

Given  $U(J)$ ,  $\text{RHO}(J)$ , and  $Z(J)$  subroutine SIPSIM calculates  $\text{SIP}(J)$  and  $\text{SIM}(J)$ . It is called at the beginning of each integration step.

Subroutine ZDZ, called at the end of the integration step, calculates  $Z(J)$  given  $U(J)$ ,  $RHO(J)$ ,  $SIP(J)$ , and  $SIM(J)$ . Width used in these calculations is the effective width,  $EFWIDTH$ . Fortran statements in these routines are almost direct translations of the formulae given in Appendices A and B of Ref. 7.

XSAREA Subroutine:

This subroutine calculates cross-sectional and surface areas of the streams. It also calculates the cross-sectional area of the duct called  $OLDA$ . This area is used in the pressure iteration formulae.

FORTRAN IV 360N-FO-479 3-8

INPUT1

DATE 08/20/79

TIME 14

SUBROUTINE INPUT1

COMMON/COM8/HEIGHT,WIDTH,HSLOPE,WSLOPE,AVWIDTH,EFWIDTH,CLDA,ARFAC

WIDTH=

HEIGHT=

WSLOPE=

HSLOPE=

ARFAC=1.

RETURN

END

```
SUBROUTINE SIPSIM(NP)
COMMON/COM1/U(50),T(50),Y(50),RHO(50),USH(50),Z(50),DZ(50)
COMMON/COM2/NJ,NJ1,NJ2,NJP,NBL,DX
COMMON/COM3/SIP(50),SIM(50),FLORAT
COMMON/COM5/AX(50),AS(50)
COMMON/COM6/ALPHA,BETA,DELTA,GAMMA,RE,VISC(50)
COMMON/COM7/DEL1,DEL2,H12,DELO
COMMON/COM8/HEIGHT,WIDTH,HSLOPE,WSLOPE,AVWIDH,EFWIDH,OLDA,ARFAC
DIMENSION RU(50)
IF(OLDA.LE.0.0)EFWIDH=WIDTH-DEL1
WIDTT=EFWIDH*0.03125
FLORAT=0.0
C**SI'S, EXCEPT SIM(2), REDUCED BY 4 TO ABSORV 1/4 APPEARING IN SI(J)/4**
DO 10 J=2,NJ
  10 RU(J)=RHO(J)*U(J)
  DO 30 J=2,NJ1
    SIP(J)=(3.*RU(J)+RU(J+1))*DZ(J+1)*WIDTT
  30 FLORAT=FLORAT+SIP(J)
    SIM(2)=RU(2)*GAMMA*DZ(2)*WIDTT*32.
    FLORAT=FLORAT+SIM(2)*.25
  DO 40 J=3,NJ
    SIM(J)=(3.*RU(J)+RU(J-1))*DZ(J)*WIDTT
  40 FLORAT=FLORAT+SIM(J)
    FLORAT=FLORAT*4.0
    IF (NP.NE.1) GO TO 100
    WRITE(6,22) ( SIM(J),J=2,NJ)
    WRITE(6,24) ( SIP(J),J=2,NJ1)
    WRITE(6,53) FLORAT
  22 FORMAT(/,' SIM',6X ,10E11.3/(10X,10E11.3))
  24 FORMAT(/,' SIP',6X ,10E11.3/(10X,10E11.3))
  53 FORMAT (1X,9X,'FLCW RATE= ',E11.4)
100 RETURN
END
```

```
SUBROUTINE ZDZ
COMMON/COM1/U(50),T(50),H(50),RHO(50),USH(50),Z(50),DZ(50)
COMMON/COM2/NJ,NJ1,NJ2,NJP,NBL,DX
COMMON/COM3/SIP(50),SIM(50),FLORAT
COMMON/COM6/ALPHA,BETA,DELTA,GAMMA,RE,VISC(50)
COMMON/COM8/HEIGHT,WIDTH,HSLOPE,WSLOPE,AVWIDTH,EFWIDTH,OLDA,ARFAC
DIMENSION RU(50)
WINV= 8.0/EFWIDTH
DO 10 J=2,NJ
10 RU(J)=RHO(J)*U(J)
   Z(2)=.125*WINV*SIM(2)/RU(2)/GAMMA
   DZ(2)=Z(2)
DO 20 J=3,NJ
   DZ(J)=(SIP(J-1)+SIM(J))/(RU(J)+RU(J-1))*WINV
20 Z(J)=Z(J-1)+DZ(J)
RETURN
END
```

```
SUBROUTINE XSAREA(NP)
COMMON/COM1/U(50),T(50),H(50),RHO(50),USH(50),Z(50),DZ(50)
COMMON/COM2/NJ,NJ1,NJ2,NJP,NBL,DX
COMMON/COM5/AX(50),AS(50)
COMMON/COM7/DEL1,DEL2,H12,DELO
COMMON/COM8/HEIGHT,WIDTH,HSLOPE,WSLOPE,AVWIDTH,EFWIDTH,OLDA,ARFAC
C**CALCULATION OF NEW DUCT CROSS-SECTION**RRRRRRRRRRRRRRRRRRRRRRRRRRRRRR
HEIGHT=HEIGHT+HSLOPE*DX
WIDTH=WIDTH+WSLOPE*DX
AVWIDTH=WIDTH+WSLOPE*DX*0.5
WIDCOR=DEL1
IF(DELO.GT.WIDTH) WIDCOR =WIDTH*DEL1/DELO
EFWIDTH=WIDTH-WIDCOR
OLDA =HEIGHT*EFWIDTH
WHF=0.5*AVWIDTH
AX(2)=WHF*(Z(3)+Z(2))
DO 10 J=3,NJ1
10 AX(J)=WHF*(Z(J+1)-Z(J-1))
AX(NJ)=WHF*(Z(NJ)-Z(NJ1))
DO 20 J=1,NJ
20 AS(J)=DX*AVWIDTH
IF(NP.NE.1)GO TO 35
WRITE(6,30) (AS(J),J=2,NJ)
30 FORMAT(/,' AS',7X,10E11.3/(10X,10E11.3))
WRITE (6,32) (AX(J),J=2,NJ)
32 FORMAT (/,' AX',7X,10E11.3/(10X,10E11.3))
35 RETURN
END
```

### 3.6 Sample Computations--Rectangular Diffuser Flow

DATA: (SI Units)

#### MAIN Program:

```
C**DYNAMIC AND THERMODYNAMIC DATA*****
      UCNTR=200.0
      ZBL=0.015
      TCNTR=300.0
      TWALL=300.0
      P=71000.0
      CP=1003.5
      GASK=1.4
      GASR=287.0
      PRNDL=0.7
      DPDFX=210000.0
C**GEOMETRIC DUCT DATA*****
      CALL INPUT1
      XEND=0.5
C**CONVERGENCE CRITERIA, GRID SIZE, AND OTHER DATA*****
      DPDTL=0.01
      DXFAC=5.0
      MAXIT=50
      NJ=21
      NPRNT=5
C**DATA FOR VSCSTY AND START SUBROUTINES*****
      VZERO=0.0000386
      TZERO=860.0
      EXPV=.7
      EXPU=7.
      EXPH=7.
```

C

#### INPUT1 Subroutine:

```
WIDTH=0.025
HEIGHT=0.05
WSLOPE=0.03
HSLOPE=0.03
```

#### JOB STATISTICS:

```
Machine: IBM 360/44 with DOS operating system.
Cards Read: 491
Core Required: 42K
Compilation Time: 3.05 mns
CPU Time: 1.97 mns
```

\*\*DIST. ALONG X= 0.0 \*\*\*\*NEAR WALL RE=1.2000E 03

Z	2.4227E-04	4.8453E-04	7.7459E-04	1.2226E-03	1.8568E-03	2.7040E-03	3.7899E-03	5.1370E-03	6.7754E-03	8.7222E-03
	1.1002E-02	1.3637E-02	1.6648E-02	2.0057E-02	2.3884E-02	2.8151E-02	3.2876E-02	3.8079E-02	4.3781E-02	5.0000E-02
U	1.1093E 02	1.2248E 02	1.3097E 02	1.3979E 02	1.4839E 02	1.5658E 02	1.6432E 02	1.7162E 02	1.7853E 02	1.8509E 02
	1.9134E 02	1.9730E 02	2.0000E 02	2.0000E 02	2.0000E 02	2.0000E 02	2.0000E 02	2.0000E 02	2.0000E 02	2.0000E 02
T	3.0000E 02	3.0000E 02	3.0000E 02	3.0000E 02	3.0000E 02	3.0000E 02	3.0000E 02	3.0000E 02	3.0000E 02	3.0000E 02
	3.0000E 02	3.0000E 02	3.0000E 02	3.0000E 02	3.0000E 02	3.0000E 02	3.0000E 02	3.0000E 02	3.0000E 02	3.0000E 02
RHO	8.2462E-01	8.2462E-01	8.2462E-01	8.2462E-01	8.2462E-01	8.2462E-01	8.2462E-01	8.2462E-01	8.2462E-01	8.2462E-01
	8.2462E-01	8.2462E-01	8.2462E-01	8.2462E-01	8.2462E-01	8.2462E-01	8.2462E-01	8.2462E-01	8.2462E-01	8.2462E-01
H	3.0105E 05	3.0105E 05	3.0105E 05	3.0105E 05	3.0105E 05	3.0105E 05	3.0105E 05	3.0105E 05	3.0105E 05	3.0105E 05
	3.0105E 05	3.0105E 05	3.0105E 05	3.0105E 05	3.0105E 05	3.0105E 05	3.0105E 05	3.0105E 05	3.0105E 05	3.0105E 05

\*\*DIST. ALONG X= 0.0006\*\*\*\*NEAR WALL RE=1.1988E 03

Z	2.4346E-04	4.8646E-04	7.7689E-04	1.2254E-03	1.8603E-03	2.7083E-03	3.7951E-03	5.1452E-03	6.7825E-03	8.7303E-03
	1.1011E-02	1.3647E-02	1.6660E-02	2.0070E-02	2.3898E-02	2.8165E-02	3.2891E-02	3.8096E-02	4.3790E-02	5.0019E-02
U	1.1034E 02	1.2219E 02	1.3068E 02	1.3949E 02	1.4809E 02	1.5628E 02	1.6402E 02	1.7134E 02	1.7826E 02	1.8482E 02
	1.9109E 02	1.9696E 02	1.9974E 02	1.9975E 02	1.9975E 02	1.9975E 02	1.9975E 02	1.9975E 02	1.9975E 02	1.9975E 02
T	3.0020E 02	3.0005E 02	3.0005E 02	3.0005E 02	3.0005E 02	3.0005E 02	3.0005E 02	3.0005E 02	3.0005E 02	3.0005E 02
	3.0005E 02	3.0005E 02	3.0005E 02	3.0004E 02	3.0005E 02	3.0004E 02	3.0004E 02	3.0004E 02	3.0004E 02	3.0005E 02
RHO	8.2450E-01	8.2491E-01	8.2492E-01	8.2492E-01	8.2492E-01	8.2492E-01	8.2492E-01	8.2492E-01	8.2492E-01	8.2492E-01
	8.2492E-01	8.2492E-01	8.2492E-01	8.2493E-01	8.2493E-01	8.2493E-01	8.2493E-01	8.2493E-01	8.2493E-01	8.2492E-01
H	3.0125E 05	3.0110E 05	3.0110E 05	3.0110E 05	3.0110E 05	3.0110E 05	3.0110E 05	3.0110E 05	3.0110E 05	3.0110E 05
	3.0110E 05	3.0110E 05	3.0110E 05	3.0109E 05	3.0110E 05	3.0109E 05	3.0109E 05	3.0109E 05	3.0109E 05	3.0110E 05

\*\*DIST. ALONG X= 0.0200\*\*\*\*NEAR WALL RE=1.1707E 03

Z	2.6072E-04	5.1872E-04	8.2382E-04	1.2912E-03	1.9485E-03	2.8220E-03	3.9367E-03	5.3165E-03	6.9844E-03	8.9632E-03
	1.1277E-02	1.3953E-02	1.7008E-02	2.0448E-02	2.4301E-02	2.8598E-02	3.3356E-02	3.8597E-02	4.4339E-02	5.0601E-02
U	1.0061E 02	1.1271E 02	1.2151E 02	1.3054E 02	1.3931E 02	1.4765E 02	1.5555E 02	1.6303E 02	1.7013E 02	1.7680E 02
	1.8289E 02	1.8808E 02	1.9174E 02	1.9268E 02	1.9255E 02	1.9257E 02	1.9257E 02	1.9257E 02	1.9257E 02	1.9257E 02
T	3.0282E 02	3.0235E 02	3.0204E 02	3.0179E 02	3.0163E 02	3.0155E 02	3.0152E 02	3.0150E 02	3.0149E 02	3.0148E 02
	3.0147E 02	3.0146E 02	3.0145E 02	3.0144E 02	3.0144E 02	3.0144E 02	3.0144E 02	3.0144E 02	3.0144E 02	3.0146E 02
RHO	8.2966E-01	8.3097E-01	8.3182E-01	8.3251E-01	8.3294E-01	8.3315E-01	8.3325E-01	8.3330E-01	8.3333E-01	8.3336E-01
	8.3338E-01	8.3341E-01	8.3343E-01	8.3346E-01	8.3345E-01	8.3346E-01	8.3345E-01	8.3345E-01	8.3345E-01	8.3342E-01
H	3.0388E 05	3.0341E 05	3.0309E 05	3.0284E 05	3.0269E 05	3.0261E 05	3.0257E 05	3.0256E 05	3.0254E 05	3.0253E 05
	3.0253E 05	3.0252E 05	3.0251E 05	3.0250E 05	3.0250E 05	3.0250E 05	3.0250E 05	3.0250E 05	3.0250E 05	3.0251E 05

\*\*DIST. ALONG X= 0.0700\*\*\*\*NEAR WALL RE=1.1247E 03

Z	2.8223E-04	5.6052E-04	8.8928E-04	1.3916E-03	2.0953E-03	3.0258E-03	4.2071E-03	5.6617E-03	7.4121E-03	9.4810E-03
	1.1893E-02	1.4676E-02	1.7839E-02	2.1375E-02	2.5307E-02	2.9683E-02	3.4532E-02	3.9871E-02	4.5721E-02	5.2102E-02
U	8.8177E 01	9.8914E 01	1.0689E 02	1.1524E 02	1.2352E 02	1.3156E 02	1.3931E 02	1.4670E 02	1.5369E 02	1.6022E 02
	1.6616E 02	1.7134E 02	1.7548E 02	1.7819E 02	1.7882E 02	1.7873E 02	1.7874E 02	1.7874E 02	1.7874E 02	1.7874E 02

REPRODUCIBILITY OF THE  
ORIGINAL PAGE IS POOR



T 3.0534E-02 3.0519E-02 3.0503E-02 3.0485E-02 3.0467E-02 3.0450E-02 3.0437E-02 3.0426E-02 3.0418E-02 3.0412E-02  
3.0408E-02 3.0405E-02 3.0402E-02 3.0400E-02 3.0400E-02 3.0400E-02 3.0400E-02 3.0400E-02 3.0400E-02 3.0402E-02

RHO 8.4503E-01 8.4545E-01 8.4589E-01 8.4640E-01 8.4690E-01 8.4736E-01 8.4774E-01 8.4803E-01 8.4826E-01 8.4842E-01  
8.4854E-01 8.4863E-01 8.4870E-01 8.4875E-01 8.4878E-01 8.4877E-01 8.4877E-01 8.4877E-01 8.4877E-01 8.4872E-01

H 3.0641E-05 3.0626E-05 3.0610E-05 3.0592E-05 3.0573E-05 3.0557E-05 3.0543E-05 3.0533E-05 3.0525E-05 3.0519E-05  
3.0515E-05 3.0511E-05 3.0509E-05 3.0507E-05 3.0506E-05 3.0506E-05 3.0506E-05 3.0506E-05 3.0506E-05 3.0508E-05

\*\*DIST. ALONG X= 0.1200\*\*\*NEAR WALL RE=1.0854E 03

Z 3.0085E-04 5.9649E-04 9.4549E-04 1.4782E-03 2.2235E-03 3.2072E-03 4.4530E-03 5.9833E-03 7.8197E-03 9.9840E-03  
1.2499E-02 1.5391E-02 1.8667E-02 2.2309E-02 2.6333E-02 3.0780E-02 3.5720E-02 4.1153E-02 4.7105E-02 5.3597E-02

U 7.8898E-01 8.8637E-01 9.5890E-01 1.0355E-02 1.1121E-02 1.1872E-02 1.2602E-02 1.3306E-02 1.3978E-02 1.4613E-02  
1.5202E-02 1.5731E-02 1.6179E-02 1.6517E-02 1.6716E-02 1.6733E-02 1.6730E-02 1.6731E-02 1.6733E-02 1.6730E-02

T 3.0684E-02 3.0692E-02 3.0692E-02 3.0686E-02 3.0676E-02 3.0665E-02 3.0653E-02 3.0641E-02 3.0631E-02 3.0621E-02  
3.0614E-02 3.0607E-02 3.0602E-02 3.0599E-02 3.0597E-02 3.0596E-02 3.0596E-02 3.0596E-02 3.0596E-02 3.0599E-02

RHO 8.5793E-01 8.5770E-01 8.5771E-01 8.5787E-01 8.5814E-01 8.5846E-01 8.5880E-01 8.5912E-01 8.5942E-01 8.5968E-01  
8.5990E-01 8.6007E-01 8.6021E-01 8.6031E-01 8.6037E-01 8.6039E-01 8.6038E-01 8.6038E-01 8.6039E-01 8.6031E-01

H 3.0791E-05 3.0799E-05 3.0799E-05 3.0793E-05 3.0784E-05 3.0772E-05 3.0760E-05 3.0748E-05 3.0738E-05 3.0729E-05  
3.0721E-05 3.0714E-05 3.0710E-05 3.0706E-05 3.0704E-05 3.0703E-05 3.0704E-05 3.0704E-05 3.0704E-05 3.0706E-05

\*\*DIST. ALONG X= 0.1700\*\*\*NEAR WALL RE=1.0513E 03

Z 3.1814E-04 6.2990E-04 9.9785E-04 1.5592E-03 2.3439E-03 3.3785E-03 4.6870E-03 6.2918E-03 8.2139E-03 1.0474E-02  
1.3095E-02 1.6099E-02 1.9490E-02 2.3245E-02 2.7373E-02 3.1915E-02 3.6928E-02 4.2449E-02 4.8498E-02 5.5097E-02

U 7.1570E-01 8.0455E-01 8.7108E-01 1.4156E-01 1.0125E-02 1.0824E-02 1.1508E-02 1.2173E-02 1.2814E-02 1.3427E-02  
1.4005E-02 1.4537E-02 1.5005E-02 1.5387E-02 1.5656E-02 1.5781E-02 1.5773E-02 1.5774E-02 1.5774E-02 1.5774E-02

T 3.0787E-02 3.0813E-02 3.0824E-02 3.0829E-02 3.0828E-02 3.0823E-02 3.0815E-02 3.0806E-02 3.0796E-02 3.0786E-02  
3.0777E-02 3.0769E-02 3.0762E-02 3.0756E-02 3.0753E-02 3.0751E-02 3.0751E-02 3.0751E-02 3.0751E-02 3.0754E-02

RHO 8.6830E-01 8.6758E-01 8.6727E-01 8.6713E-01 8.6715E-01 8.6730E-01 8.6751E-01 8.6777E-01 8.6805E-01 8.6832E-01  
8.6858E-01 8.6881E-01 8.6901E-01 8.6917E-01 8.6927E-01 8.6933E-01 8.6933E-01 8.6932E-01 8.6932E-01 8.6924E-01

H 3.0895E-05 3.0921E-05 3.0932E-05 3.0937E-05 3.0936E-05 3.0931E-05 3.0923E-05 3.0914E-05 3.0904E-05 3.0894E-05  
3.0885E-05 3.0877E-05 3.0870E-05 3.0864E-05 3.0860E-05 3.0858E-05 3.0858E-05 3.0858E-05 3.0858E-05 3.0861E-05

\*\*DIST. ALONG X= 0.2200\*\*\*NEAR WALL RE=1.0211E 03

Z 3.3498E-04 6.6236E-04 1.0486E-03 1.6377E-03 2.4606E-03 3.5448E-03 4.9146E-03 6.5924E-03 8.5990E-03 1.0955E-02  
1.3680E-02 1.6797E-02 2.0305E-02 2.4178E-02 2.8417E-02 3.3057E-02 3.8153E-02 4.3756E-02 4.9897E-02 5.6596E-02

U 6.5502E-01 7.3685E-01 7.9825E-01 8.6352E-01 9.2941E-01 9.9472E-01 1.0589E-02 1.1217E-02 1.1828E-02 1.2418E-02  
1.2981E-02 1.3508E-02 1.3985E-02 1.4393E-02 1.4711E-02 1.4918E-02 1.4966E-02 1.4959E-02 1.4960E-02 1.4959E-02

T 3.0863E-02 3.0902E-02 3.0922E-02 3.0936E-02 3.0942E-02 3.0943E-02 3.0940E-02 3.0934E-02 3.0926E-02 3.0918E-02  
3.0909E-02 3.0900E-02 3.0892E-02 3.0885E-02 3.0880E-02 3.0876E-02 3.0875E-02 3.0875E-02 3.0875E-02 3.0879E-02

RHO 8.7670E-01 8.7559E-01 8.7502E-01 8.7464E-01 8.7466E-01 8.7443E-01 8.7452E-01 8.7469E-01 8.7490E-01 8.7514E-01  
8.7539E-01 8.7564E-01 8.7587E-01 8.7607E-01 8.7623E-01 8.7633E-01 8.7637E-01 8.7635E-01 8.7635E-01 8.7626E-01

H 3.0971E-05 3.1010E-05 3.1030E-05 3.1044E-05 3.1050E-05 3.1051E-05 3.1048E-05 3.1042E-05 3.1035E-05 3.1026E-05  
3.1017E-05 3.1008E-05 3.1000E-05 3.0993E-05 3.0988E-05 3.0984E-05 3.0983E-05 3.0983E-05 3.0983E-05 3.0987E-05

\*\*DIST. ALONG X= 0.2700\*\*\*\*NEAR WALL RE=9.8469E 02

Z	3.6020E-04	7.1050E-04	1.1225E-03	1.7487E-03	2.6204E-03	3.7648E-03	5.2060E-03	6.9659E-03	9.0643E-03	1.1521E-02	1.4354E-02	1.7585E-02	2.1209E-02	2.5196E-02	2.9543E-02	3.4280E-02	3.9452E-02	4.5120E-02	5.1330E-02	5.8105E-02
U	5.8322E 01	6.5847E 01	7.1575E 01	7.7720E 01	8.3965E 01	9.0184E 01	9.6325E 01	1.0273E 02	1.0926E 02	1.1400E 02	1.1952E 02	1.2477E 02	1.2962E 02	1.3388E 02	1.3741E 02	1.4000E 02	1.4138E 02	1.4137E 02	1.4137E 02	1.4136E 02
T	3.0939E 02	3.0989E 02	3.1016E 02	3.1036E 02	3.1048E 02	3.1054E 02	3.1055E 02	3.1053E 02	3.1048E 02	3.1041E 02	3.1033E 02	3.1025E 02	3.1016E 02	3.1009E 02	3.1002E 02	3.0997E 02	3.0994E 02	3.0994E 02	3.0994E 02	3.0994E 02
RHO	8.8454E-01	8.8311E-01	8.8234E-01	8.8177E-01	8.8142E-01	8.8125E-01	8.8122E-01	8.8129E-01	8.8143E-01	8.8162E-01	8.8184E-01	8.8208E-01	8.8232E-01	8.8254E-01	8.8273E-01	8.8297E-01	8.8296E-01	8.8296E-01	8.8296E-01	8.8284E-01
H	3.1047E 05	3.1097E 05	3.1124E 05	3.1144E 05	3.1157E 05	3.1163E 05	3.1164E 05	3.1161E 05	3.1156E 05	3.1150E 05	3.1142E 05	3.1133E 05	3.1125E 05	3.1117E 05	3.1111E 05	3.1105E 05	3.1102E 05	3.1102E 05	3.1102E 05	3.1107E 05

\*\*DIST. ALONG X= 0.3200\*\*\*\*NEAR WALL RE=9.5409E 02

Z	3.8037E-04	7.4906E-04	1.1824E-03	1.8406E-03	2.7559E-03	3.9559E-03	5.4648E-03	7.3036E-03	9.4917E-03	1.2047E-02	1.4989E-02	1.8334E-02	2.2076E-02	2.6181E-02	3.0640E-02	3.5482E-02	4.0742E-02	4.6479E-02	5.2754E-02	5.9601E-02
U	5.3194E 01	6.0131E 01	6.5406E 01	7.1092E 01	7.6908E 01	8.2742E 01	8.8545E 01	9.4289E 01	9.9947E 01	1.0549E 02	1.1088E 02	1.1605E 02	1.2090E 02	1.2527E 02	1.2904E 02	1.3203E 02	1.3403E 02	1.3459E 02	1.3451E 02	1.3452E 02
T	3.0991E 02	3.1050E 02	3.1084E 02	3.1110E 02	3.1128E 02	3.1133E 02	3.1143E 02	3.1144E 02	3.1141E 02	3.1137E 02	3.1130E 02	3.1123E 02	3.1115E 02	3.1107E 02	3.1100E 02	3.1094E 02	3.1089E 02	3.1087E 02	3.1088E 02	3.1092E 02
RHO	8.9089E-01	8.8919E-01	8.8823E-01	8.8749E-01	8.8693E-01	8.8667E-01	8.8655E-01	8.8653E-01	8.8659E-01	8.8673E-01	8.8691E-01	8.8712E-01	8.8735E-01	8.8757E-01	8.8778E-01	8.8796E-01	8.8809E-01	8.8814E-01	8.8813E-01	8.8799E-01
H	3.1100E 05	3.1159E 05	3.1193E 05	3.1219E 05	3.1237E 05	3.1247E 05	3.1252E 05	3.1253E 05	3.1250E 05	3.1246E 05	3.1239E 05	3.1232E 05	3.1224E 05	3.1216E 05	3.1208E 05	3.1202E 05	3.1198E 05	3.1196E 05	3.1196E 05	3.1201E 05

\*\*DIST. ALONG X= 0.3700\*\*\*\*NEAR WALL RE=9.2340E 02

Z	4.0496E-04	7.9573E-04	1.2539E-03	1.9483E-03	2.9115E-03	4.1712E-03	5.7510E-03	7.6717E-03	9.9518E-03	1.2608E-02	1.5658E-02	1.9118E-02	2.2977E-02	2.7198E-02	3.1770E-02	3.6715E-02	4.2066E-02	4.7872E-02	5.4200E-02	6.1103E-02
U	4.8116E 01	5.4550E 01	5.9470E 01	6.4804E 01	7.0294E 01	7.5827E 01	8.1355E 01	8.6850E 01	9.2292E 01	9.7655E 01	1.0291E 02	1.0800E 02	1.1284E 02	1.1727E 02	1.2120E 02	1.2448E 02	1.2692E 02	1.2824E 02	1.2824E 02	1.2823E 02
T	3.1039E 02	3.1105E 02	3.1143E 02	3.1174E 02	3.1195E 02	3.1209E 02	3.1218E 02	3.1221E 02	3.1221E 02	3.1219E 02	3.1214E 02	3.1208E 02	3.1200E 02	3.1193E 02	3.1185E 02	3.1179E 02	3.1173E 02	3.1170E 02	3.1169E 02	3.1175E 02
RHO	8.9633E-01	8.9443E-01	8.9334E-01	8.9247E-01	8.9185E-01	8.9145E-01	8.9121E-01	8.9111E-01	8.9111E-01	8.9118E-01	8.9132E-01	8.9149E-01	8.9170E-01	8.9192E-01	8.9213E-01	8.9233E-01	8.9248E-01	8.9259E-01	8.9259E-01	8.9244E-01
H	3.1148E 05	3.1214E 05	3.1252E 05	3.1283E 05	3.1304E 05	3.1319E 05	3.1327E 05	3.1330E 05	3.1331E 05	3.1328E 05	3.1323E 05	3.1317E 05	3.1310E 05	3.1302E 05	3.1295E 05	3.1288E 05	3.1282E 05	3.1279E 05	3.1279E 05	3.1284E 05

\*\*DIST. ALONG X= 0.4200\*\*\*\*NEAR WALL RE=9.9735E 02

Z	4.2430E-04	8.3274E-04	1.3116E-03	2.0369E-03	3.0423E-03	4.3559E-03	6.0015E-03	7.9994E-03	1.0367E-02	1.3122E-02	1.6278E-02	1.9851E-02	2.3829E-02	2.8168E-02	3.2856E-02	3.7911E-02	4.3362E-02	4.9250E-02	5.5639E-02	6.2597E-02
U	4.4466E 01	5.0411E 01	5.4989E 01	5.9965E 01	6.5104E 01	7.0309E 01	7.5638E 01	8.0765E 01	8.5970E 01	9.1132E 01	9.6222E 01	1.0120E 02	1.0597E 02	1.1042E 02	1.1444E 02	1.1792E 02	1.2071E 02	1.2256E 02	1.2304E 02	1.2295E 02
T	3.1074E 02	3.1146E 02	3.1188E 02	3.1222E 02	3.1247E 02	3.1264E 02	3.1275E 02	3.1281E 02	3.1284E 02	3.1283E 02	3.1280E 02	3.1275E 02	3.1269E 02	3.1261E 02	3.1254E 02	3.1247E 02	3.1241E 02	3.1237E 02	3.1235E 02	3.1241E 02

REPRODUCIBILITY OF THE  
ORIGINAL PAGE IS POOR

RHO 9.0077E-01 8.9869E-01 8.9748E-01 8.9649E-01 8.9577E-01 8.9528E-01 8.9497E-01 8.9480E-01 8.9473E-01 8.9476E-01  
 8.9484E-01 8.9499E-01 8.9517E-01 8.9537E-01 8.9558E-01 8.9577E-01 8.9595E-01 8.9608E-01 8.9614E-01 8.9597E-01

H 3.1183E 05 3.1255E 05 3.1297E 05 3.1332E 05 3.1357E 05 3.1374E 05 3.1385E 05 3.1391E 05 3.1393E 05 3.1392E 05  
 3.1389E 05 3.1384E 05 3.1378E 05 3.1371E 05 3.1364E 05 3.1357E 05 3.1351E 05 3.1346E 05 3.1344E 05 3.1350E 05

\*\*DIST. ALONG X= 0.4700\*\*\*NEAR WALL RE=8.7183E 02

Z 4.4957E-04 8.8055E-04 1.3846E-03 2.1462E-03 3.1993E-03 4.5719E-03 6.2875E-03 8.3659E-03 1.0824E-02 1.3678E-02  
 1.6940E-02 2.0627E-02 2.4721E-02 2.9176E-02 3.3977E-02 3.9139E-02 4.4687E-02 5.0657E-02 5.7104E-02 6.4103E-02

U 4.0609E 01 4.6162E 01 5.0473E 01 5.5188E 01 6.0072E 01 6.5032E 01 7.0026E 01 7.5035E 01 8.0041E 01 8.5029E 01  
 8.9973E 01 9.4841E 01 9.9552E 01 1.0399E 02 1.0807E 02 1.1169E 02 1.1473E 02 1.1696E 02 1.1810E 02 1.1905E 02

T 3.1108E 02 3.1184E 02 3.1229E 02 3.1265E 02 3.1293E 02 3.1313E 02 3.1326E 02 3.1334E 02 3.1339E 02 3.1339E 02  
 3.1338E 02 3.1334E 02 3.1329E 02 3.1322E 02 3.1316E 02 3.1309E 02 3.1302E 02 3.1297E 02 3.1294E 02 3.1299E 02

RHO 9.0460E-01 9.0241E-01 9.0112E-01 9.0006E-01 8.9926E-01 8.9870E-01 8.9832E-01 8.9809E-01 8.9797E-01 8.9794E-01  
 8.9798E-01 8.9809E-01 8.9824E-01 8.9842E-01 8.9861E-01 8.9881E-01 8.9899E-01 8.9915E-01 8.9925E-01 8.9909E-01

H 3.1217E 05 3.1293E 05 3.1338E 05 3.1375E 05 3.1403E 05 3.1422E 05 3.1436E 05 3.1444E 05 3.1448E 05 3.1449E 05  
 3.1447E 05 3.1444E 05 3.1438E 05 3.1432E 05 3.1425E 05 3.1418E 05 3.1412E 05 3.1407E 05 3.1403E 05 3.1409E 05

\*\*DIST. ALONG X= 0.5200\*\*\*NEAR WALL RE=8.4911E 02

Z 4.7024E-04 9.1974E-04 1.4452E-03 2.2387E-03 3.3350E-03 4.7624E-03 6.5441E-03 8.6994E-03 1.1245E-02 1.4195E-02  
 1.7562E-02 2.1359E-02 2.5569E-02 3.0141E-02 3.5056E-02 4.0328E-02 4.5978E-02 5.2038E-02 5.8552E-02 6.5590E-02

U 3.7700E 01 4.2893E 01 4.6922E 01 5.1341E 01 5.5942E 01 6.0638E 01 6.5389E 01 7.0175E 01 7.4979E 01 7.9786E 01  
 8.4577E 01 8.9321E 01 9.3947E 01 9.8348E 01 1.0244E 02 1.0616E 02 1.0937E 02 1.1192E 02 1.1357E 02 1.1390E 02

T 3.1134E 02 3.1214E 02 3.1261E 02 3.1301E 02 3.1331E 02 3.1352E 02 3.1367E 02 3.1377E 02 3.1382E 02 3.1385E 02  
 3.1385E 02 3.1382E 02 3.1378E 02 3.1373E 02 3.1367E 02 3.1360E 02 3.1354E 02 3.1348E 02 3.1344E 02 3.1348E 02

RHO 9.0784E-01 9.0552E-01 9.0415E-01 9.0301E-01 9.0216E-01 9.0154E-01 9.0111E-01 9.0083E-01 9.0066E-01 9.0059E-01  
 9.0059E-01 9.0066E-01 9.0078E-01 9.0094E-01 9.0112E-01 9.0130E-01 9.0149E-01 9.0165E-01 9.0178E-01 9.0167E-01

H 3.1243E 05 3.1323E 05 3.1371E 05 3.1410E 05 3.1440E 05 3.1462E 05 3.1477E 05 3.1487E 05 3.1492E 05 3.1495E 05  
 3.1495E 05 3.1492E 05 3.1488E 05 3.1483E 05 3.1476E 05 3.1470E 05 3.1464E 05 3.1458E 05 3.1453E 05 3.1457E 05

REPRODUCIBILITY OF THE  
 ORIGINAL PAGE IS POOR

EX	PRESS	P-RECV	WALL SHEAR (Pa)	HEAT FLX (W/m <sup>2</sup> )	B.L. THK	DISP THK	MOM THK	SHAPE FAC
0.0	7.100E 04	0.0	3.967E 01	0.0	1.553E-02	1.913E-03	1.471E-03	1.301E 00
3.906E-05	7.100E 04	1.536E-04	3.963E 01	7.372E 00	1.554E-02	1.913E-03	1.471E-03	1.301E 00
7.812E-05	7.100E 04	2.583E-04	3.961E 01	1.378E 01	1.554E-02	1.914E-03	1.471E-03	1.301E 00
1.562E-04	7.101E 04	5.340E-04	3.955E 01	2.754E 01	1.555E-02	1.915E-03	1.472E-03	1.301E 00
3.125E-04	7.102E 04	1.054E-03	3.945E 01	5.365E 01	1.556E-02	1.917E-03	1.473E-03	1.301E 00
6.250E-04	7.104E 04	2.084E-03	3.925E 01	1.027E 02	1.559E-02	1.921E-03	1.476E-03	1.301E 00
1.250E-03	7.107E 04	4.119E-03	3.890E 01	1.899E 02	1.564E-02	1.929E-03	1.481E-03	1.302E 00
2.500E-03	7.115E 04	8.195E-03	3.829E 01	3.364E 02	1.574E-02	1.945E-03	1.492E-03	1.304E 00
5.000E-03	7.129E 04	1.624E-02	3.727E 01	5.637E 02	1.592E-02	1.978E-03	1.513E-03	1.308E 00
1.000E-02	7.157E 04	3.189E-02	3.565E 01	8.906E 02	1.625E-02	2.043E-03	1.555E-03	1.314E 00
2.000E-02	7.211E 04	6.176E-02	3.306E 01	1.330E 03	1.690E-02	2.172E-03	1.641E-03	1.324E 00
3.000E-02	7.252E 04	8.508E-02	3.159E 01	1.596E 03	1.814E-02	2.282E-03	1.717E-03	1.329E 00
4.000E-02	7.294E 04	1.085E-01	2.994E 01	1.822E 03	1.902E-02	2.401E-03	1.798E-03	1.335E 00
5.000E-02	7.333E 04	1.301E-01	2.862E 01	1.997E 03	1.970E-02	2.517E-03	1.878E-03	1.340E 00
6.000E-02	7.371E 04	1.512E-01	2.727E 01	2.149E 03	2.032E-02	2.639E-03	1.963E-03	1.344E 00
7.000E-02	7.405E 04	1.705E-01	2.616E 01	2.272E 03	2.092E-02	2.759E-03	2.047E-03	1.348E 00
8.000E-02	7.438E 04	1.889E-01	2.509E 01	2.377E 03	2.150E-02	2.881E-03	2.131E-03	1.352E 00
9.000E-02	7.470E 04	2.067E-01	2.407E 01	2.468E 03	2.265E-02	3.007E-03	2.219E-03	1.355E 00
1.000E-01	7.500E 04	2.234E-01	2.313E 01	2.546E 03	2.354E-02	3.135E-03	2.307E-03	1.359E 00
1.100E-01	7.528E 04	2.391E-01	2.229E 01	2.612E 03	2.427E-02	3.262E-03	2.396E-03	1.362E 00
1.200E-01	7.555E 04	2.542E-01	2.148E 01	2.668E 03	2.493E-02	3.392E-03	2.486E-03	1.365E 00
1.300E-01	7.581E 04	2.686E-01	2.071E 01	2.717E 03	2.556E-02	3.524E-03	2.577E-03	1.367E 00
1.400E-01	7.606E 04	2.823E-01	1.997E 01	2.758E 03	2.617E-02	3.660E-03	2.671E-03	1.370E 00
1.500E-01	7.629E 04	2.952E-01	1.931E 01	2.792E 03	2.678E-02	3.794E-03	2.764E-03	1.373E 00
1.600E-01	7.651E 04	3.076E-01	1.867E 01	2.821E 03	2.776E-02	3.930E-03	2.858E-03	1.375E 00
1.700E-01	7.672E 04	3.196E-01	1.805E 01	2.845E 03	2.878E-02	4.071E-03	2.954E-03	1.378E 00
1.800E-01	7.693E 04	3.309E-01	1.746E 01	2.865E 03	2.962E-02	4.213E-03	3.052E-03	1.380E 00
1.900E-01	7.712E 04	3.416E-01	1.693E 01	2.881E 03	3.034E-02	4.354E-03	3.149E-03	1.383E 00
2.000E-01	7.730E 04	3.520E-01	1.641E 01	2.893E 03	3.101E-02	4.497E-03	3.247E-03	1.385E 00
2.100E-01	7.748E 04	3.619E-01	1.591E 01	2.902E 03	3.166E-02	4.644E-03	3.347E-03	1.388E 00
2.200E-01	7.766E 04	3.717E-01	1.539E 01	2.907E 03	3.230E-02	4.796E-03	3.449E-03	1.390E 00
2.300E-01	7.784E 04	3.822E-01	1.472E 01	2.904E 03	3.295E-02	4.969E-03	3.562E-03	1.395E 00
2.400E-01	7.801E 04	3.917E-01	1.421E 01	2.903E 03	3.370E-02	5.137E-03	3.673E-03	1.399E 00
2.500E-01	7.819E 04	4.014E-01	1.362E 01	2.895E 03	3.491E-02	5.318E-03	3.789E-03	1.404E 00
2.600E-01	7.838E 04	4.122E-01	1.287E 01	2.876E 03	3.590E-02	5.528E-03	3.918E-03	1.411E 00
2.700E-01	7.854E 04	4.212E-01	1.244E 01	2.869E 03	3.674E-02	5.716E-03	4.038E-03	1.415E 00
2.800E-01	7.870E 04	4.298E-01	1.198E 01	2.858E 03	3.750E-02	5.905E-03	4.159E-03	1.420E 00
2.900E-01	7.884E 04	4.378E-01	1.161E 01	2.849E 03	3.821E-02	6.087E-03	4.277E-03	1.423E 00
3.000E-01	7.898E 04	4.456E-01	1.122E 01	2.836E 03	3.890E-02	6.276E-03	4.398E-03	1.427E 00
3.100E-01	7.911E 04	4.530E-01	1.086E 01	2.823E 03	3.958E-02	6.465E-03	4.519E-03	1.430E 00
3.200E-01	7.924E 04	4.602E-01	1.051E 01	2.808E 03	4.026E-02	6.657E-03	4.642E-03	1.434E 00
3.300E-01	7.936E 04	4.670E-01	1.019E 01	2.794E 03	4.093E-02	6.849E-03	4.765E-03	1.437E 00
3.400E-01	7.948E 04	4.735E-01	9.890E 00	2.780E 03	4.214E-02	7.042E-03	4.887E-03	1.441E 00
3.500E-01	7.962E 04	4.813E-01	9.334E 00	2.741E 03	4.326E-02	7.288E-03	5.031E-03	1.449E 00
3.600E-01	7.974E 04	4.879E-01	9.042E 00	2.726E 03	4.419E-02	7.504E-03	5.164E-03	1.453E 00
3.700E-01	7.985E 04	4.941E-01	8.735E 00	2.705E 03	4.500E-02	7.718E-03	5.295E-03	1.458E 00
3.800E-01	7.995E 04	4.999E-01	8.489E 00	2.690E 03	4.575E-02	7.925E-03	5.424E-03	1.461E 00
3.900E-01	8.005E 04	5.056E-01	8.234E 00	2.671E 03	4.646E-02	8.135E-03	5.553E-03	1.465E 00
4.000E-01	8.015E 04	5.110E-01	8.002E 00	2.653E 03	4.716E-02	8.345E-03	5.683E-03	1.468E 00
4.100E-01	8.024E 04	5.162E-01	7.775E 00	2.635E 03	4.785E-02	8.556E-03	5.813E-03	1.472E 00
4.200E-01	8.033E 04	5.212E-01	7.557E 00	2.616E 03	4.854E-02	8.770E-03	5.944E-03	1.475E 00
4.300E-01	8.042E 04	5.260E-01	7.347E 00	2.598E 03	4.922E-02	8.986E-03	6.076E-03	1.479E 00
4.400E-01	8.050E 04	5.307E-01	7.149E 00	2.579E 03	5.010E-02	9.204E-03	6.209E-03	1.482E 00
4.500E-01	8.059E 04	5.356E-01	6.886E 00	2.551E 03	5.141E-02	9.446E-03	6.351E-03	1.487E 00
4.600E-01	8.068E 04	5.408E-01	6.562E 00	2.515E 03	5.251E-02	9.720E-03	6.505E-03	1.494E 00
4.700E-01	8.076E 04	5.453E-01	6.382E 00	2.497E 03	5.348E-02	9.966E-03	6.650E-03	1.499E 00
4.800E-01	8.084E 04	5.496E-01	6.183E 00	2.474E 03	5.437E-02	1.022E-02	6.797E-03	1.503E 00
4.900E-01	8.091E 04	5.537E-01	6.029E 00	2.457E 03	5.521E-02	1.046E-02	6.942E-03	1.506E 00
5.000E-01	8.099E 04	5.577E-01	5.858E 00	2.436E 03	5.604E-02	1.071E-02	7.090E-03	1.510E 00
5.100E-01	8.105E 04	5.615E-01	5.712E 00	2.418E 03	5.684E-02	1.096E-02	7.238E-03	1.514E 00

REPRODUCIBILITY OF THE  
ORIGINAL PAGE IS POOR

REPRODUCIBILITY OF THE  
ORIGINAL PAGE IS POOR

#### REFERENCES

- [1] H. Schlichting, Boundary-Layer Theory (McGraw-Hill, New York, 1968).
- [2] P.J. Roache, Computational Fluid Dynamics (Hermosa Publishers, Albuquerque, NM, 1972).
- [3] R.M. Nelson and R.H. Pletcher, An Explicit Scheme for the Calculation of Confined Flows with Heat Transfer, Heat Transfer and Fluid Mechanics Inst. Proceedings, Oregon State University, Corvallis, June 12-14, 1974, pp. 154-170.
- [4] S.V. Pantankar and D.B. Spalding, Heat and Mass Transfer in Boundary Layers (Margon-Grampian, London, 1967).
- [5] E. Doss and H. Geyer, Two-Dimensional Subsonic Diffuser Code, ANL/MHD-77-1, Argonne National Laboratory, Argonne, Illinois.
- [6] R.A. Gentry, R.E. Martin and R.J. Daly, An Eulerian Differencing Method for Unsteady Compressible Flow Problems, Journ. of Comp. Phys. 1 (1966), pp. 87-117.
- [7] M.S. Greywall, Streamwise Computation of Duct Flows, Computer Methods in Applied Mechanics and Engineering (to appear).
- [8] J.A. Frisch, Pressure Iteration and Convergence Criteria for Pipe Flows, M.S. Thesis (1979), Dept. of Mechanical Engineering, Wichita State University, Wichita, KS.
- [9] L.R. Reneau and J.P. Johnston, A Performance Prediction Method for Unstalled Two-Dimensional Diffusers, J. of Basic Engineering, ASME Transactions, 89 (1967), pp. 643-652.

## APPENDIX A

In the computation of confined flows the pressure gradient along the flow is usually the unknown parameter to be calculated. The finite difference equations given in section 2, along with the supporting relations given in Appendix A of Ref. 7, favor the case in which the pressure gradient is the specified variable and the duct area along the flow is the unknown quantity to be calculated. When the pressure gradient is the unknown quantity these equations, as discussed earlier, are solved iteratively. Two questions arise in regard to the pressure iteration. One, how to adjust the previously used  $\Delta p$  (pressure drop across  $\Delta x$ ) for the succeeding iteration. Second, how best to estimate starting  $\Delta p$  at the beginning of a new integration step. In this appendix we have summarized our current know-how in regard to these two questions.

Applying conservation principles approximately across  $x$  and  $x + \Delta x$  we can derive the following equations:

$$p' = \frac{\dot{m}U_2}{A_1A_2\left(1 - \frac{\dot{m}U_2}{A_1p_2}\right)} A' \quad (A-1)$$

$$U' = \frac{U_2}{A_2\left(\frac{\dot{m}U_2}{A_1p_2} - 1\right)} A' = -\frac{A_1}{\dot{m}} p' \quad (A-2)$$

Equation (A-1) is derived in Appendix C of Ref. 7 and Eq. (A-2) follows easily from the equations given in that appendix. In these equations

$U_2$  is average velocity at  $x + \Delta x$

$A_1$  duct area at  $x$ ,

$A_2$  duct area at  $x + \Delta x$

$\dot{m}$  mass flow rate

$p_2$  pressure at  $x + \Delta x$

$A'$  small change in  $A_2$

$p'$  small change in  $\Delta p$

$U'$  small change in  $U_2$

$\theta = \infty$  for incompressible flows

$\gamma =$  ratio of specific heats for compressible flows

We also introduce the following nomenclature for later use:

DPDTL specified tolerance within which the pressure gradient is to be calculated (put into the program as a dimensionless number, DPDTL = 0.01 means that the pressure gradient is to be calculated within  $\pm 1\%$ ),

ZTLRN tolerance for the calculation of the duct area,

UTLRN tolerance in the calculation of velocity at  $x + \Delta x$ .

At the beginning of the MAIN program DPDTL is specified through an assignment statement. Given DPDTL ( $p'$ ) Eq. (A-1) specifies the tolerance limit within which the duct area must be calculated to meet the pressure gradient tolerance. Equation (A-2) tells how closely  $U_2$  must be calculated during the velocity iteration loop. At the beginning of a new integration step Eqs. (A-1) and (A-2) are used to calculate ZTLRN ( $A'$ ) and UTLRN ( $U'$ ) from the specified DPDTL ( $p'$ ). Then with an initial estimate of  $\Delta p$  we start the velocity iteration loop until  $U_2$  at  $x + \Delta x$  converges within

UTLRN. We next check calculated  $A_2$  against the specified  $A_2$ . If the difference, called  $A'$ , is greater than ZTLRN we change  $\Delta p$  by  $p'$ , calculated from Eq. (A-1) using  $A'$ , for the succeeding pressure iteration. Note Eq. (A-1) does double duty--at the beginning of a new integration step it is used to calculate ZTLRN for that integration step and then during the pressure iteration loop it is used to correct  $\Delta p$  for the next iteration using  $A'$  from the last iteration. In the actual computations Eqs. (A-1) and (A-2) are used with  $U_2$  replaced by the known center-line velocity at  $x$ ,  $p_2$  by  $p_1$ ,  $A_2$  by  $A_1$ , and  $U'$  as the variation of  $U_2$  ( $U$  along streamline 2). To make up partly for these approximations and partly for those that went into the derivation of Eq. (A-1), Eq. (A-1) when employed within the pressure iteration loop, to calculate adjustment to  $\Delta p$  from  $A'$ , is used along with a damping factor. Correction  $p'$  calculated from (A-1) is decreased by the factor

$$\text{DPDAMP} = 0.5 \times \exp \left( -0.115 \frac{\text{distance along the duct}}{\text{half duct width or radius}} \right) . \quad (\text{A-3})$$

We next turn our attention to the estimation of initial  $\Delta p$ , call it  $\Delta p_I$ , at the beginning of each new integration step. Denote the final calculated  $\Delta p$  at the given integration step by  $\Delta p_F$ . In our earlier computations  $\Delta p_I$  at  $x_i$  was calculated from  $\Delta p_F$  at  $x_{i-2}$  and  $x_{i-1}$  using straight line projection. In Fig. (A-1a) is shown the distribution, using this approach, of  $\Delta p_I(x)$  and  $\Delta p_F(\odot)$  along part of a duct. The flow is through a rectangular diffuser. Note the flip-flop nature of the distribution of  $\Delta p_I$  with respect to mean  $\Delta p/\Delta x$  versus  $x$  curve. Note



X Initial estimates of  $\Delta p/\Delta X$

○ Final calculated values of  $\Delta p/\Delta X$

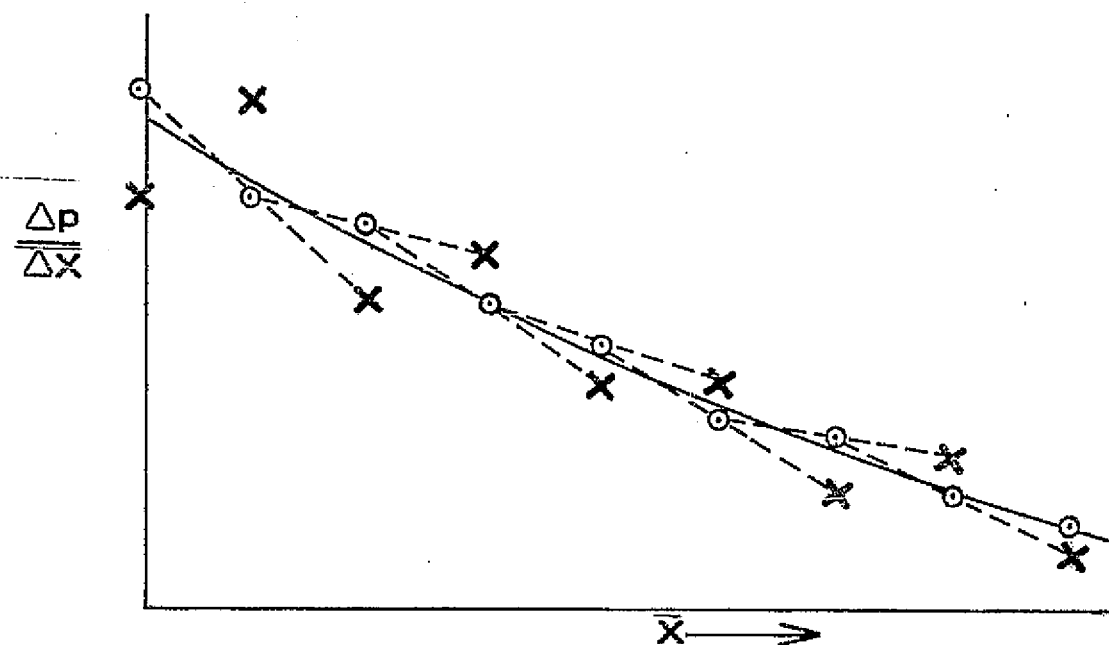


Fig. (A-1a). Initial pressure gradient estimated from previous two calculated values using a linear relation.

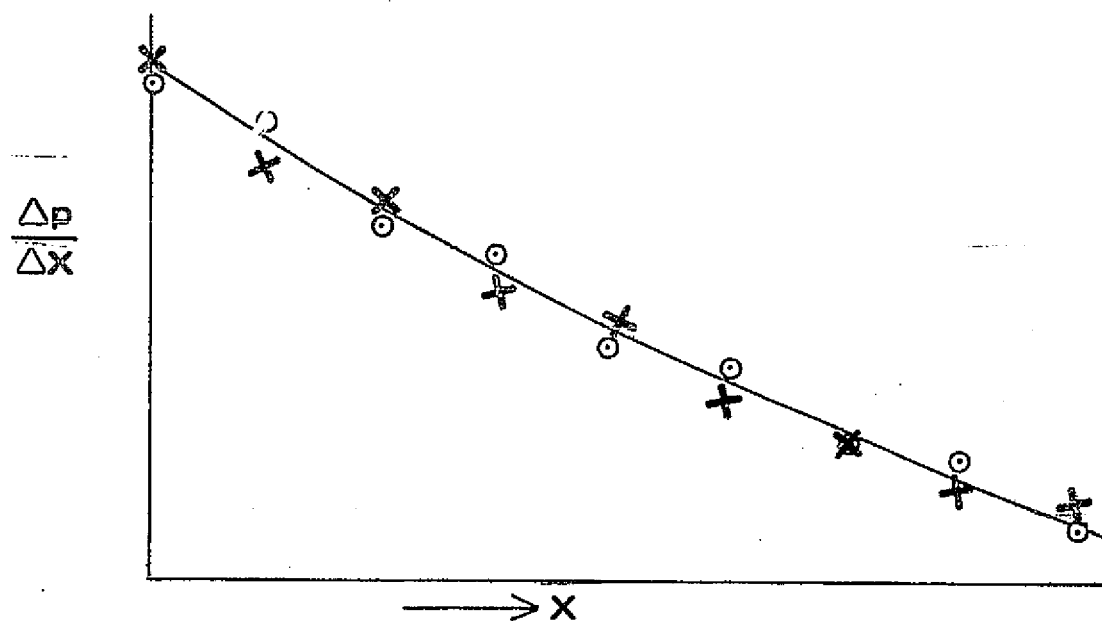


Fig. (A-1b). Initial pressure gradient estimated from previous three calculated values using regression analysis.

also that to estimate  $\Delta p_I$  by fitting second order curve through  $\Delta p_F$  at  $x_{i-3}$ ,  $x_{i-2}$ , and  $x_{i-1}$  will worsen the estimate of  $\Delta p_I$ .

Since  $\Delta p_F$  is calculated not exactly but within a specified limit, the values of  $\Delta p_F$  will fall randomly about the mean  $\Delta p/\Delta x$  versus  $x$  curve. Thus  $\Delta p_I$  at  $x_i$  should be calculated from  $\Delta p_F$  at previous steps on statistical basis. In our later computations  $\Delta p_I$  at  $x_i$  was projected from  $\Delta p_F$  at  $x_{i-3}$ ,  $x_{i-2}$ , and  $x_{i-1}$  using regression analysis. Distribution of  $\Delta p_I$  and  $\Delta p_F$  using this approach is shown in Fig. (A-1b). Figures (A-1a) and (A-1b) are for the same flow over the same section of the duct. Estimation of  $\Delta p_I$  using regression analysis has improved the convergence rate in our computations.

In the program listing given in section 3  $\Delta p_I$  at  $x_i$  is calculated from previous three values of  $\Delta p_F$  using the following formulae:

$$\Delta p = \text{DPSLOP } x_i + \text{DPZERO} \quad (\text{A-4})$$

$$\text{DPSLOP} = \frac{3 \sum \Delta p_i x_i - (\sum \Delta p_i)(\sum x_i)}{3 \sum x_i^2 - (\sum x_i)^2} \quad (\text{A-5})$$

$$\text{DPZERO} = \frac{(\sum \Delta p_i)(\sum x_i^2) - (\sum x_i)(\sum x_i \Delta p_i)}{3 \sum x_i^2 - (\sum x_i)^2} \quad (\text{A-6})$$

In the program  $x$  at the first of the three points to be projected is taken equal to zero. Near the entrance before three  $\Delta p_F$  are available  $\Delta p_I$  is set simply equal to the last  $\Delta p_F$ .

## APPENDIX B

### STREAMWISE COMPUTATION OF DUCT FLOWS

Mahesh S. Greywall  
Department of Mechanical Engineering  
Wichita State University  
Wichita, Kansas 67208

#### ABSTRACT

A computational method to calculate momentum and energy transport in two-dimensional viscous compressible duct flows is presented. The flow in the duct is partitioned into finite streams. The difference equations are then obtained by applying momentum and energy conservation principles directly to the individual streams. The method is applicable to laminar and turbulent flows.

## I. INTRODUCTION

Two-dimensional effects in duct flows, such as the growth of momentum and thermal boundary layers, have been studied for a long time by separating the flow into a core flow and a boundary layer [1]. Two-dimensional effects associated with sudden changes in duct shape in incompressible flows have been successfully computed using vorticity transport equation [2]. In high temperature compressible flows such as those encountered in magnetohydrodynamic (MHD) channels separation of flow into a uniform core and a boundary layer is difficult except at the very beginning of the channel. The difficulties arise from (1) large temperature differences between the wall and the core flow which lead to temperature gradients within the core and (2) shrinking size of the core as the flow proceeds down the channel. Also in calculating performance of diffusers with high inlet blockage factor, as in MHD diffusers, one cannot separate the flow into a core and a boundary layer. Computation of such flows have been recently carried out mostly using equations obtained by von Mises transformation of boundary layer equations [3,4,5]. Some MHD channel calculations have also been carried out using Fluid-in-Cell Method [6,7].

We have in this article presented a new approach to compute internal flows without separating the flow into a core and a boundary layer. A novel feature of this approach is the method by which the difference equations are obtained. In most of the approaches one starts with the differential equations, such as energy equation, Navier-Stokes equations, which are obtained from the conservation principles. These equations

either in their primitive forms or in transformed forms are then differenced to obtain the finite difference equations needed to compute the flow. In the present approach the flow in the duct is portioned into finite streams and the finite difference equations are then obtained by applying conservation principles directly to the individual streams. The resulting equations are similar to the ones obtained previously [3,4] by the procedure: derive boundary layer equations from the conservation principles via energy and Navier-Stokes equations--carry out von Mises transformation of the boundary layer equations--finite difference the transformed equations using integral method finite differencing. In contrast, in the present approach there is direct relationship between the finite difference equations and their roots, the conservation principles. This direct relationship, we think, makes it easier to introduce approximations allowed by the flow being simulated and also to incorporate any special features of the flow.

In section II we have presented the finite difference equations based on the new approach and in section III discussed their solution techniques. The discussion is limited to two-dimensional flows. The application of the present approach to compute three-dimensional effects is straightforward and is indicated at the end of section III. In the main body of the paper we have tried to present the new approach in broad and general terms to make its application easier to specific problems requiring individual handling. Some specific details are given in Appendices A and B. To provide an assessment of the present approach we have carried out sample computations of turbulent flow in a smooth pipe. The results are shown in Appendix C and are compared

with experimental data and other works. We have also used this approach to compute two-dimensional viscous compressible turbulent flows in hydrogen-oxygen combustion driven MHD ducts [8] and are currently using it to calculate diffuser performance with high inlet blockage factors.

## II. FINITE DIFFERENCE EQUATIONS

Consider two dimensional duct flow as shown in Fig. 1. The direction  $x$  is taken along the flow and  $z$ , measured from the duct wall, normal to it. For circular ducts  $z$  represents the radial distance from the wall. For rectangular ducts the variation of flow properties normal to  $z$  and  $x$  are neglected. We partition the total flow in the duct into a sequence of finite streams. To accomplish this partitioning we draw a series of streamlines  $1, 2, \dots, N$  as shown in Fig. 1. Streamline 1 is taken along the wall and streamline  $N$  represents the duct center or the symmetry line. The spacing between any two consecutive streamlines is determined by the desired resolution of the local gradients normal to the flow. We define streamline  $j+1/2$  as the streamline passing through the middle of  $j$  and  $j+1$ . Streamline  $j-1/2$  is defined similarly. The stream  $j$ , in general, is now defined to be the flow bounded by streamlines  $j-1/2$  and  $j+1/2$ . The shape of the stream, of course, depends on the shape of the duct: in rectangular ducts the streams will be plane layers and in circular ducts the streams will be cylindrical shells. Stream 2 is defined to be the flow between the wall and streamline  $2+1/2$ . Stream  $N$  is defined to be the flow between the streamline  $N-1/2$  and the center or symmetry line  $N$ .

We introduce the following nomenclature:

$\psi_j^+$ ; mass flow rate between the streamline  $j$  and  $j+1/2$ .

$\psi_j^-$ ; mass flow rate between the streamline  $j$  and  $j-1/2$ .

Note  $\psi_j^+ + \psi_j^-$  represents the mass flow rate through stream  $j$ . For calculations of  $\psi_j$ 's see Appendix A.

$u_j(x)$ ,  $T_j(x)$ ,  $\rho_j(x)$ ,  $h_j(x)$ ,  $C_j(x)$ ; velocity, temperature, density, enthalpy and constant pressure specific heat along the streamline  $j$ .

$z_j(x)$ ; distance of streamline  $j$  from the wall.

$A_j^x$ ; cross-sectional area of stream  $j$  (see Appendix A).

$\mu_{j+1/2}(x)$ ,  $k_{j+1/2}(x)$ ; effective viscosity and thermal conductivity (including turbulent contribution when the flow is turbulent) along streamline  $j+1/2$ . These are the coefficients that are later used to calculate momentum and energy transfer between the stream  $j$  and  $j+1$  across the interface at  $j+1/2$ .

Other nomenclature is introduced as we go along.

The difference equations to calculate the flow properties are now obtained by applying conservation principles directly to the individual streams. We assume that the streamlines are chosen sufficiently close so that the variation of the flow properties between any two successive streamlines  $j$  and  $j+1$  can be approximated as linear. Note the flow properties  $u_j$ ,  $T_j$ , etc., though not their gradients, are continuous across these streamlines. However, across the interface of the streams, i.e. across streamlines  $j+1/2$ , the gradients are also continuous thus determining, unambiguously, momentum and energy transfer between the adjoining streams.

Applying momentum balance to stream  $j$  between  $x$  and  $x+\Delta x$ , i.e. applying the momentum balance to the control volume bounded by  $x$ ,  $x+\Delta x$ ,  $j-1/2$ , and  $j+1/2$ , we obtain,

$$\begin{aligned} & \text{Momentum Flux Out} \Big|_{\text{at } x+\Delta x} - \text{Momentum Flux In} \Big|_{\text{at } x} \\ & = \text{Pressure Forces} + \text{Viscous Forces} + \text{Body Forces} \end{aligned} \quad (1)$$



Estimation of the various quantities in Eq. (1) allows a great deal of flexibility to accommodate the desired accuracy and any special features of the given flow. We here present one such approximation for stream  $j$ , (streams 2 and  $N$  require special treatment and are considered later separately).

$$\begin{aligned}
 & \left[ \psi_j^+ \left( \frac{3u_j^+ + u_{j+1}^+}{4} \right) + \psi_j^- \left( \frac{3u_j^+ + u_{j-1}^+}{4} \right) \right] \\
 & - \left[ \psi_j^+ \left( \frac{3u_j^+ + u_{j+1}}{4} \right) + \psi_j^- \left( \frac{3u_j^+ + u_{j-1}}{4} \right) \right] \\
 & = -\Delta p A_j^x + \frac{1}{2} \left[ V_{j+1/2}^+ (u_{j+1}^+ - u_j^+) + V_{j+1/2}^- (u_{j+1} - u_j) \right] \\
 & - \frac{1}{2} \left[ V_{j-1/2}^+ (u_j^+ - u_{j-1}^+) + V_{j-1/2}^- (u_j - u_{j-1}) \right] + F_j \quad (2)
 \end{aligned}$$

On the left hand side of Eq. (2) the expressions involving  $\psi_j^+$  represents the momentum flux between  $j$  and  $j+1/2$  and those involving  $\psi_j^-$  the momentum flux between  $j-1/2$  and  $j$ . The superscript  $+$  indicates the unknown velocities at  $x+\Delta x$ ,  $\Delta p$  the pressure difference between  $x+\Delta x$  and  $x$ , and  $F_j$  the sum of body forces on the control volume. Also we have introduced

$$V_{j+1/2}^+ = \frac{z_{j+1} - z_j}{z_{j+1} - z_j} A_{j+1/2}^s, \quad V_{j-1/2}^+ = \frac{z_j - z_{j-1}}{z_j - z_{j-1}} A_{j-1/2}^s \quad (3)$$

where  $A_{j+1/2}^s$  and  $A_{j-1/2}^s$  represent the upper and lower surface areas of the control volume (see Appendix A for calculation of  $A^s$ 's). Terms  $V_{j+1/2}^+$  and  $V_{j-1/2}^+$  are defined similarly with  $\mu$ 's and  $z$ 's evaluated at  $x+\Delta x$ . Note we have estimated the viscous forces on a given surface by taking the average

of those at  $x$  and  $x + \Delta x$ . Rewriting Eq. (2) with all the unknown velocities collected on the left hand side we obtain,

$$\begin{aligned}
 & -u_{j+1}^+ \left[ -\frac{\psi_j^+}{4} + \frac{1}{2}v_{j+1/2}^+ \right] + u_j^+ \left[ \frac{3}{4}\psi_j^+ + \frac{3}{4}\psi_j^- + \frac{1}{2}v_{j+1/2}^+ + \frac{1}{2}v_{j-1/2}^+ \right] \\
 & - u_{j-1}^+ \left[ -\frac{\psi_j^-}{4} + \frac{1}{2}v_{j-1/2}^+ \right] \\
 & = -\Delta p A_j^x + u_{j+1} \left[ \frac{\psi_j^+}{4} + \frac{1}{2}v_{j+1/2} \right] + u_j \left[ \frac{3}{4}\psi_j^+ + \frac{3}{4}\psi_j^- - \frac{1}{2}v_{j+1/2} - \frac{1}{2}v_{j-1/2} \right] \\
 & + u_{j-1} \left[ \frac{\psi_j^-}{4} + \frac{1}{2}v_{j-1/2} \right] + F_j \\
 & j = 3, 4, \dots, N-1
 \end{aligned} \tag{4}$$

Similarly, application of momentum balance to stream  $N$ , after some rearrangement, yields

$$\begin{aligned}
 & u_N^+ \left[ \frac{3}{4}\psi_N^- + \frac{1}{2}v_{N-1/2}^+ \right] - u_{N-1}^+ \left[ -\frac{\psi_N^-}{4} + \frac{1}{2}v_{N-1/2}^+ \right] \\
 & = -\Delta p A_N^x + u_N \left[ \frac{3}{4}\psi_N^- - \frac{1}{2}v_{N-1/2} \right] + u_{N-1} \left[ \frac{\psi_N^-}{4} + \frac{1}{2}v_{N-1/2} \right] + F_N
 \end{aligned} \tag{5}$$

We note that Eq. (4) will yield Eq. (5) for  $j=N$  if we were to set  $\psi_N^+$ ,  $v_{N+1/2}^+$ ,  $v_{N+1/2}$ , and  $u_{N+1}$  equal to zero. Thus by initializing these quantities equal to zero at the beginning of a computer program stream  $N$  can be treated by the general formula for stream  $j$ .

Next we will treat Stream 2. This stream requires considerably more computational finesse. The sources of the difficulty are (1) occurrence of steep

gradients normal to the flow near the wall and (2) reckoning of wall surface roughness for turbulent flows. For laminar flows the wall surface roughness does not affect the flow and the gradients are not as steep and the flow can be simulated by taking streams sufficiently thin next to the wall. For turbulent flows we let go of the assumption that the velocity varies linearly between the wall and streamline 2. The momentum flux through the lower half of the stream 2 is estimated as some  $\alpha$  times  $\psi_2^- u_2$  where  $\alpha$  takes into account the nonlinearity of the velocity distribution next to the wall. Also the viscous force at the lower face of stream 2, that is at the wall, is calculated from the Reynold's number along streamline 2 taking into account the wall surface roughness. Proceeding accordingly, we obtain by applying momentum balance to stream 2

$$\begin{aligned}
 & \left[ \psi_2^+ \left( \frac{3u_2^+ + u_3^+}{4} \right) + \psi_2^- \alpha u_2^+ \right] - \left[ \psi_2^+ \left( \frac{3u_2^+ + u_3}{4} \right) + \psi_2^- \alpha u_2 \right] \\
 &= -\Delta p A_2^x + \frac{1}{2} \left[ V_{2+1/2}^+ (u_3^+ - u_2^+) + V_{2+1/2} (u_3 - u_2) \right] \\
 &= -\frac{1}{2} \left[ V_1^+ u_2^+ + V_1 u_2 \right] + F_2 \tag{6}
 \end{aligned}$$

Coefficients  $V_{2+1/2}^+$  and  $V_{2+1/2}$  are given by the general expression for  $V_{j+1/2}$  presented earlier. For programming ease viscous forces along the wall have been expressed as  $V_1 u_2$  similar to viscous forces at the other interfaces. However  $V_1$  is defined differently from other  $V$ 's. Estimations of  $V_1$  and  $\alpha$  for turbulent flows are discussed in Appendix B. When the flow is laminar Eq. (6) can be used for the momentum balance for stream 2 with  $\alpha$  set equal to one half and  $V_1$  determined by

$$V_1 = \frac{\mu_1}{z_2} A_1^S \quad (\text{Laminar Flow}) \quad (7)$$

where the  $A_1^S$  represents the area of the lower surface of stream 2 and  $\mu_1$  the viscosity at the wall ( $V_1^+$  is determined similarly). Rearranging Eq. (6) we obtain

$$\begin{aligned} & -u_3^+ \left[ -\frac{\psi_2^+}{4} + \frac{1}{2}V_{2+1/2}^+ \right] + u_2^+ \left[ \frac{3}{4}\psi_2^+ + \alpha\psi_2^- + \frac{1}{2}V_{2+1/2}^+ + \frac{1}{2}V_1^+ \right] \\ & = -\Delta p A_2^X + u_3^+ \left[ \frac{\psi_2^+}{4} + \frac{1}{2}V_{2+1/2}^+ \right] + u_2^+ \left[ \frac{3}{4}\psi_2^+ + \alpha\psi_2^- - \frac{1}{2}V_{2+1/2}^+ - \frac{1}{2}V_1^+ \right] + F_2 \end{aligned} \quad (8)$$

Equations (4), (5), and (8) provide  $N-1$  equations to solve for the  $N-1$  unknown velocities  $u_2^+, u_3^+, \dots, u_N^+$ .

Equations for the unknown enthalpies  $h_j^+$  at  $x + \Delta x$  are obtained by applying conservation of energy to the control volume under consideration;

$$\text{Energy Flux Out} \Big|_{\text{at } x + \Delta x} - \text{Energy Flux In} \Big|_{\text{at } x} =$$

Heat Added By Conduction + Work Done by Viscous Forces +

$$Q_j \text{ (Internal Heat Generated)} + W_j \text{ (Work Done by the Body Forces)} \quad (9)$$

The different terms in Eq. (9) can be estimated with varying degree of accuracy (and the accompanying complexity) to reflect their relative importance for the flow being simulated. One estimate for stream  $j$  is as follows:

$$\begin{aligned} \text{Energy Flux In} &= \frac{\psi_j^+}{4} \left[ 3h_j + h_{j+1} + \frac{1}{2}(3u_j^2 + u_{j+1}^2) \right] \\ &+ \frac{\psi_j^-}{4} \left[ 3h_j + h_{j-1} + \frac{1}{2}(3u_j^2 + u_{j-1}^2) \right] \end{aligned}$$

Expression for energy flux out is obtained from the expression for the energy flux in by adding superscript + to h's and u's.

$$\begin{aligned} & \text{Heat added by conduction across the upper surface of the control volume} \\ &= \frac{1}{2} H_{j+1/2}^+ (h_{j+1}^+ - h_j^+) + \frac{1}{2} H_{j+1/2} (h_{j+1} - h_j) \end{aligned}$$

where we have introduced

$$H_{j+1/2}^+ = \frac{k_{j+1/2}^+}{C_j^+ (z_{j+1}^+ - z_j^+)} A_{j+1/2}^S \quad \text{and} \quad H_{j+1/2} = \frac{k_{j+1/2}}{C_j (z_{j+1} - z_j)} A_{j+1/2}^S \quad (10)$$

The H terms can be expressed in terms of  $\nu$  by using  $Pr$ , the Prandtl number.

Thus we can write

$$H_{j+1/2} = \frac{\nu_{j+1/2}}{Pr_{j+1/2}} \quad \text{where} \quad Pr_{j+1/2} = \frac{\mu_{j+1/2} C_j}{k_{j+1/2}} \quad (11)$$

Work done by the viscous forces on the upper surface

$$\begin{aligned} &= \frac{1}{2} \left[ \nu_{j+1/2}^+ (u_{j+1}^+ - u_j^+) \left( \frac{u_{j+1}^+ + u_j^+}{2} \right) + \nu_{j+1/2} (u_{j+1} - u_j) \left( \frac{u_{j+1} + u_j}{2} \right) \right] \\ &= \frac{1}{4} \left[ \nu_{j+1/2}^+ (u_{j+1}^{+2} - u_j^{+2}) + \nu_{j+1/2} (u_{j+1}^2 - u_j^2) \right] \end{aligned}$$

Expressions for the heat transferred and the work done across the lower surface can be written down from the corresponding one's for the upper surface by replacing  $j+1$  by  $j$ ,  $j$  by  $j-1$ , and  $j+1/2$  by  $j-1/2$ . Substituting the various estimates into Eq. (7) and rearranging to get all the unknown  $h_j^+$ 's on the left hand side of the equation we get,

$$\begin{aligned}
& -h_{j+1}^+ \left[ -\frac{\psi_j^+}{4} + \frac{1}{2}H_{j+1/2}^+ \right] + h_j^+ \left[ \frac{3}{4}\psi_j^+ + \frac{3}{4}\psi_j^- + \frac{1}{2}H_{j+1/2}^+ + \frac{1}{2}H_{j-1/2}^+ \right] \\
& - h_{j-1}^+ \left[ -\frac{\psi_j^-}{4} + \frac{1}{2}H_{j-1/2}^+ \right] \\
= & h_{j+1}^+ \left[ \frac{\psi_j^+}{4} + \frac{1}{2}H_{j+1/2}^+ \right] + h_j^+ \left[ \frac{3}{4}\psi_j^+ + \frac{3}{4}\psi_j^- - \frac{1}{2}H_{j+1/2}^+ - \frac{1}{2}H_{j-1/2}^+ \right] \\
& + h_{j-1}^+ \left[ \frac{\psi_j^-}{4} + \frac{1}{2}H_{j-1/2}^+ \right] + \frac{u_{j+1}^+}{2} \left[ -\frac{\psi_j^+}{4} + v_{j+1/2}^+ \right] \\
& - \frac{u_j^+}{2} \left[ \frac{3}{4}\psi_j^+ + \frac{3}{4}\psi_j^- + v_{j+1/2}^+ + v_{j-1/2}^+ \right] + \frac{u_{j-1}^+}{2} \left[ -\frac{\psi_j^-}{4} + v_{j-1/2}^+ \right] \\
& + \frac{u_{j+1}^2}{2} \left[ \frac{\psi_j^+}{4} + v_{j+1/2}^+ \right] + \frac{u_j^2}{2} \left[ \frac{3}{4}\psi_j^+ + \frac{3}{4}\psi_j^- - v_{j+1/2}^+ - v_{j-1/2}^+ \right] \\
& + \frac{u_{j-1}^2}{2} \left[ \frac{\psi_j^-}{4} + v_{j-1/2}^+ \right] + Q_j + W_j
\end{aligned}$$

(12)

for  $j = 3, 4, \dots, N-1$

The equation that results on applying the energy balance to stream N can be obtained from Eq. (12) by letting j equal to N and setting  $\psi_N^+$ ,  $h_{n+1}^+$ ,  $h_{n+1}$ ,  $u_{N+1}^+$ ,  $u_{N+1}$ ,  $H_{N+1/2}^+$ ,  $H_{N+1/2}$ ,  $v_{N+1/2}^+$ , and  $v_{N+1/2}$  equal to zero.

Next, following the procedure outlined for the momentum balance, we apply energy balance to stream 2 to obtain,

$$\begin{aligned}
& \frac{\psi_2^+}{4} \left[ (3h_2^+ + h_3^+) + \frac{1}{2}(3u_2^{+2} + u_3^{+2}) \right] \\
& - \frac{\psi_2^+}{4} \left[ (3h_2 + h_3) + \frac{1}{2}(3u_2^2 + u_3^2) \right] \\
& + \psi_2^- \left[ \beta(h_2^+ - h_w^+) + \delta \frac{1}{2}u_2^{+2} \right] - \psi_2^- \left[ \beta(h_2 - h_w) + \frac{1}{2}\delta u_2^2 \right] \\
& = \frac{1}{2} \left[ H_{2+1/2}^+(h_3^+ - h_2^+) + H_{2+1/2}(h_3 - h_2) \right] - q_w \\
& + \frac{1}{4} \left[ V_{2+1/2}^+(u_3^{+2} - u_2^{+2}) + V_{2+1/2}(u_3^2 - u_2^2) \right] + Q_2 + W_2
\end{aligned} \tag{13}$$

In Eq. (13)  $\beta$  and  $\delta$  are correction factors to take care of nonlinear variation between wall and the streamline 2 when the flow is turbulent and are further discussed in Appendix B. Also in Eq. (13)  $h_w$  represents the enthalpy evaluated at the wall temperature and  $q_w$  the heat transfer to the wall. For flows with wall temperature specified  $q_w$  can be written as

$$q_w = \frac{1}{2} \left[ H_1^+(h_2^+ - h_w^+) + H_1(h_2 - h_w) \right] \tag{14}$$

where  $H_1$  is calculated from  $V_1$  via the relation given in Eq. (11). When  $q_w$  is specified Eq. (14) is used to eliminate  $h_w$  and  $h_w^+$  appearing on the left hand side of Eq. (13). Equations (12), (13) and (14) provide  $N$  equations for the  $N$  unknowns  $h_N, h_{N-1}, \dots, h_2$  and either one of  $h_w$  or  $q_w$ .

The proceeding equations for the calculations of  $u_j^+$ 's and  $h_j^+$ 's are to be supplemented with equations given in Appendices A and B to calculate the duct width at  $x + \Delta x$  in terms of  $u_j^+$ 's and  $\rho_j^+$ 's.

In summary, Eqs. (4), (5), (8), (12), (13), (14), (B-2), (A-13) [or (B-3), (A-14), and (A-15)], along with the thermodynamic relations interrelating  $h$ ,  $\rho$ ,  $T$ , and  $p$  are our basic set of equations to calculate the two dimensional duct flow.



### III. SOLUTION TECHNIQUE

Overall methodology adopted to solve the duct flow equations will depend upon the given design specifications, e.g. pressure gradient is specified or variation of duct width is specified, etc. In any case one has to solve the momentum and energy difference equations given in section II. The set of simultaneous equations to solve for new  $u_j^+$ , as also the set to solve for new  $h_j^+$ , are of the general form

$$-a_j X_{j+1} + b_j X_j - c_j X_{j-1} = d_j, \quad (15)$$

where  $X_j$  stands for the unknowns  $u_j^+$  or  $h_j^+$ . Coefficients  $a_j$ ,  $b_j$  and  $c_j$  due to their dependence on  $V_j^+$  or  $H_j^+$  are indirectly functions of  $X_j$ . Thus Eq. (15) is nonlinear. If we had approximated the viscous forces and the heat transfer across stream interfaces by their values at  $x$  rather than by their averages between  $x$  and  $x + \Delta x$  coefficients  $a_j$ ,  $b_j$  and  $c_j$  would have been independent of  $X_j$ . In that case Eq. (15) will constitute a set of linear tri-diagonal equations and can be solved directly by the standard algorithm to solve such equations. In the present case these equations are solved by iteration.

At first we calculate  $a_j$ ,  $b_j$ , and  $c_j$  for the momentum difference equations setting  $V^+$  equal to  $V$  and solve for new  $u_j^+$  using the algorithm to solve directly tri-diagonal equations. With these new  $u_j^+$  and  $H^+$  set equal to  $H$  we calculated  $a_j$ ,  $b_j$ ,  $c_j$  and  $d_j$  for the energy difference equations and solve for  $h_j^+$ . Next we calculate  $z_j^+$  using newly calculated flow properties at  $x + \Delta x$ . The procedure is then repeated this time around calculating  $V^+$  and  $H^+$  using the newly calculated values of  $u_j^+$ ,  $z_j^+$ , etc. The iteration

is continued until the desired convergence is achieved. The number of required iterations increases, in regions of rapidly changing temperature and velocity profiles. These are also the regions where had we calculated  $a_j$ ,  $b_j$  and  $c_j$  from  $V$  and  $H$  alone (instead  $V$ ,  $V^+$  and  $H$ ,  $H^+$ ) the error introduced by such approximation would have been the greatest.

When the pressure gradient is specified the  $z_j^+$ 's calculated at the end of the last iteration give the channel width at  $x + \Delta x$ . When the channel width is specified iteration on pressure gradient is required. The iteration in the pressure gradient can be performed either over and above the iteration on  $V^+$  and  $H^+$  or combined into the  $V^+$ - $H^+$  iteration loop. In the latter case at the end of each iteration when new  $z_j^+$  and thus the channel width at  $x + \Delta x$  is calculated the assumed pressure gradient is readjusted.

We conclude this section by indicating how the present approach can be used to calculate three-dimensional flows. In three-dimensional case one will partition the flow in the duct into three-dimensional streams. In rectangular channels the streams now instead of being plane layers as in two-dimensional case will be rectangular bars. The difference equations to calculate the flow can now be written down as in the two dimensional case except now when calculating viscous forces acting upon the control volume and the heat conducted into it one will have to take into account four neighboring streams. The resulting equations now will be pentadiagonal and will require more computational time to solve.

## APPENDIX A

In this appendix we present formulae for calculating  $\psi_j^+$ ,  $\psi_j^-$ ,  $A_j^x$ ,  $A_j^s$ , and  $z_j$  for the rectangular and cylindrical ducts. These are the formulae we have used in our computational works and can be easily modified to fit the requirements of other problems. For cylindrical ducts we introduce  $r_j$ , the distance of streamline  $j$  from the centerline. For duct of radius  $R_0$ ,  $r_j$  and  $z_j$  are related by

$$r_j = R_0 - z_j \quad (A-1)$$

For rectangular ducts the formulae are for a duct of unit width. (Formulae are presented in forms to reveal their origin. They can be further contracted or simplified for computational efficiency.)

### MASS FLOW RATES

#### (a) Rectangular Ducts

$$\psi_j^+ = \left( \frac{3\rho_j u_j + \rho_{j+1} u_{j+1}}{4} \right) \left( \frac{z_{j+1} + z_j}{2} - z_j \right)$$

$$j = 2, 3, \dots, N-1 \quad (A-2)$$

$$\psi_j^- = \left( \frac{3\rho_j u_j + \rho_{j-1} u_{j-1}}{4} \right) \left( z_j - \frac{z_j + z_{j-1}}{2} \right)$$

$$j = 3, 4, \dots, N \quad (A-3)$$

(b) Cylindrical Ducts

$$\psi_j^+ = \left( \frac{3\rho_j u_j + \rho_{j+1} u_{j+1}}{4} \right) \pi \left[ r_j^2 - \left( \frac{r_j + r_{j+1}}{2} \right)^2 \right]$$

$$j = 2, 3, \dots, N-1 \quad (A-4)$$

$$\psi_j^- = \left( \frac{3\rho_j u_j + \rho_{j-1} u_{j-1}}{4} \right) \pi \left[ \left( \frac{r_j + r_{j-1}}{2} \right)^2 - r_j^2 \right]$$

$$j = 3, 4, \dots, N-1 \quad (A-5)$$

$$\psi_N^- = \left( \frac{3\rho_N u_N + \rho_{N-1} u_{N-1}}{4} \right) \pi r_{N-1}^2 / 4 \quad (A-6)$$

Calculations of  $\psi_2^-$  are discussed in Appendix B.

CROSS-SECTIONAL AREAS

(a) Rectangular Ducts

$$A_2^x = \frac{z_3 + z_2}{2} \quad (A-7)$$

$$A_j^x = \frac{z_{j+1} - z_{j-1}}{2} \quad (A-8)$$

$$j = 3, 4, \dots, N-1$$

$$A_N^x = \frac{z_N - z_{N-1}}{2} \quad (A-9)$$

(b) Cylindrical Ducts

$$A_2^x = \pi \left[ r_1^2 - \left( \frac{r_2 + r_3}{2} \right)^2 \right] \quad (A-10)$$

$$A_j^x = \pi \left[ \left( \frac{r_j + r_{j-1}}{2} \right)^2 - \left( \frac{r_j + r_{j+1}}{2} \right)^2 \right] \quad (A-11)$$

$$j = 3, 4, \dots, N-1$$

$$A_N^x = \pi r_{N-1}^2 / 4 \quad (A-12)$$

$z_j$  AND  $r_j$  TERMS

When the  $p$ 's and  $u$ 's have been calculated at a new position along the duct the  $z$ 's and  $r$ 's at the new position are then calculated by the following formulae,

(a) Rectangular Ducts

After  $z_2$  has been calculated as discussed in Appendix B we calculate  $z_3, z_4, \dots, z_N$  by

$$z_j = z_{j-1} + \frac{2(\psi_{j-1}^+ + \psi_j^-)}{\rho_j u_j + \rho_{j-1} u_{j-1}} \quad (A-13)$$

(b) Circular Ducts

$$r_{N-1} = \left[ \frac{8(\psi_{N-1}^+ + \psi_N^-)}{\pi(3\rho_N u_N + 5\rho_{N-1} u_{N-1})} \right]^{1/2} \quad (A-14)$$

$$r_{j-1} = \left[ \frac{4\psi_{j-1}^+}{\pi(3u_{j-1} + u_j)} + \frac{4\psi_j^-}{\pi(3u_j + u_{j-1})} + r_j^2 \right]^{1/2}$$

$$j = N-1, \dots, 3.$$

(A-15)

Radius  $r_j$  is calculated as discussed in Appendix B.

#### SURFACE AREAS

##### (a) Rectangular Ducts

for all interfaces

$$A_{j+1/2}^S = \Delta x$$

(A-16)

##### (b) Circular Duct

for all interfaces

$$A_{j+1/2}^S = \Delta x \pi (r_j + r_{j+1})$$

(A-17)

## APPENDIX B

In this appendix we will discuss how to calculate the various correction factors that take into account the non-linear nature of velocity distribution between streamline 2 and the wall. There are many approaches possible to calculate these correction factors. The discussion that follows presents a method rather than the only one. For flow through circular pipes thickness of stream 2, i.e.  $z_2 - z_1$ , is assumed so small compared with the duct radius that we can neglect the curvature of stream 2. In evaluating the various integrals we have held  $\rho$  constant equal to some  $\bar{\rho}$ . For incompressible flows  $\bar{\rho}$  is, of course, just equal to  $\rho$ . For compressible flows  $\bar{\rho}$  is taken to be the average of  $\rho$  between streamline 2 and the wall.

We introduce mass flux correction factor,  $\gamma$ , by

$$\gamma = \frac{1}{u_2 z_2} \int_0^{z_2} u \, dz \quad (\text{B-1})$$

In terms of  $\gamma$  we can write

$$\psi_2^- = \gamma \bar{\rho} u_2 z_2 \quad (\text{B-2})$$

Equation (B-2) is used at the beginning to calculate  $\psi_2^-$  and later on to calculate  $z_2$  for rectangular ducts. For circular ducts  $r_1$  is calculated by

$$r_1 = r_2 + \psi_2^- / \gamma u_2 z_2 \quad (\text{B-3})$$

From their definitions we have for the correction factors  $\alpha$  and  $\delta$ ,

$$\alpha \psi_2^{-1} u_2 = \int_0^{z_2} \rho u^2 dz, \text{ that is}$$

$$\alpha = \frac{1}{\gamma u_2^2 z_2} \int_0^{z_2} u^2 dz, \quad (\text{B-4})$$

and similarly,

$$\delta = \frac{1}{\gamma u_2^3 z_2} \int_0^{z_3} u^3 dz \quad (\text{B-5})$$

If one assumes as is often done, that the variation of  $h$  in the near wall region is similar to  $u$  then the correction factor  $\beta$  will be obviously equal to  $\alpha$ . If some other variation of  $h$  is assumed then the integral

$$\beta = \frac{1}{\gamma u_2^2 z_2 h_2} \int_0^{z_2} h u dz$$

evaluated with the assumed variation of  $h$  will yield  $\beta$ .

The velocity distribution in the near wall region, needed to evaluate the proceeding integrals, is calculated from the relation

$$\mu_t \frac{du}{dz} = \tau_w \quad (\text{B-6})$$

where  $\tau_w$  is the shear stress at the wall and  $\mu_t$  is the viscosity including the turbulent contributions. To proceed further one must select some expression for  $\mu_t$ . To illustrate the procedure we use von Driest's relation [8]



for  $\mu_t$  (this relation has been successfully used in our own computations [7] and by several other authors [3,4]). For smooth walls we have from [8]

$$\mu_t = \mu + \rho k^2 z^2 \left[ 1 - \exp(-z\sqrt{\tau_w \rho}/\mu A) \right]^2 \frac{du}{dz} \quad (B-7)$$

where  $\mu$  is the laminar viscosity and  $k$  and  $A$  are constants. Introducing non-dimensional variables

$$z_* = z\sqrt{\tau_w \rho}/\mu, \quad \text{and} \quad u_* = \rho u/\sqrt{\tau_w \rho} \quad (B-8)$$

we obtain on integrating (B-6) using (B-7)

$$u_* = \int_0^{z_*} \frac{2dz_*}{1 + \left[ 1 + 4k^2 z_*^2 \{1 - \exp(-z_*/A)\}^2 \right]^{1/2}} \quad (B-9)$$

In terms of the non-dimensional variables integrals (B-1), (B-4), and (B-5) become, omitting the subscript 2,

$$\gamma = \frac{1}{u_* z_*} \int_0^{z_*} u_* dz_* \quad (B-10)$$

$$\alpha = \frac{1}{2 \gamma u_* z_*} \int_0^{z_*} u_*^2 dz_*, \quad \text{and} \quad (B-11)$$

$$\delta = \frac{1}{\gamma u_*^3 z_*} \int_0^{z_*} u_*^3 dz_* \quad (B-12)$$

Introducing friction factor,  $f$ , and Reynolds number,  $Re$ , we have in terms of non-dimensional variables

$$f = \frac{\tau_w}{\rho u^2} = \frac{1}{u_*^2}, \quad \text{and} \quad (B-13)$$

$$Re = \frac{\rho u z}{\mu} = u_* z_* . \quad (B-14)$$

After having calculated the velocity distribution from (B-9)  $\gamma$ ,  $\alpha$ ,  $\delta$ , and  $f$  can be next evaluated as functions of  $Re$  once and for all and the results then later used during the flow field computations. We have numerically integrated these integrals using  $k=0.4$  and  $A=26$ , the values recommended by Van Driest [8] for smooth walls. The results of the calculations are shown in Figs. (B-1) and (B-2). The numerically obtained relation between any of the factors and  $Re$  can now be stored for later use either by fitting a high order polynomial over the whole range of  $Re$  of interest or by breaking the range of  $Re$  into small segments and then approximating the relation over each segment by a straight line. The quantity  $V_1$  introduced in section II in Eq. (6) is in terms of  $f$  given by

$$V_1 = f \frac{\rho_1 + \rho_2}{2} u_2 \quad (B-15)$$

and  $V_1^+$  is given similarly with the quantities in the right hand side of (B-15) evaluated at  $x + \Delta x$ .

## APPENDIX C

In this appendix we present two sets of computations of turbulent flow in smooth pipes using the present approach. In these computations shear stress at the wall was calculated from the local Reynolds' number as discussed in Appendix B. Turbulent shear stress,  $\mu_t$ , in the main body of the flow was calculated using Prandtl's mixing length hypothesis,

$$\mu_t = \rho \ell^2 \left( \frac{du}{dz} \right)^2 \quad (C-1)$$

Variation of the mean free path,  $\ell$ , along  $z$ , the radial distance from the wall, was calculated from the equation

$$\frac{\ell}{R} = 0.14 - 0.08 \left( 1 - \frac{z}{R} \right)^2 - 0.06 \left( 1 - \frac{z}{R} \right)^4 \quad (C-2)$$

where  $R$  is the radius of the pipe. Relation given in (C-2) is obtained from the experimental data for pipes as discussed in Ref. [1].

### DEVELOPING FLOW

In the first set of the computations we calculated the developing velocity profiles in the inlet region of a smooth pipe starting with slug flow (radially uniform velocity) condition at the inlet. Computations were carried out with twenty radial grid points, with the grid spacing increasing as we moved away from the wall. Axial integration step,  $\Delta x$ , was taken at start equal to  $R/256$ . This  $\Delta x$  was doubled after each integration step until it reached the value  $R/4$ ; from there on

$\Delta x$  was held constant. The iteration in the pressure gradient was carried out over and above the iteration on  $V^+$  (refer to section III). The formula used to iterate on pressure gradient is discussed at the end of this appendix. The  $V^+$  iteration was carried until the velocity next to the wall varied less than 0.02 percent, and the pressure iteration was carried out until the pipe diameter at the new  $x$  was within 0.02 percent of its specified constant value. For each integration step it took a combined total of 5 to 6 iterations to meet both  $V^+$  and pipe diameter convergence criteria. The initial guess for pressure gradient at each new  $x$  was obtained from the previous two values using a linear relation.

The results of the computations are shown in Figs. (C-1) and (C-2). In these figures  $u_b$  represents the bulk velocity,  $\rho$  the density,  $r$  the distance from the center line,  $x$  the distance from the entrance, and  $D$  the pipe diameter. In Fig. (C-1) we have plotted the computed radial velocity profiles at three values of  $x/D$ . Also shown in this figure are experimental values obtained by Barbin and Jones [10]. Small differences between the measured and the computed values are, we think, due to the following reason: in the computations we used for the radial variation of  $\lambda$  Eq. (C-2), which is for fully developed turbulent flow; in the experiment, as noted by the authors from their turbulent intensity measurements, in the inlet region the turbulent shear stresses near the center of the pipe are below their fully developed values whereas near the wall they exceed their fully developed values. In Fig. (C-2) we have shown the computed pressure drop in the entry region. Also shown in this figure are the experimental values obtained in Ref. [10].

The computed pressure gradient after about fifteen pipe diameters becomes essentially constant and is equal to the pressure gradient calculated using Moody chart [1].

#### FULLY DEVELOPED VELOCITY PROFILES

In the second set of computations we calculated velocity profiles for fully developed flow in a smooth pipe. These profiles were obtained by setting momentum flux out of the control volume equal to the momentum flux into the control volume. This can be accomplished easily, although not most economically with respect to computing time, by setting all the  $\psi_j$ 's equal to zero in the program designed to compute developing flows. The results of the computations are shown in Fig. (C-3). The computed values are shown by discrete points to indicate the logarithmic nature of the radial grid spacing used in these computations. The non-dimensional parameters used in the figure are defined by

$$z = \frac{z \sqrt{\tau_w \rho}}{\mu} \quad \text{and} \quad u^* = \frac{\rho u}{\sqrt{\tau_w \rho}}$$

where  $\tau_w$  is the shear stress at the wall. Also shown in this figure are van Driest's calculations and the relation  $u^* = 5.5 + 2.5 \ln z^*$ , both of which compare well with the experimental data.

#### PRESSURE GRADIENT CORRECTION FORMULA

As discussed in section III in the present approach when the pressure gradient along the duct is not specified it is obtained by iteration. The area of the duct at  $x + \Delta x$  is calculated during the computations using a guessed  $\Delta p$ , the pressure drop across  $\Delta x$ . The guessed  $\Delta p$  is then

iterated upon until the calculated area at  $x + \Delta x$  meets the requirements. To better guess  $\Delta p$  at the beginning of each new iteration a formula, based on approximate application of conservation principles, has been derived. We denote area, average density, and average velocity by  $A_1, \rho_1, U_1$  at  $x$ , and by  $A_2, \rho_2, U_2$  at  $x + \Delta x$ . Applying mass and momentum balance across  $\Delta x$  we obtain

$$A_1 \rho_1 U_1 = A_2 \rho_2 U_2 \quad (C-3a)$$

$$\dot{m}(U_2 - U_1) = -\Delta p A_1 - F_v \quad (C-3b)$$

where  $\dot{m}$  represents mass flow rate and  $F_v$  the viscous forces. Now we ask the question that to produce a small change in  $A_2$  how much change in  $\Delta p$  is required? Let  $A_2, \rho_2, U_2, p_2$  be another set of values at  $x + \Delta x$  that also satisfies Eqs. (C-3) and differ from  $A_2, U_2, \rho_2, p_2$  by only small amounts. We set

$$A_2' = A_2 + A', \quad U_2' = U_2 + U', \quad \rho_2' = \rho_2 + \rho', \quad p_2' = p_2 + p' \quad (C-4)$$

Substituting relations from (C-4) into (C-3) we obtain after neglecting second and higher order terms in small quantities  $A', \rho',$  etc.,

$$p' = \frac{\dot{m} U_2}{A_1 A_2 \left( 1 - \frac{\dot{m} U_2}{A_1 p_2} \right)} A' \quad (C-5)$$

In obtaining Eq. (C-5) we have assumed (a) the small changes in  $A_2', \rho_2',$  etc., induce negligible change in  $F_v$ , and (b) changes  $p'$  and  $\rho'$  are related by

$$\frac{p'}{p_2} = \theta \frac{p'}{p_2} \quad (C-6)$$

where  $\theta$  is some constant. Equation (C-5) tells, approximately, that  $\Delta p$  when incremented by  $p'$  will produce a change equal to  $A'$  in  $A_2$ . During computations at the end of each pressure iteration the difference between the computed and the specified area is calculated, calling it  $A'$ . Eq. (C-5) is solved for  $p'$ . The  $p'$ , thus obtained, is in turn used to adjust  $\Delta p$  for the next iteration. In our experience so far, the most satisfactory value of  $\theta$  seemed to depend on the flow being computed. In the sample calculations given in this appendix, of incompressible flow,  $\theta$  was set equal to infinity.

The sample calculations were carried out using FORTRAN IV programming language on IBM 360/44 with DOS operating system. For the case of developing flow, discussed in this appendix, the program required 34 K of core memory. The computational CPU time was 2 minutes and 22 seconds to carry out the calculations to 60 pipe radii (approximately 240 integration steps).

## REFERENCES

- [1] H. Schlichting, Boundary-Layer Theory (McGraw-Hill, New York, 1968).
- [2] P.J. Roache, Computational Fluid Dynamics (Hermosa Publishers, Albuquerque, NM, 1972).
- [3] S.V. Pantankar and D.B. Spalding, Heat and Mass Transfer in Boundary Layers (Margon-Grampian, London, 1967).
- [4] A.D. Gosman, W.M. Pun, A.K. Runchal, D.B. Spalding, and M. Wolfshtein, Heat and Mass Transfer in Recirculating Flows (Academic Press, New York, 1969).
- [5] E.D. Doss, G.S. Argyropoulos, and S.T. Demetriades, Two Dimensional Flow in MHD Ducts with Transverse Asymmetries, AIAA Journal 13 (1975), pp. 545-546.
- [6] R.A. Gentry, R.E. Martin and R.J. Daly, An Eulerian Differencing Method for Unsteady Compressible Flow Problems, Journ. of Comp. Phys. 1 (1966), pp. 87-117.
- [7] P. Fritzer, L.L. Lengyel and K.J. Witte, Self Consistent Calculation of the Gasdynamic and Electrical Properties of a Two-Dimensional MHD Flow, in Proceedings of the 12th Symposium on Engineering Aspects of MHD (1972), pp. III.7.1 - III.7.8.
- [8] M.S. Greywall, and C.C.P. Pian, Velocity, Temperature and Conductivity Profiles in Hydrogen-Oxygen MHD Duct Flows, Symposium on Fluids Engineering in Advanced Energy Conversion Systems, 1978 ASME Winter Annual Meeting (1978), pp. 111-120.
- [9] E.R. van Driest, On Turbulent Flow Near a Wall, Journ. of the Aero. Sciences 23 (1966), pp. 1011-1011, 1036.
- [10] A.R. Barbin and J.B. Jones, Turbulent Flow in the Inlet Region of a Smooth Pipe, Journ. of Bas. Engr. 85 (1963), pp. 29-34.



### ACKNOWLEDGEMENTS

We would like to thank Dr. J.M. Smith and Dr. C.C.P. Pian of NASA-Lewis Research Center for many helpful discussions during the course of these investigations.

The work was partly supported by the National Aeronautics and Space Administration Grant NSG-3186 and partly by NASA-ASEE summer faculty program.

## LIST OF FIGURES

- Fig. 1. Partitioning of the flow in the duct into streams.
- Fig. B-1. Variation of friction factor  $f$  with Reynolds number.
- Fig. B-2. Variations of mass, momentum, and kinetic energy correction factors  $\gamma$ ,  $\alpha$ , and  $\delta$  with Reynolds number.
- Fig. C-1. Comparison of computed developing velocity profiles in the inlet region of a pipe with experimental data.
- Fig. C-2. Comparison of computed pressure drop in the inlet region of a circular pipe with experimental data.
- Fig. C-3. Computed fully developed velocity profiles in circular pipes.

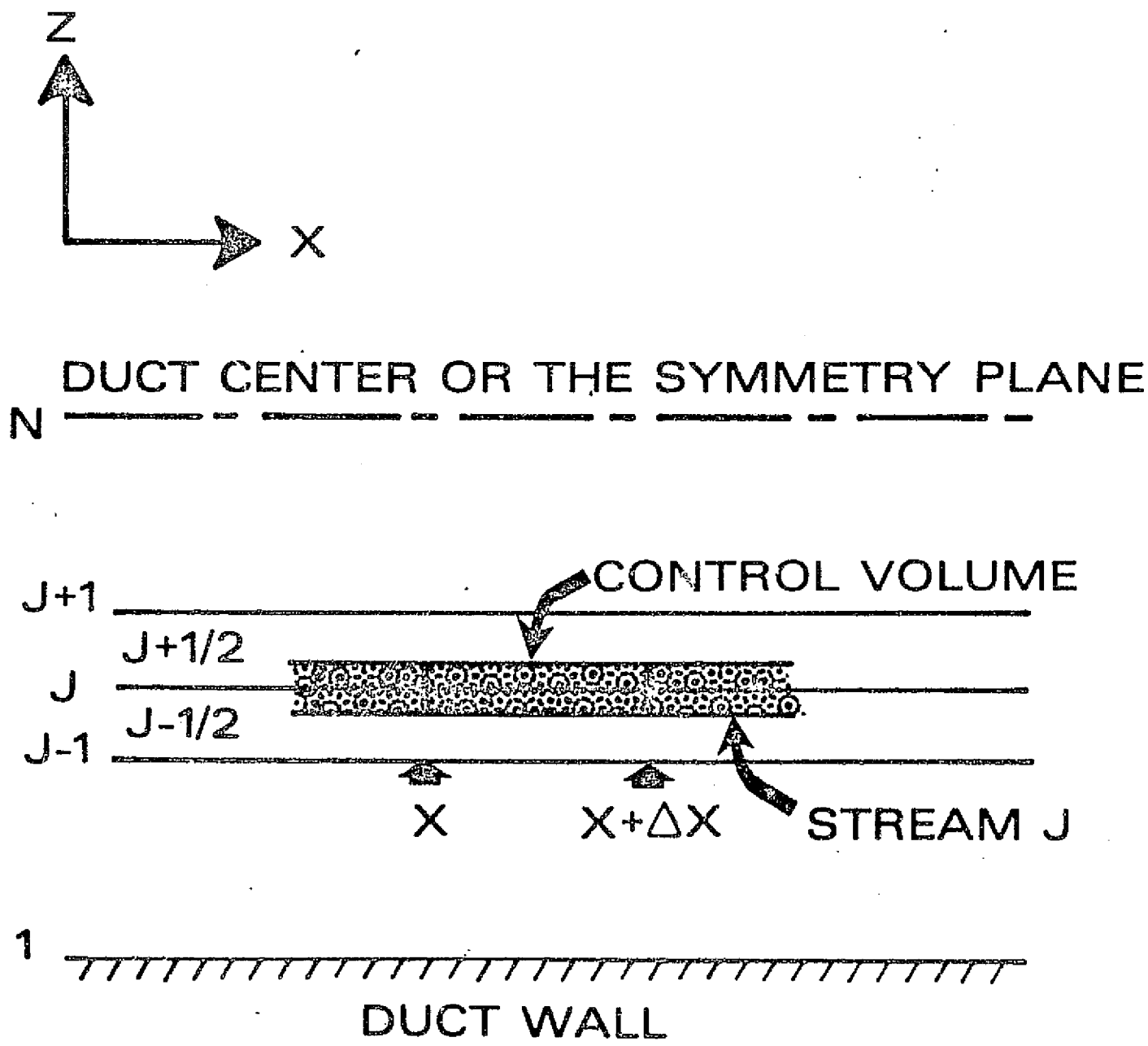


FIG. 1

8

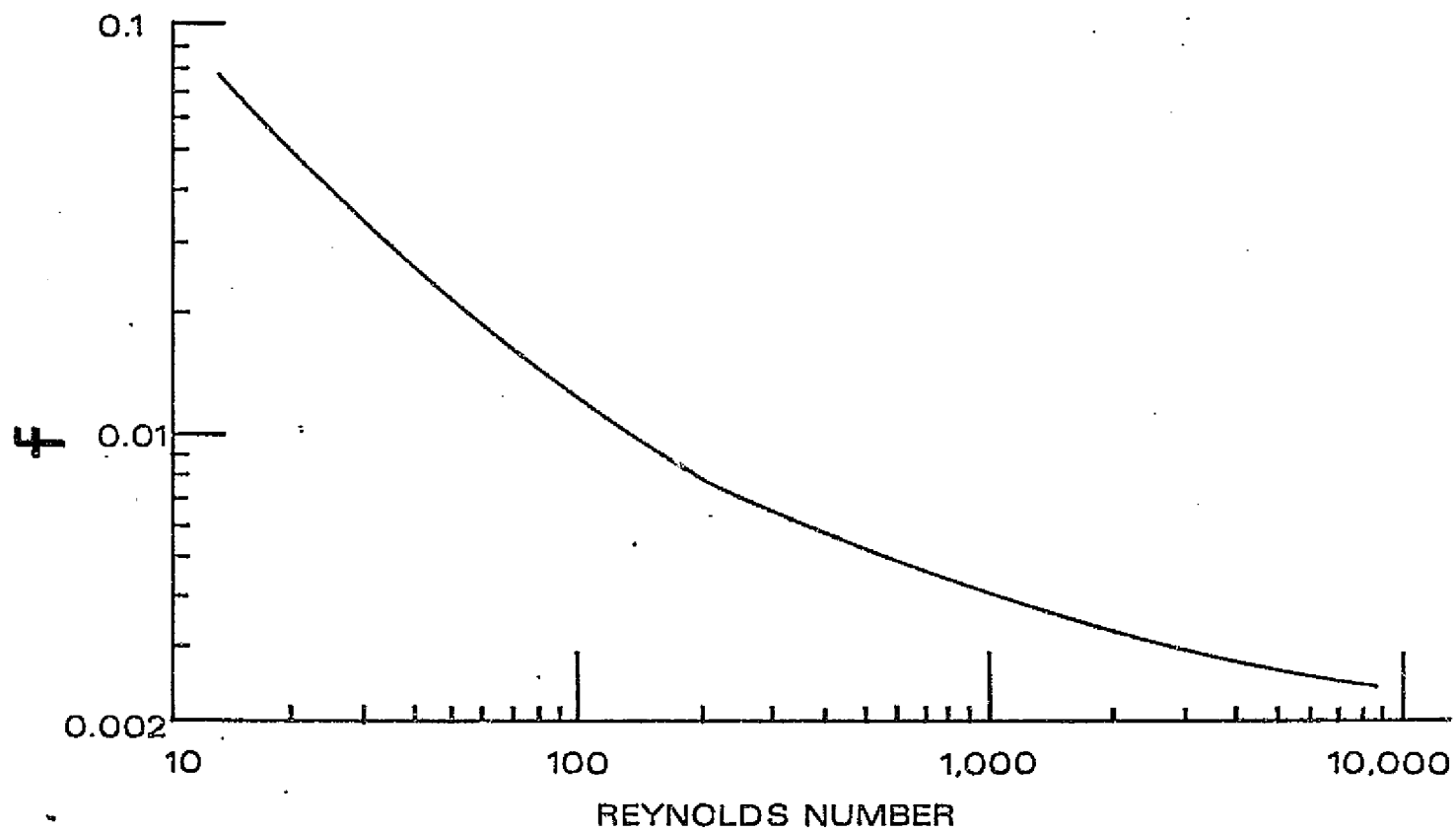


FIG. B-1

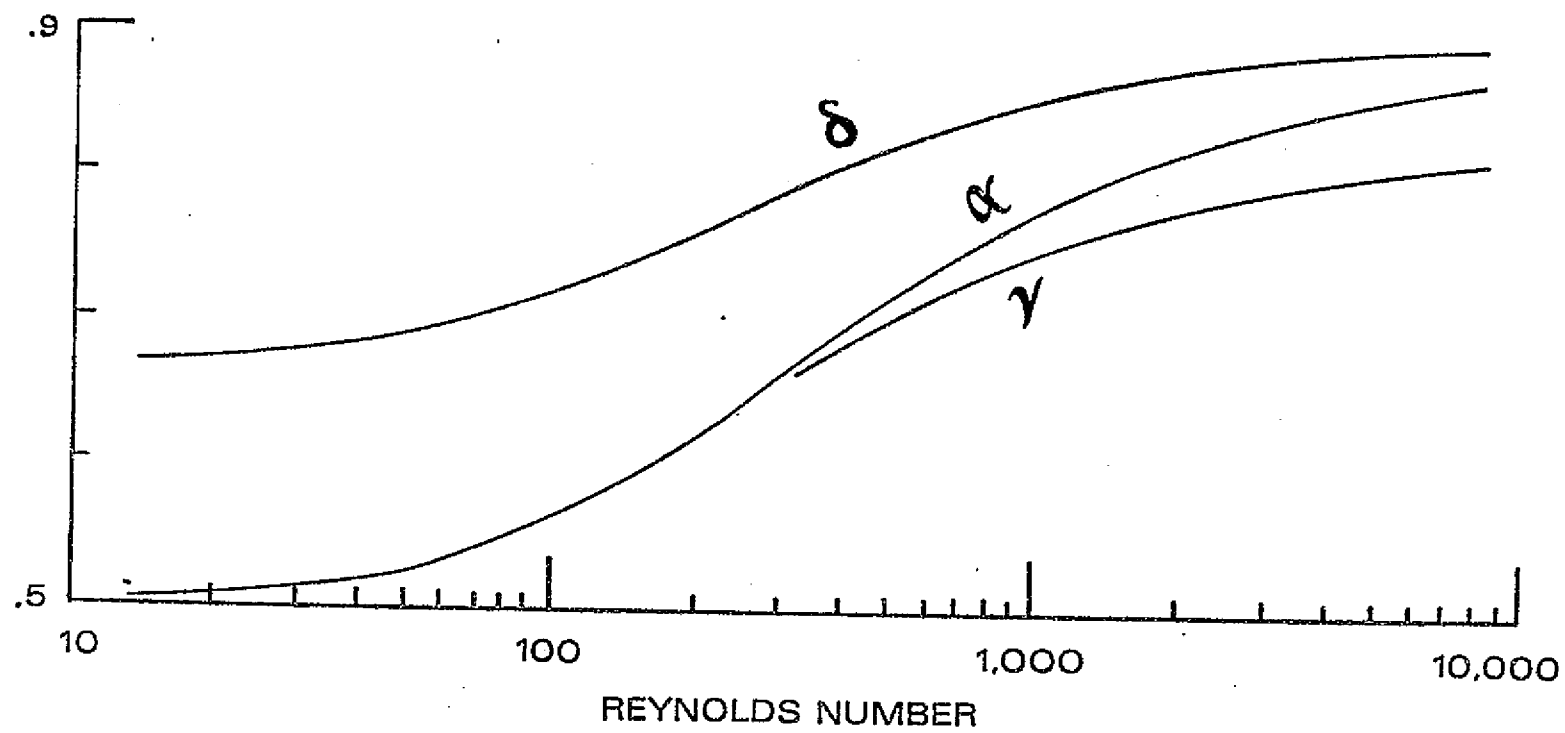


FIG. B-2

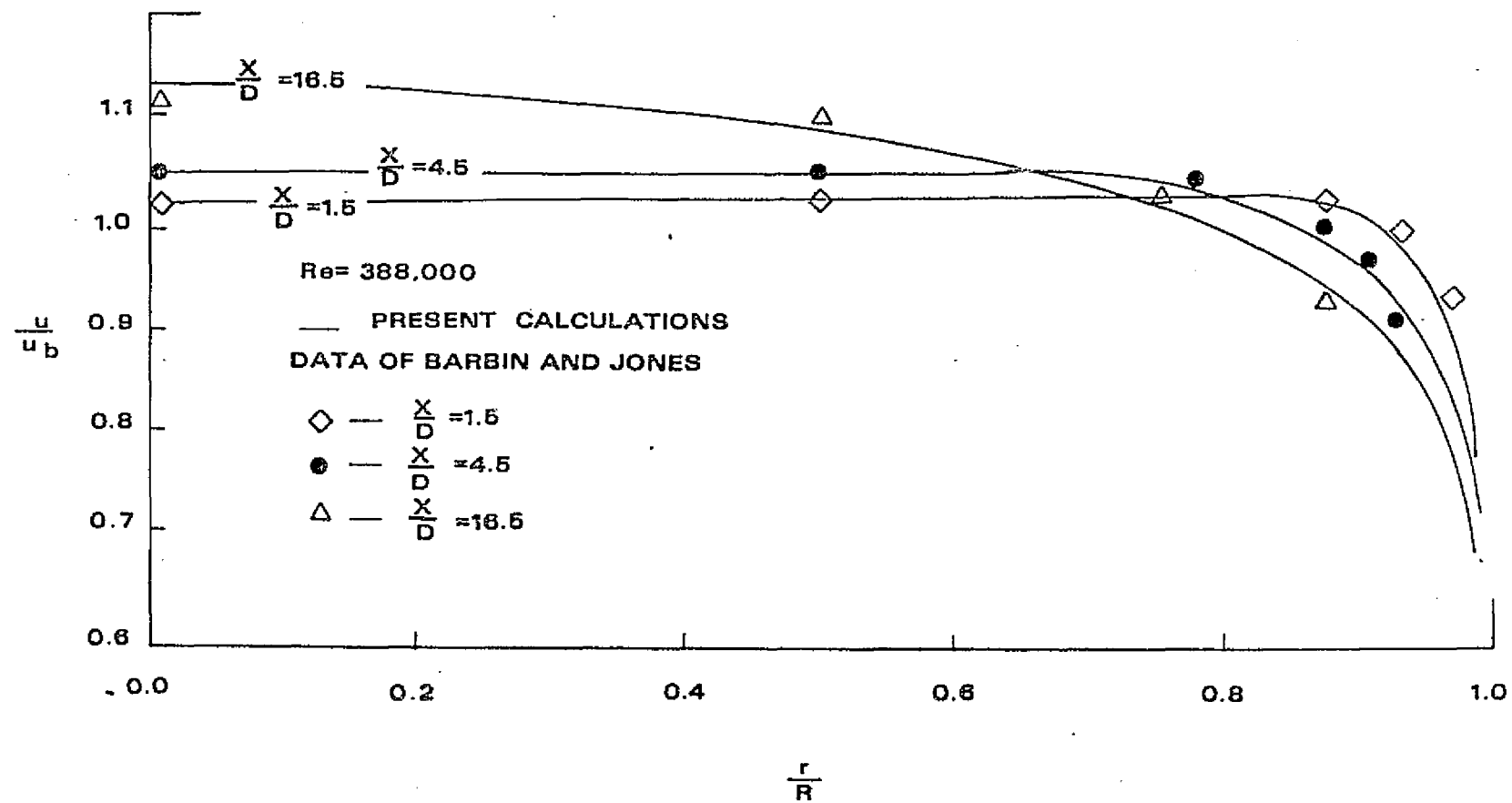


FIG. C-1

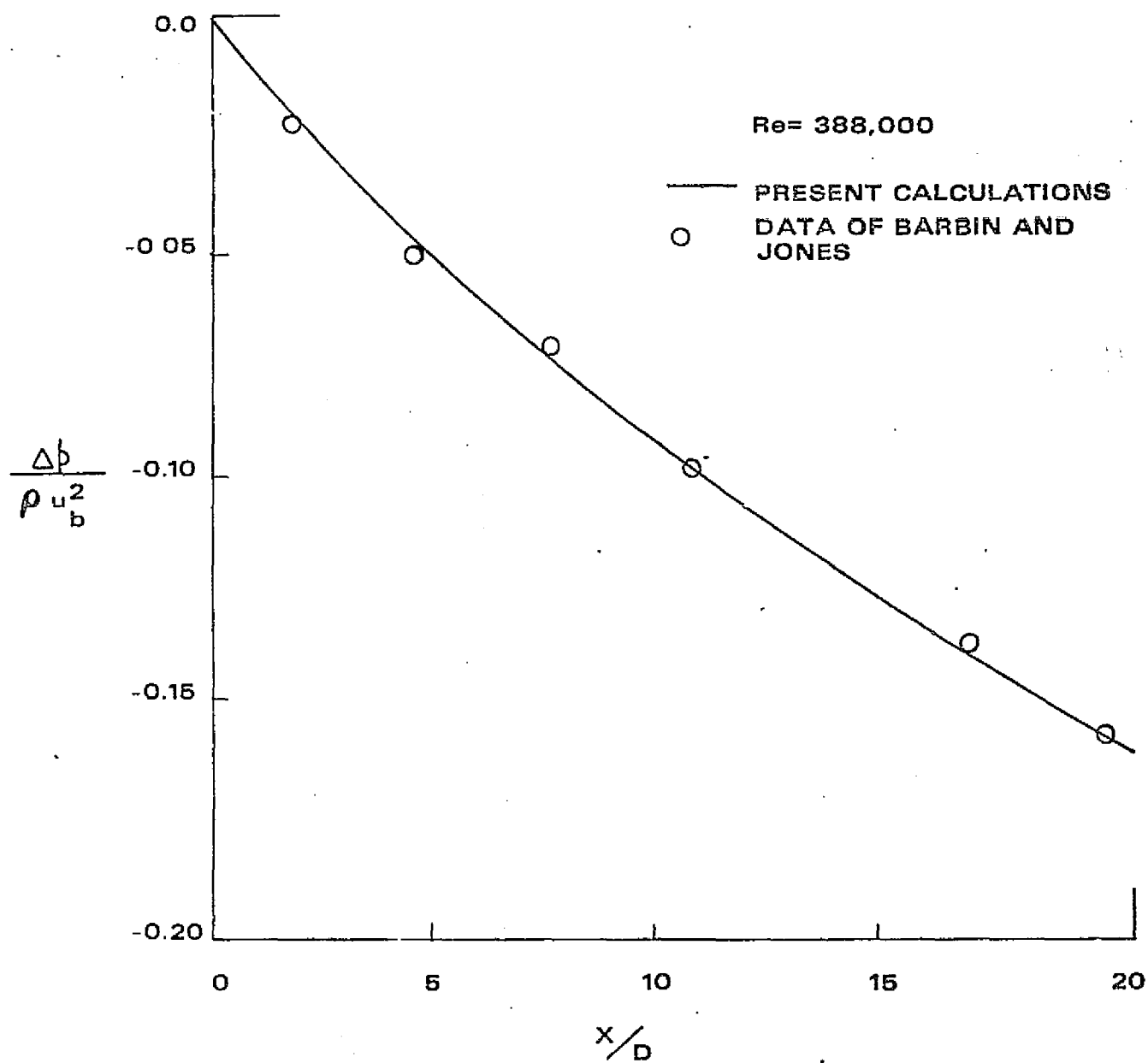


FIG. C-2

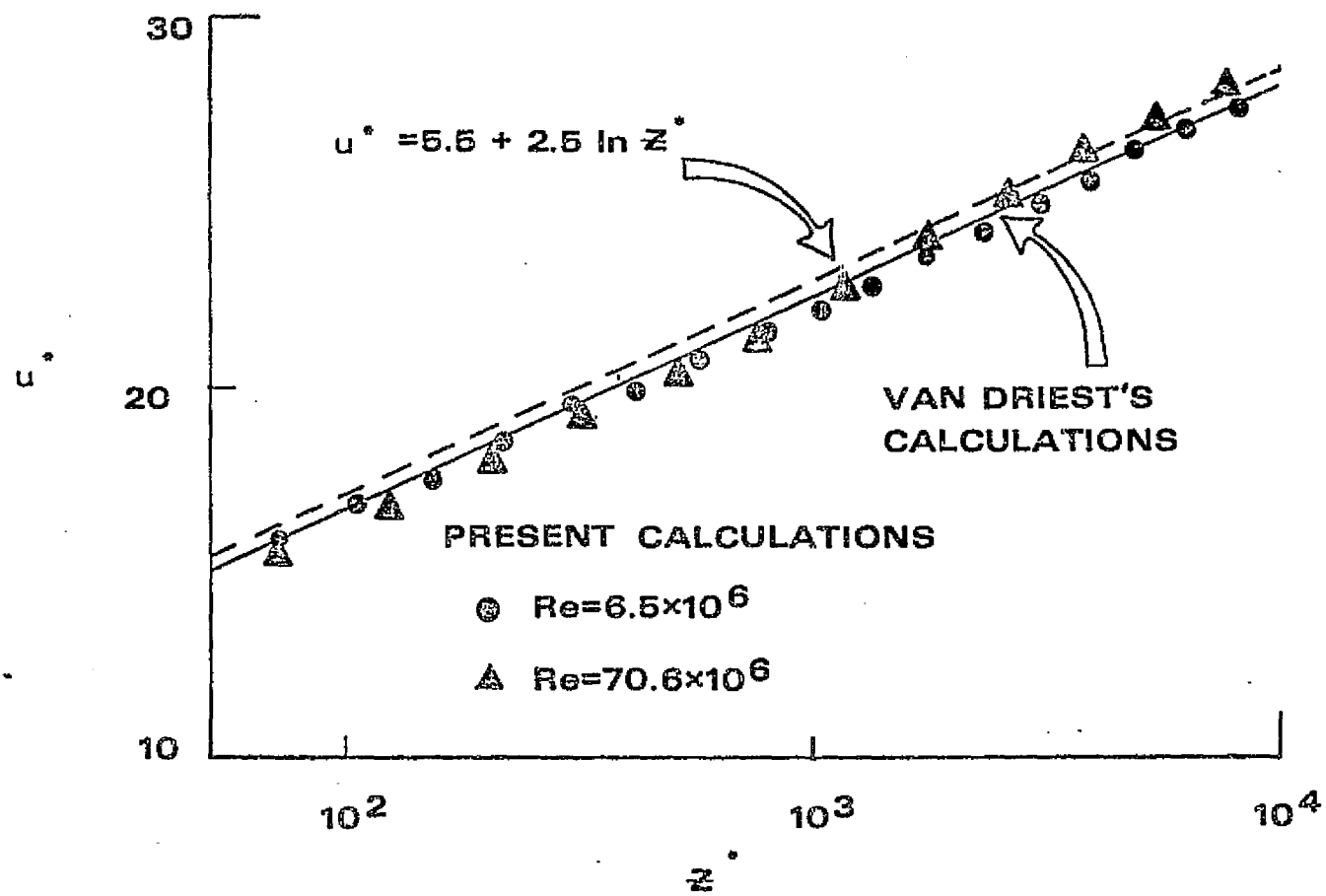


FIG. C-3